UNIVERSIDADE DE SÃO PAULO
INSTITUTO DE FÍSICA DE SÃO CARLOS

Guilherme Camargo Fiusa

Geometric bounds for approximate quantum error correction and a few words about holography

São Carlos

2022

Guilherme Camargo Fiusa

Geometric bounds for approximate quantum error correction and a few words about holography

Dissertation presented to the Graduate Program in Physics at the Instituto de Física de São Carlos da Universidade de São Paulo, to obtain the degree of Master in Science.

Concentration area: Theoretical and Experimental Physics

Advisor: Prof. Dr. Diogo de Oliveira Soares Pinto

Corrected version

(Original version available on the Program Unit)

São Carlos

2022

Fiusa, Guilherme Camargo
Geometric bounds for approximate quantum error correction and a few words about holography / Guilherme Camargo Fiusa; advisor Diogo de Oliveira Soares Pinto - corrected version -- São Carlos 2022.
126 p.

Dissertation (Master's degree - Graduate Program in Theoretical and Experimental Physics) -- Instituto de Física de São Carlos, Universidade de São Paulo - Brasil , 2022.

1. Quantum error correction. 2. Quantum information theory. 3. Quantum resource theory. 4. AdS/CFT. I. Pinto, Diogo de Oliveira Soares, advisor. II. Title.

This work is dedicated to my older brother,
who is and has always been my best friend.

ACKNOWLEDGEMENTS

Em proêmio, menciono meus pais, o "doutor" e a dona Rosa, indivíduos fulcrais que sempre fizeram o possível e impossível para proporcionar a vida que tenho, em sentido literal, lato e estrito. "*Se cheguei até aqui foi porque me apoiei no ombro de gigantes*". A citação de um ilustre cientista pode também ser atribuida ao meu irmão Gustavo, a quem esta tese é dedicada, e ao meu primo Filipe, fonte inesgotável de inspiração.

Reiterando a afirmação de Belchior, "*presentemente eu posso me considerar um sujeito de sorte*", tenho imensa fortuna de estar repleto de pessoas das quais tenho grande estima. A seguir, menciono algumas figuras do supracitado conjunto. Ao Rodrigo (Eskeleto), agradeço por muito me ensinar sobre a carreira acadêmica e como como o "jogo" é "jogado", e também pela incalculável ajuda recente com a burocracia alemã. Ao Wilson, demonstro minha gratidão pelas boas conversas e pelo auxílio inestimável em duras decisões; mal posso esperar pelo início de nossa roda de samba em Tübingen. Ao Luan, agradeço por ser um bom amigo, pelos inúmeros cafés, pelos conselhos pessoais e profissionais, e também pelas conversas sobre a vida, o Universo, e tudo mais. À Alexandra, Pedro, Mauro, Luke, David, Dave, Chris e admins do Zoro, agradeço pelos momentos de expressão artística. Ao Igaum, pela fritação. À *ela*, *você-sabe-quem*, permito que Fernando Pessoa diga por mim: "*não há saudades mais dolorosas do que as das coisas que nunca foram*".

"Cuidado com o golpe" foi uma despretensiosa frase proferida entre amigos numa noite de sexta-feira no apartamento 61 enquanto caíamos num golpe. Por ironia do destino, tal frase acabou nomeando este seleto conjunto de pessoas cuja importância me é inestimável. Felipe(s), Gabriel, Giuliano, e Mateus são os nomes das feras. Deveras grato pelas horas de física, várzea, cafés, rolês, prévias, papo furado, jogos do Fluminense e do Cruzeiro. Menciono também os(as) matemáticos(as) do i^i, a velha (e a nova) geração da Astrofísica, os enxadristas, os lúcidos da PPG, e o grupo de Informação Quântica.

Meu egrégio orientador merece congratulações dobradas. Primeiro, agradeço ao Diogo na figura de orientador pelo apoio, confiança, infinitas cartas de recomendação, e sobretudo pelo exemplo de pessoa, cientista, e profissional. Segundo, agradeço ao Diogo na figura de amigo por ser alguém com quem eu sempre pude contar nas mais diversas esferas da vida, seja para tirar dúvidas de física ou para conversar sobre os maiores sambistas

da nossa geração. Tenho plena ciência de que seu altruísmo é uma das virtudes mais belas que já vi num ser humano. Meu conselho, para qualquer pessoa e independente das circunstâncias, é “procure o Diogo e troque uma ideia com ele”.

Não poderia deixar de citar o professor Vitor pelos fundamentais anos de orientação, pelo exemplo de cientista e pessoa, pelos conselhos, e também pelas infinitas cartas de recomendação. O nome dos protagonistas dos Capítulos 3 e 5 é uma singela homenagem à sua contribuição. Aponto também outros professores essenciais em minha formação, a saber, Daniel Vanzella, Leo Maia, Luiz Agostinho, e Reginaldo Napolitano.

Em desfecho, agradeço à população brasileira e seus esforços para a manutenção de uma Universidade pública de qualidade. Não menos digno de mérito são os servidores do IFSC, por tornarem tudo isto possível. Em particular, o Ricardeus que resolveu toda burocracia com acurácia e celeridade ímpares e a Neusa da biblioteca que gentilmente corrigiu meus (inúmeros) erros nas referências e me orientou em relação às (frustradas) tentativas de burlar o template, e.g. usar [ ] e não ( ) nas citações.

This study was financed in part by the Coordenação de Aperfeiçoamento de Pessoal de Nível Superior – Brasil (CAPES) – Finance Code 001.

"We have no choice but to laugh at such paradox."

Yang Wenli

ABSTRACT

FIUSA, G. **Geometric bounds for approximate quantum error correction and a few words about holography**. 2022. 126p. Dissertation (Master in Science) - Instituto de Física de São Carlos, Universidade de São Paulo, São Carlos, 2022.

In this work, we investigate some applications of quantum information theory motivated by high-energy physics. There is strong evidence suggesting that entanglement is deeply connected with the geometry of spacetime, which leads to surprising applications of quantum information theory in the AdS/CFT correspondence and holography. We start by reviewing the fundamental concepts of the AdS/CFT correspondence which play a key role in bulk-boundary reconstruction, in particular, we explore some features which suggest that one must interpret the encoding of information in the correspondence as a quantum error-correcting code. We discuss the fundamentals of error correction, exploring the formalisms of operator algebra and stabilizer codes. Then, we establish the concrete connection between the two main concepts by showing examples of quantum error-correcting codes that serve as a toy model for AdS/CFT. We illustrate how the 3-qutrit code and the HaPPY code can be powerful tools to explore the correspondence analytically and to solve apparent paradoxes. Following recent results, using quantum error correction, that suggest an intrinsic incompatibility of quantum gravity with global symmetries, we explore approximate error-correcting codes and asymmetric codes as a way to better understand the consequences in a quantum resource-theoretic way. Finally, we discuss our original contribution: geometric bounds for approximate quantum error correction. We calculate our bounds for three typical quantum channels that model the lack of exactness in error correction, namely, dephasing, depolarizing, and amplitude damping channels. The implications of our bounds for AdS/CFT are somewhat elusive; nonetheless, we provide a new approach to benchmark approximations in error correction performance, which may be of high interest for AdS/CFT and its corresponding absence of global symmetries.

Keywords: Quantum error correction. Quantum information theory. Quantum resource theory. AdS/CFT.

RESUMO

FIUSA, G. **Desigualdades geométricas para correção de erros aproximada e algumas palavras sobre holografia**. 2022. 126p. Dissertação (Mestrado em Ciências) - Instituto de Física de São Carlos, Universidade de São Paulo, São Carlos, 2022.

Neste trabalho, investigamos algumas aplicações de teoria de informação quântica motivadas pela física de altas energias. Há fortes evidências apontando uma profunda conexão entre emaranhamento e a geometria do espaço-tempo, nos levando à aplicações surpreendentes de teoria de informação quântica na correspondência AdS/CFT e em holografia. Iniciamos com uma revisão dos conceitos fundamentais acerca da correspondência AdS/CFT no tocante à reconstrução *bulk-boundary*, em particular, exploramos alguns aspectos que sugerem que a codificação de informação na correspondência é análoga ao que ocorre em códigos de correção de erros. Discutimos os fundamentos de correção de erros, explorando os formalismos de álgebra de operadores e códigos de estabilizadores. Em seguida, estabelecemos a relação concreta entre as duas ideias principais através de exemplos de códigos de correção de erros que servem de *toy model* para AdS/CFT. Ilustramos como o código de 3-qutrits e o código HaPPY podem ser ferramentas poderosas para explorar a correspondência de forma analítica e para solucionar aparentes paradoxos. Seguindo resultados recentes, usando de correção de erros, que sugerem uma incompatibilidade intrínseca entre gravitação quântica e simetrias globais, exploramos correção de erros aproximada e códigos com assimetria como uma forma de melhor entender as consequências sob o ponto de vista de teorias quânticas de recursos. Por fim, discutimos nossa contribuição original: desigualdades geométricas para correção de erros aproximada. Calculamos nossas desigualdades para três canais quânticos típicos que modelam a falta de exatidão em correção de erros, a saber, *dephasing*, *depolarizing*, e *amplitude damping*. As implicações de nossas desigualdades para AdS/CFT permanecem difusas; de todo modo, fornecemos uma nova abordagem para classificar o desempenho em códigos aproximados, o que pode ser de elevado interesse para AdS/CFT e ausência de simetrias globais.

Palavras-chave: Correção de erros. Teoria de informação quântica. Teoria quântica de recursos. AdS/CFT.

CONTENTS

1 INTRODUCTION AND MOTIVATION

"Porque é assim que é, renascendo das cinzas
Firme e forte, guerreiro de fé."
Mano Brown

The quest for a unified description of Nature remains the biggest challenge for fundamental physics. All possible interactions are classified into four fundamental interactions that govern the Universe. We have two very good theories that describe those fundamental interactions, namely, the Standard Model (SM) of particle physics (1) which consists of renormalizable quantum field theories describing electromagnetism, weak interactions and strong interactions; and General Relativity (GR) which describes gravity. (2, 3) The catch is that those two theories describe different objects on different scales; GR is neither quantum nor renormalizable, and the SM deals with scales in which gravity is negligible. Therefore, unifying those two theories under the same framework is a tall task.

The unification of all fundamental interactions has been restlessly pursued by theoretical physicists over the past eighty years. In fact, even Albert Einstein himself dedicated his later life to this mission; albeit unsuccessful, Einstein (once more) laid down the path in which hordes of brilliant physicists would stroll. From the point of view of understanding Nature in its most intimate settings, it is obvious why a unified description of every possible interaction is of immense importance; nonetheless, there is more to it than simply seeking beauty. There are extreme phenomena in our Universe that we cannot describe with the theories we currently have, hence there are practical reasons why we need a unified description. In particular, the two honorable mentions are the beginning of the Universe (the Big Bang and early Universe cosmology) and the interior of black holes.

Among the candidates for the unification, there is a wonderful theory known as string theory (4–7) which, funnily enough, was originally developed as a way to describe strong interactions as one could model the flux tubes between quarks as a string of gluon energy density between the quark pairs. (8–11) Things took a wild turn when it was discovered in the '70s that in the spectra of this theory there was a spin-2 boson, affectionately named the "graviton". With a few modifications, string theory could actually

be used to describe gravity! (12, 13) Yet another chapter in the history of unification was written throughout the '80s when it was discovered that string theory could be used as a single framework to describe all particles and their interactions. (14–17) The pinnacle of string theory came from an unpretentious conjecture: motivated by the pioneer study of black hole entropy and microstates (18, 19), it was argued that a consistent unification of quantum gravity must be described by an effective theory with one less dimension. (20, 21) The first concrete example of this conjecture was provided by Maldacena (22), culminating in the exorbitantly famous AdS/CFT correspondence[1], which consists of a correspondence between two different physical theories, in particular, one string theory and one quantum field theory. The stunning consequence is the fact that a theory that possesses gravity can be described by a pure quantum field theory, in a sense, it suggests that gravity is an emergent phenomenon from quantum degrees of freedom.

Up to this day, the AdS/CFT correspondence is the best description[2] we have for a unified theory of quantum gravity; although its general validity is still a conjecture, there are several pieces of evidences in its favor. (23–26) In particular, it transcended its original context of string theory and unification, as there are several applications of AdS/CFT in various areas of physics. By fate's sense of humor or divine inspiration, Ryu and Takayanagi realized that entropy equals gravity in the context of the correspondence. (27, 28) This brilliant insight opened the floodgates for other ideas concerning information theory and quantum gravity. In particular, it took seventeen years for exceptionally clever physicists to realize that the way information is encoded in the AdS/CFT correspondence is precisely the way information is encoded in quantum error correction. (29–32) This happy and fortuitous insight is the catalyst of the present work.

Taking a complete turnaround, the history of quantum error correction begins from a much more practical standpoint. Quantum computers will promote a revolution just like the advent of classical computers did, and thus are among the most awaited technological advances of the present century. (33) The problem, however, is that quantum computers

[1] The term "exorbitantly famous" is indeed appropriate. As of the time of writing, Maldacena's original paper has over 22000 citations according to the google scholar database.

[2] The reader may think that this affirmation is somewhat pretentious. There are several reasons why AdS/CFT is the current leading theory in the race for a complete theory of quantum gravity. On top of that, string theorists are not particularly known for their humbleness, had the author been an actual string theorist, he would have said that AdS/CFT is the *only consistent* theory of quantum gravity.

are difficult beasts to tame, as they strongly interact with the environment, losing the stored information and having unreliable computations. (34, 35) Given this context, the theory of quantum error correction begins with the search for ways to protect information stored and transmitted by quantum computers, this protection is accomplished through the exploitation of redundancy. Given a piece of information, one seeks to store it redundantly such that if an error occurs or some information is lost, the damaged piece is precisely the redundant information; this way, the actual information stays pristine. (36–39)

As we shall see, the redundancy exploited in quantum error correction is somehow a built-in feature of the AdS/CFT correspondence. The fact that quantum error correction seems to be the way the Universe found to encode information in quantum gravity is nothing short of a blissful miracle. Furthermore, the use of error correction methods in AdS/CFT has proven over and over to be very fruitful in unveiling its layers and secrets. A recent motivating example is the work by Harlow and Ooguri (40, 41) where it was shown, using quantum error correction methods, that the AdS/CFT correspondence is incompatible with global symmetries. That is quite the affirmation.

Motivated by this keen result, we reinterpret this statement under the light of another famous result in error correction theory, the so-called Eastin-Knill theorem, which states that quantum error-correcting codes cannot simultaneously recover errors exactly, have continuous symmetries and a universal set of transversal gates. (42) In this sense, global symmetries are not quite "incompatible" but rather "in conflict" with the correspondence. This reinterpretation is supported and enhanced by the introduction of quantum resource theories (43), which is a very general and powerful framework to deal with quantum phenomena; employed in our context to quantify "approximate" quantum error correction and "approximate symmetries". (44–51) In our original contribution, we propose a distance measure based on sub- and super-fidelities (52, 53) to bound and quantify approximations in lack of exact error correction. The great advantage of our proposal is the fact that it is significantly easier to calculate than the standard approach. On top of that, it also defines a genuine metric and thus may be employed to explore geometric properties.

The present work is inserted in this broad context. We studied and employed quantum error correction methods and concepts motivated by the AdS/CFT correspondence and quantum resource theories. As a twist of fate, our main result (the proposal and

calculation of distance measures based on sub- and super-fidelity) deals with "pure" error correction, as its consequences for AdS/CFT remain somewhat elusive. Nonetheless, our work sheds light on this incredibly active and perhaps exotic relation: information encoding in quantum computers and Nature in its most fundamental constituents.

This dissertation is the result of sixteen months of work (including a global pandemic and coursework) and is organized as follows: in Chapter 2, we present a review of the pertinent literature on the AdS/CFT correspondence, in particular, we discuss reconstruction procedures which point out a redundancy structure just like in quantum error correction. In Chapter 3, we present the fundamentals of error correction and its main approaches, the idea is to rigorously provide substance to carry on the connections with holography and AdS/CFT. In Chapter 4, we establish those connections by discussing the quintessential Ryu-Takayanagi result, and the quantum error-correcting codes that play a role in holography. We also discuss a recent result pointing out inconsistencies between symmetries and AdS/CFT and use those to motivate the introduction of quantum resource theories. In Chapter 5, we introduce quantum resource theories with particular attention to the asymmetry resource theory, and how it can be used to systematically approach the aforementioned inconsistency through the ideas of approximate quantum error-correcting codes and asymmetric codes. In the end, we discuss our original proposal of the distance measure based on sub- and super-fidelities, point out that they generate a metric and thus can be used to study geometry, and obtain the closed-form expression for common quantum channels that arise in the theory of error correction. Moreover, we calculate those bounds numerically and discuss the obtained results. In Chapter 6, we conclude giving a brief overview of the content of this dissertation and point out further work.

2 THE WORLD AS A HOLOGRAM: MEET THE ADS/CFT CORRESPONDENCE

"We don't know how we can
Decode this anagram
We have lost our true selves
Within this hologram
Nothing is what it seems
Our soul is lost."
Epica: A Profound Understanding of Reality

In this chapter, we review the AdS/CFT correspondence and its main properties to provide solid ground in which we will develop its connections with quantum error correction. This is done through error-correcting toy models which are complex enough to capture meaningful physics but simple enough to be solvable. In particular, we talk about two important reconstruction procedures, known as global and AdS-Rindler reconstruction. In the end, we mention two apparent "paradoxes" that arise from the AdS/CFT description, rephrase them as puzzles and use them to motivate the quantum error correction interpretation of AdS/CFT.

2.1 Motivating the correspondence

The idea of holographic principle (and holography) began in the '70s with the works of S. Hawking and J. Bekenstein. They showed that black holes are thermodynamical objects that possess a well-defined entropy (18, 19), given by

$$S_{BH} = \frac{4GM^2}{\hbar c} = \frac{c^3 A}{4\hbar G} \sim A \tag{2.1}$$

where A denotes the area of the black hole event horizon[1]. The remarkable property of the black hole entropy is that it scales with the area of the horizon, rather than the volume, as expected for a usual thermodynamical system. This way, the number of microstates of a black hole grows with its area, which means that those microstates are somehow encoded into the horizon area. That is the first realization of a so-called holographic principle.

[1] The constants are denoted as usual: M is the mass of the black hole, G is Newton's constant, c is the speed of light and $\hbar$ is Planck's constant. Unless stated otherwise, we will take all of those constants equal to one throughout the text.

Motivated by this idea, L. Susskind and G. 't Hooft conjectured (20, 21) that a quantum theory of gravity must obey the holographic principle, that is, there must be an effective field theory, living in a spacetime with one less spatial dimension than the spacetime where the quantum gravity theory lives, that describes the same physical phenomena. Although revolutionary, the ideas of Susskind and 't Hooft were far from being concrete, as they could not provide an example or how this holographic principle would manifest in an actual theory.

A concrete manifestation of the holographic principle was provided a few years later by Maldacena (22), he showed that a type IIB superstring theory compactified in five spacetime dimensions (on an Anti de-Sitter background) as $\mathrm{AdS}_5 \times S^5$, which is a theory of quantum gravity, is equivalent in the large N limit (where this theory is well approximated by semiclassical gravity), to the $\mathcal{N} = 4$ super Yang-Mills theory, which is a supersymmetric conformal field theory in four spacetime dimensions. Apart from providing a concrete example of the holographic principle, Maldacena also conjectured that this duality relation between a quantum theory of gravity on an Anti de-Sitter (AdS) background and a conformal field theory (CFT) is a generic property, and should be valid for various theories.

Those ideas evolved into an incredibly active area of research, and although it is still a conjecture, there is plenty of evidence in favor of its validity (for a review of the main arguments, we refer to (23–26)) and applications in a wide variety of phenomena, from heavy-ion collisions (54), quark-gluon plasma (55), and superconductivity (56) to fluid dynamics. (57)

2.2 Anti de-Sitter spacetimes, the left side

In this section, we describe the basic ideas behind Anti de-Sitter spacetimes and mention the important results for AdS/CFT, particularly in the context of symmetries. For details of the derivations presented in this section, we refer to. (2, 3)

Einstein's equation is the apex of General Relativity (GR), it is a tensor equation that describes how energy and matter curve spacetime through precise geometric definitions. It is given by

$$R_{\mu\nu} - \frac{1}{2} R g_{\mu\nu} = 8\pi G T_{\mu\nu}, \tag{2.2}$$

where $R_{\mu\nu}$ denotes the Ricci tensor, R is the scalar curvature, $g_{\mu\nu}$ is the metric tensor, G is Newton's constant and $T_{\mu\nu}$ is the energy-momentum tensor. The first claim is that AdS spacetimes are solutions of Einstein's equations. To show that, consider the Einstein-Hilbert action (in arbitrary d spatial dimensions) with a cosmological constant

$$I_{EH} = \frac{1}{16\pi G_{d+1}} \int \sqrt{-g}(R - 2\Lambda) d^{d+1}x, \tag{2.3}$$

variations of the action with respect to the metric yields

$$\frac{\delta I_{EH}}{\delta g^{\mu\nu}} = 0 \rightarrow R_{\mu\nu} - \frac{1}{2} R g_{\mu\nu} + \Lambda g_{\mu\nu} = 0 \tag{2.4}$$

by contracting the result (2.4) with the metric tensor $g^{\mu\nu}$, we arrive at the scalar curvature

$$R = \frac{2(d+1)}{d-1}\Lambda. \tag{2.5}$$

The scalar curvature is already enough to characterize the solutions. When $R = 0$, we recover flat spacetime[2], when $R > 0$, we obtain a de-Sitter solution and when $R < 0$, we obtain an Anti de-Sitter solution, which is the solution we are interested in. A solution to Einstein's equation is said to be *maximally symmetric* if and only if the Riemann tensor obeys

$$R_{\mu\nu\alpha\beta} \propto g_{\mu\alpha} g_{\nu\beta} - g_{\mu\beta} g_{\nu\alpha}.$$

The AdS solution is indeed a maximally symmetric solution. (3)

There are two convenient coordinate systems for AdS spacetimes, the first one is known as Poincaré coordinates $(t, r, x_1, ..., x_{d-2})$ and the line element is

$$ds^2 = \frac{r^2}{\ell^2}\left(-dt^2 + \sum_i^{d-2} dx_i^2\right) + \frac{\ell^2}{r^2} dr^2 \tag{2.6}$$

where $r \in [0, \infty)$, $t \in (-\infty, +\infty)$, and ℓ denotes the AdS radius; one drawback of this choice of coordinates is that it does not cover the entire manifold. The second convenient coordinate system is known as global coordinates[3] $(t, r, \Omega_1, ..., \Omega_{d-2})$ and its line element is given by

$$ds^2 = -\left(1 + \frac{r^2}{\ell^2}\right) dt^2 + \frac{dr^2}{\left(1 + \frac{r^2}{\ell^2}\right)} + r^2 d\Omega_{d-2}^2 \tag{2.7}$$

[2] We use flat spacetime and Minkowski spacetime as synonyms, and whenever necessary we adopt a mostly plus convention to the metric signature. Einstein's summation convention is always implied.

[3] Note that the (t, r) coordinates from Poincaré coordinates and from global coordinates are different, we choose to denote them using the same letters for convenience. Most of the time, global coordinates are more convenient because, unlike Poincaré coordinates, it covers the entire manifold.

where $r \in [0, \infty)$, $t \in (-\infty, +\infty)$, and ℓ denotes the AdS radius. AdS spacetimes have two remarkable properties which are cornerstones of the AdS/CFT correspondence. The first one is the existence of a horizon at spatial infinity ($r \to \infty$ in the global coordinates or $r \to 0$ in the Poincaré coordinates) which has topology $\mathbb{R} \times S^{d-1}$. The second property is the fact that AdS spacetimes have $SO(2, d-1)$ symmetry, the group acts transitively which means that any two points are connected by a symmetry transformation and therefore the space is homogeneous. Turns out that a $(d-1)$-dimensional conformal field theory also possesses $SO(2, d-1)$ symmetry, this happy coincidence indeed has profound implications on the structure of the AdS/CFT correspondence.

2.3 Conformal Field Theories, the right side

In this section, we give a brief overview of what is a conformal field theory and explore its symmetry properties, giving some intuition behind the relation between the symmetries that are manifested in $(d+1)$-dimensional AdS spacetimes and d-dimensional conformal field theories. We mention the main properties and results which are useful in the context of AdS/CFT; for derivations and details, we refer to. (58, 59)

Quantum Field Theory (QFT) is a mathematical framework used to describe fundamental interactions of nature, and it is not an overstatement to say it is one of the most accurate frameworks physicists have ever developed (60). QFTs work in accordance with Special Relativity (SR) and thus are symmetric under Poincaré transformations[4].

Conformal Field Theory (CFT) is a QFT that, in addition to Poincaré symmetry, also possesses conformal symmetry, which can be divided into two categories, *special conformal transformations* and *dilations* which are described by, respectively,

$$x'^{\mu} = \frac{x^{\mu} + a^{\mu} x^2}{1 + a^2 x^2 + 2 a_{\nu} x^{\nu}}, \qquad x'^{\mu} = \lambda x^{\mu}, \tag{2.8}$$

where $a^2 = a_{\mu} a^{\mu}$, a^{μ} is a four-vector and λ is some parameter.

The symmetry group of a d-dimensional CFT is $SO(2, d)$, the Lie algebra associated with the group have generators which can be classified as rotations $J_{\mu\nu} = i(x_{\mu}\partial_{\nu} - x_{\nu}\partial_{\mu})$, translations $P_{\mu} = -i\partial_{\mu}$, dilations $D = -ix^{\mu}\partial_{\mu}$, and special conformal transformations $K_{\mu} = -2x_{\mu}D + x^2 P_{\mu}$.

[4] Poincaré transformations in the context of Special Relavitiy have nothing to do with the Poincaré coordinates of AdS spacetimes we saw in the last section.

From symmetry considerations, we see that there is already a relation between the two sides of the correspondence. As we have seen, AdS_{d+1} is a homogeneous space as every point can be mapped to another through symmetry transformations. On distance scales which are much smaller than the AdS radius ℓ, the AdS space looks like a flat space $\mathbb{R}^{1,d}$, and thus the isometries compose $d+1$ translations, $d(d-1)/2$ rotations and d boosts. These symmetry transformations make up $SO(2,d)$, which is the isometry group of AdS_{d+1}. However, as we have seen through the generators of the conformal algebra, this is also the symmetry of the conformal group in d-dimensions. This way, from the CFT point of view, the isometries of the AdS space are conformal symmetries. The extra dimension of the AdS space is typically associated with scales in the CFT side (61), as conformal symmetry is manifested as a symmetry of scales. On the AdS side, it is manifested as a symmetry between different radial slices of the geometry.

In conformal field theories, one is typically interested in two objects of the theory, namely, *primary operators* and *correlation functions*. Primary operators are local operators defined as the lowest dimension operators in a given representation of the conformal algebra, however, the practical reason why those are interesting is their transformation properties: $e^{iD\xi}\mathcal{O}(x)e^{-iD\xi} = e^{\xi\Delta}\mathcal{O}(e^{\xi}x)$, where D is the generator of dilations, Δ is the *scaling dimension* of the operator $\mathcal{O}(x)$ and ξ is some parameter. For the remaining of this work, whenever a CFT operator is considered, it is taken to be a primary operator. Correlation functions are the main object of study in quantum field theories, because a number of important observables can be cast as sums of correlation functions, such as scattering amplitudes and propagators. (60, 62)

In CFTs, correlation functions are heavily constrained from the symmetry properties of the theory, as the overall result must be symmetric under rotations, translations, dilations, and special conformal transformations. For example, the two-point correlation function is given by

$$\langle \mathcal{O}_1(x_1)\mathcal{O}_2(x_2)\rangle = \frac{k_{12}}{|x_1 - x_2|^{\Delta_1+\Delta_2}}, \tag{2.9}$$

where k_{12} is some constant, Δ_1 and Δ_2 are the scaling dimension of the operators $\mathcal{O}_1$ and $\mathcal{O}_2$, respectively. Higher-point correlation functions have the same form as equation (2.9). We will not reproduce higher-point functions because the notation and indexes get rather cumbersome, the idea was to illustrate how those correlation functions behave.

2.4 A precise correspondence

After a brief review of the properties and symmetries of AdS spacetimes and CFTs, we are ready to present a more precise statement about the AdS/CFT correspondence and to discuss two procedures known as global reconstruction and AdS-Rindler reconstruction. Those reconstruction protocols will be of utmost importance when we rephrase and explore AdS/CFT in the language of quantum error correction. From now on, we choose to work with units such that the AdS radius ℓ is equal to one unless explicitly said otherwise.

The claim is (30): any conformal field theory on $\mathbb{R} \times S^{d-1}$ is equivalent to a theory of quantum gravity in an asymptotically $\mathrm{AdS}_{d+1} \times M$ spacetime, where M is a compact manifold.

In other words, the correspondence is an equivalence between two distinct physical theories. As such, we may view the correspondence as an isomorphism between two Hilbert spaces

$$\Phi : \mathcal{H}_{AdS} \to \mathcal{H}_{CFT}. \tag{2.10}$$

This interpretation suggests that there is a way to map observables from one side of the correspondence to the other; indeed, although incomplete, this collection of maps which tells us how to go from one side to the other is known as the *dictionary*. Exploring this dictionary will be the main focus of the remaining of this section. From this point onward, we will frequently refer to the theory that lives in AdS background as the *bulk* theory and the CFT theory that lives in flat background as the *boundary* theory, for a graphical representation, see Figure 1.

Before discussing how to relate observables from the bulk to the boundary, we ought to discuss which conformal field theories are dual to "semiclassical" gravity theories, where the AdS radius ℓ is much larger than the Planck length ℓ_P, and the string coupling g_S is small. Whenever this regime is satisfied, the gravity in the bulk theory (originally described by superstring theory) can be approximately described by Einstein gravity. It is hard to further enhance our dictionary without formulating a precise set of rules in which we have a CFT dual to a semiclassical theory of gravity, since we do not know which observables to study in a quantum theory of gravity in the scales of Planck length. We say that a d-dimensional CFT has a semiclassical dual near the vacuum if, for a given finite set of conformal operators $\{\mathcal{O}_i\}$, a local effective bulk action $I_{eff}[\phi_i, \Lambda]$ and a finite set of

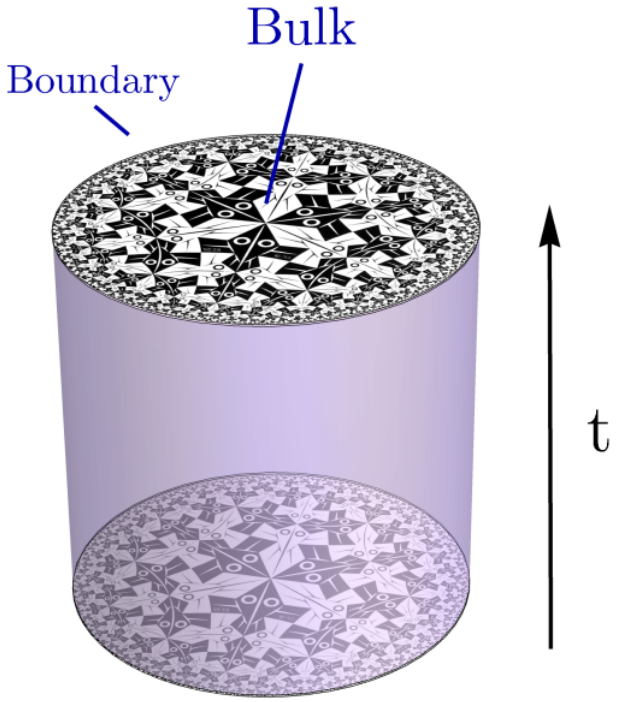

Figure 1 – Illustration of the AdS/CFT correspondence. The bulk corresponds to the theory that lives in the AdS background, which is represented by the hyperbolic tesselation. The boundary corresponds to the conformal field theory which lives in a flat background. The time coordinate is also represented, for each fixed time; there is a static time-slice of the bulk and boundary.
Source: JAHN. (63)

bulk fields $\{\phi_i\}$, the following approximately holds (30):

$$\langle \mathcal{O}_{i_1}(t_1)\mathcal{O}_{i_2}(t_2)...\mathcal{O}_{i_n}(t_n)\rangle_{CFT} \simeq \int e^{iI_{eff}[\phi_i,\Lambda]}\mathcal{O}_{i_1}(t_1)\mathcal{O}_{i_2}(t_2)...\mathcal{O}_{i_n}(t_n)\ \mathcal{D}\phi_i \tag{2.11}$$

where Λ is some convenient cutoff. The semiclassical limit is also associated with the large N limit, where N denotes the parameter of the internal symmetry Lie group. As long as equation (2.11) is satisfied, the superstring theory in the bulk is weakly coupled and can be described classically.

One aspect which is important when considering a one-to-one relation between operators on the AdS side and the CFT side is *locality*. A rigorous set of rules describing the mechanism behind the emergence of bulk locality remains elusive, however, locality near the boundary is manifested through the following relation (64, 65)

$$\lim_{r\to\infty} r^{\Delta}\phi(r,x) = \mathcal{O}(x), \tag{2.12}$$

since the CFT respects locality (it is a quantum field theory afterall), this relation manifestly respects locality in the x directions. However, the radial direction is more complicated,

when we naively consider locality in the radial direction and try to relate bulk operators with boundary operators, we run into the so-called "radial commutativity puzzle". For now, we limit our discussion to methods of relating bulk operators to boundary operators, later on, this puzzle will play an important role.

One concrete approach to relate fields in the AdS background with operators in the CFT, not necessarily in the limit where a point in the bulk approaches the boundary, is due to Witten (66), where the claim is that the partition functions are equivalent

$$Z_{\text{bulk}}[\phi] \equiv Z_{\text{boundary}}[\mathcal{O}]. \tag{2.13}$$

Taking the boundary value of a bulk field ϕ to be $\tilde{\phi}$, the bulk configuration of ϕ may be determined by a boundary value problem from a given $\tilde{\phi}$ according to the prescription (2.12). Furthermore, the bulk action then follows from

$$Z_{\text{bulk}}[\phi] \equiv Z_{\text{bulk}}[\tilde{\phi}] = \left\langle \exp \int \tilde{\phi}\mathcal{O}\ d^d x \right\rangle. \tag{2.14}$$

Interestingly, the bulk partition function (after some algebraic work) from equation (2.14) provides the relation $\Delta(\Delta - d) = m^2$ between the scaling dimension Δ of the conformal operator $\mathcal{O}$, the mass m of the scalar bulk field ϕ and the spacetime dimension d. This relation serves not only as evidence, where it explicitly relates quantities associated with asymptotic bulk fields and conformal operators as well as a consistency condition that must be satisfied by the two sides of the correspondence.

2.5 Global reconstruction

The first reconstruction procedure we explore is known as global AdS reconstruction[5], which was first proposed in (67) and enhanced in. (68, 69) We work in global coordinates (2.7) in the AdS space. The idea is to describe a formula for the bulk operator $\phi(x)$ in the boundary in terms of non-local operators in the CFT as if the bulk operator is "smeared out" in the boundary. In practice, one construct operators in the CFT which obey the equations of motion of the bulk with the boundary conditions given by equation (2.12). The first step is to solve the bulk equations of motion for a scalar field $\phi(x)$ in the curved background:

$$\nabla^2\phi = \frac{1}{\sqrt{-g}}\partial_\mu(\sqrt{-g}g^{\mu\nu}\partial_\nu\phi) = m^2\phi. \tag{2.15}$$

[5] The global reconstruction procedure is sometimes called the HKLL procedure, where the letters are an acronym for the names of the authors.

with the boundary condition given by equation (2.12). The solution for the equations of motion can be written as[6]

$$\phi(x) = \int_{\mathbb{R}\times S^{d-1}} K(x;Y)\mathcal{O}(Y)\ dY, \tag{2.16}$$

where the integration is carried over the conformal boundary, and the function $K(x;Y)$ is known as the *smearing function*, it essentially links the boundary operator with the bulk field in a way that it obeys the bulk equations of motion and recovers precisely equation (2.12) as we take x going to the boundary. For details of this derivation, see Appendix A. This boundary-value problem is not a usual one, the reason is that the existence of a solution and its uniqueness is not guaranteed[7]. In a special case (pure AdS), one can find an explicit solution for the smearing function, the procedure, however, is quite complicated and out of the scope of this text, for that, we refer to the aforementioned papers where this method was developed. (67–69)

The smearing function can be chosen in a way that it only has support when the separation between the bulk coordinate x and the boundary coordinate Y is spacelike, in other words, when x and Y are in the same Cauchy time-slice. For the case of AdS_3, we refer to Figure 2, where the point x is represented by an integral over the region that is shaded green and Σ represents the Cauchy time-slice in which x belongs.

One subtlety associated with this reconstruction process is the fact that as long as we have the representation (2.16) which connects bulk fields with boundary operators, we may rewrite the operators in the boundary in a single Cauchy time-slice Σ using the Heisenberg picture with the Hamiltonian that characterizes the CFT. (29) An interesting but somewhat problematic property that arises from this procedure is that if one takes a bulk field close to the boundary, the corresponding single-time CFT representation will still involve operators with support on the entire time-slice Σ. The reason why this is indeed a flaw will be made clear later, for now, it suffices to say that this motivates another reconstruction procedure which has a CFT representation of the bulk fields whose boundary support gets smaller as the bulk field gets closer to the boundary. This new procedure is called "AdS-Rindler" reconstruction.

[6] From now on, lowercase letters represent bulk coordinates and uppercase letters represent boundary coordinates.

[7] In fact, that is an interesting open problem for mathematicians interested in partial differential equations.

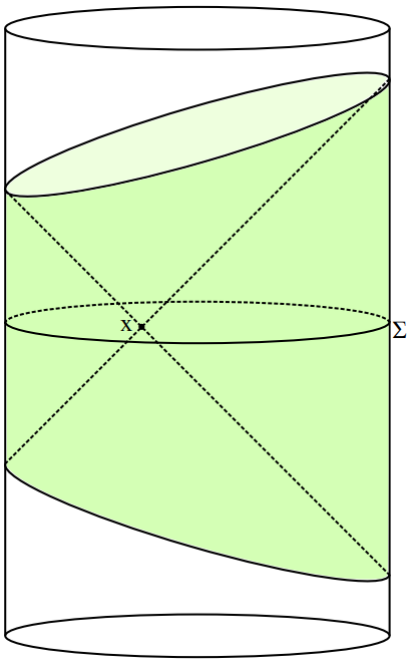

Figure 2 – Global reconstruction procedure in AdS_3. The integration is carried over the shaded green region and the CFT representation of a bulk field in x has support over the whole boundary of the time-slice Σ.
Source: ALMHEIRI. (29)

2.6 AdS-Rindler reconstruction

In the global reconstruction picture, a bulk field $\phi(x)$ has a CFT representation which has support on an entire boundary time-slice Σ. In this section, we explore the AdS-Rindler reconstruction procedure, where the spatial support of a CFT representation is restricted to some subregion A of a boundary time-slice. The AdS-Rindler is the first manifestation we encounter of the principle of *subregion duality* (70, 71), that is, a spatial subregion of the boundary CFT which has enough information to completely determine a corresponding subregion of the bulk.

The mechanism in which the reconstruction is based is the same for the global case, we construct operators in the CFT which obey the equations of motion of the bulk with the boundary conditions set by equation (2.12). The difference is that instead of integrating over the whole conformal boundary, we restrict our integration to a region $D[A]$, called the *domain of dependence of* A, which is defined as the set of points in the boundary in which if a causal curve passes through any of those points it also must intersect A. This

amounts to solving

$$\phi(x) = \int_{D[A]} \tilde{K}(x;Y)\mathcal{O}(Y)dY \tag{2.17}$$

where $\tilde{K}(x;Y)$ is a smearing function[8]. For the AdS_3 case, the procedure is illustrated in Figure 3, where the region of integration of equation (2.17), i.e. the domain of dependence $D[A]$, is shaded green.

For any boundary region A, one can consider its *bulk causal future* $\mathcal{J}^+[A]$, which is defined as the set of causally connected bulk points to a region A, analogously, one defines the *bulk causal past* $\mathcal{J}^-[A]$. By "causally connected" we mean points that can be connected to (or from) region A by bulk causal curves, which are curves whose tangent vector is null or timelike at all points. The *causal wedge* of a region A (72, 73) is defined as the intersection between the region's bulk causal future and past, that is,

$$W_C[A] := \mathcal{J}^+[A] \cap \mathcal{J}^-[A]. \tag{2.18}$$

The causal wedge of a region A is illustrated in Figure 3 as the region between $D[A]$ (the green shaded region) and the dotted lines, what determines the endpoint of the dotted lines is a surface (or a geodesic in the case of AdS_3) called the Ryu-Takayanagi surface, which we shall discuss in Chapter 4. The claim is that the construction of representations in the boundary of the bulk fields can be implemented purely within the causal wedge, that is, for any bulk field $\phi(x)$ with $x \in W_C[A]$, we obtain a representation of $\phi(x)$ in the boundary region A through equation (2.17), with the integration carried over $D[A]$ instead of the whole conformal boundary. It is now clear that the AdS-Rindler reconstruction has the property that only a small boundary region A localized close to x is needed to obtain the CFT representation of $\phi(x)$.

AdS-Rindler reconstruction satisfies the property we were looking for in a reconstruction procedure, namely that the boundary support gets smaller as the bulk field gets closer to the boundary. This property, which motivated the procedure in the first place, has a staggering feature: a given bulk field operator $\phi(x)$ lies in many different causal wedges and thus has different boundary representations according to which causal wedge one chooses. In particular, one pathological case is such that one chooses three equal causal wedges in a way that the whole boundary is covered, however, a bulk field in the center

[8] The smearing function of the global reconstruction is, in general, different from the smearing function of the AdS-Rindler reconstruction, hence why we denote the latter using a tilde.

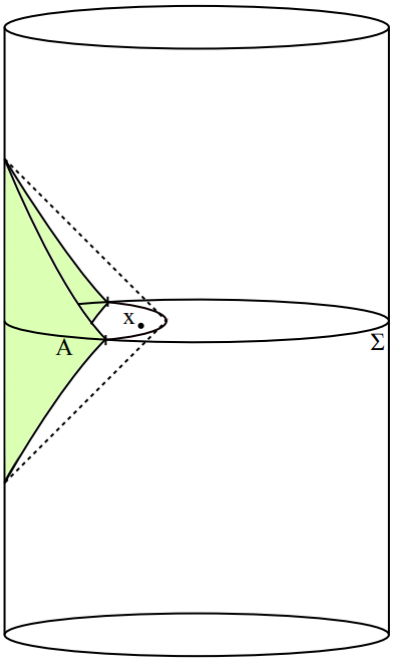

Figure 3 – AdS-Rindler reconstruction procedure in AdS_3. The integration is carried over the shaded green region, which represents the domain of dependence of region A. The causal wedge $W_C[A]$ of the region A lies between the dotted lines and $D[A]$. As the point x gets closer to the boundary, only a small region A is needed to obtain the boundary representation of a bulk field localized in x. Source: Adapted from ALMHEIRI. (29)

of the AdS space cannot be reconstructed in any of the three wedges. It is clear that if we have information about the entire boundary we should be able to obtain a boundary representation of any bulk field, according to the global and AdS-Rindler reconstruction protocols. This apparent paradox is known as the "ABC puzzle" and has an enormous impact when we reinterpret the AdS/CFT correspondence in the language of quantum error correction later on.

2.7 Two puzzles to be solved

In the previous sections, as we described the properties of AdS/CFT and the reconstruction methods, we stumbled across two features that are in apparent contradiction with the expected properties. We called the first contradictory feature the "radial commutativity puzzle" and the second one the "ABC puzzle". We will discuss them in detail and use them as motivation to reinterpret AdS/CFT in the language of quantum error correction. In advance, although those puzzles are apparently paradoxical, they present no problem in the description of AdS/CFT, they are just unexpected features that can be reinterpreted

under the light of quantum error correction.

2.7.1 The radial commutativity puzzle

Before discussing the puzzle in our setting, consider first a quantum field theory without gravity. In a usual QFT, we have causality, which means that we cannot instantaneously influence physical phenomena which is spacelike separated from where we are. Causality is enforced by locality, as physical phenomena in a QFT are always local. The statement of locality is: if we take any two operators $\mathcal{O}_1(X)$ and $\mathcal{O}_2(Y)$ in the QFT, as long as they are spacelike separated, that is, $X^2 - Y^2 > 0$, they commute, which means that $[\mathcal{O}_1(X), \mathcal{O}_2(Y)] = 0$.

We expect that this statement also holds for the bulk theory in AdS/CFT, because the bulk is well described by quantum field theory weakly coupled to semiclassical gravity, and therefore causality holds. Indeed, let us consider that this property is present in the bulk. Then, we have an operator $\phi(x)$ in the bulk and a local boundary operator $\mathcal{O}(Y)$ which are in the same time-slice Σ, this setup is illustrated in Figure 4.

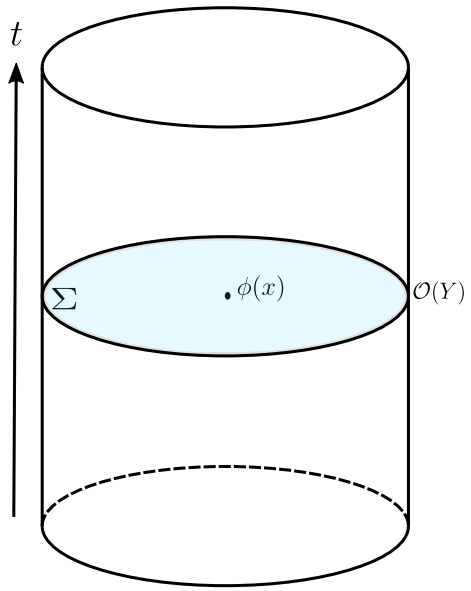

Figure 4 – Schematic representation of AdS/CFT where we have a bulk operator $\phi(x)$ and a local boundary operator $\mathcal{O}(Y)$ in the same time-slice Σ (shaded light blue). The time coordinate points upwards, for each fixed time value, we have a time-slice similar to Σ.
Source: By the author.

Given that causality holds in the bulk, the statement becomes: if a bulk operator $\phi(x)$ and a local boundary operator $\mathcal{O}(Y)$ are in the same time-slice Σ, they are spacelike

separated in the radial direction and $x^2 - Y^2 > 0$, furthermore, from causality, they must commute, which means that $[\phi(x), \mathcal{O}(Y)] = 0$. In this case, when we consider the commutation relation between $\phi(x)$ and $\mathcal{O}(Y)$, we should think of $\phi(x)$ as a highly non-local operator in the CFT, whose relation to the bulk is given by the boundary conditions (2.12) and the global/AdS-Rindler reconstruction equations (2.16, 2.17). This way, the commutation relation statement is actually a statement purely about the CFT, which says that a non-local and complicated CFT operator $\phi(x)$ commutes with a local operator $\mathcal{O}(Y)$ of the CFT.

However, the statement presented in the previous paragraph contradicts a very important feature of *any* QFT, the so-called *time-slice axiom* (74), which states, using *Schur's lemma*, that *any* operator commuting with all local operators at a fixed time must be trivial, i.e, a complex number proportional to the identity[9]. As the boundary CFT is indeed a quantum field theory, it must satisfy the time-slice axiom, and therefore the causality statement cannot be true.

There seems to be a way to guarantee that causality and the time-slice axiom are both satisfied. The solution is trivial, literally. If *every* bulk operator $\phi(x)$ is the identity, no problem in the commutation relations arises from causality, and it satisfies the time-slice axiom. The problem is physical: if that were the case, why would holography be interesting in the first place? There is a way to circumvent this issue, the actual solution of this puzzle lies in the interpretation that the structure of AdS/CFT is a quantum error-correcting code. For now, we claim that this puzzle is not a problem as is it perfectly solvable within the context of quantum error correction. (29, 30) We will explore this consideration in Chapter 4.

2.7.2 The ABC puzzle

The ABC puzzle is another apparently paradoxical feature that arose when we discussed the AdS-Rindler reconstruction. The idea is to consider a single fixed time-slice with a bulk operator $\phi(x)$ in the center and to divide the boundary into three equal regions, A, B, and C; each region has a corresponding causal wedge $W_C[A]$, $W_C[B]$, and $W_C[C]$.

[9] A more concrete way to see this is to consider a n-spin chain in a one-dimensional manifold, we may consider the set of products of Pauli operators $\{1, X, Y, Z\}^{\otimes n}$, this set form a basis of all operators in the Hilbert space of the spin chain, therefore, any operator commuting with all these products must be proportional to the identity.

We show the three regions and their respective causal wedges in Figure 5.

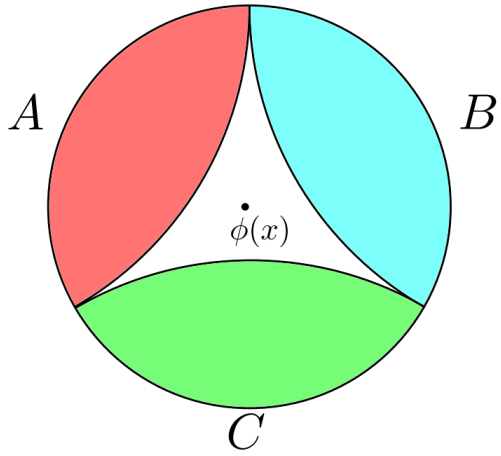

Figure 5 – Fixed time-slice where the boundary is divided in three equal regions, labelled A, B and C. Each region has its respective causal wedge. The bulk operator $\phi(x)$ in the center does not belong to any causal wedge, this is the core of the ABC puzzle.
Source: Adapted from HARLOW. (32)

The ABC puzzle arises from the fact that the bulk operator $\phi(x)$ does not lie within any of the three causal wedges from the boundary regions. As we have seen in the discussion about AdS-Rindler, a necessary condition to obtain a CFT representation of a bulk field in a given boundary region is that the bulk field must lie within the causal wedge of that boundary region. This is not the case in our setup.

This means that the bulk field $\phi(x)$ has no representation in A, B or C, however, if we take the union of any two regions, for instance, $A \cup B$, we have a situation where $A \cup B = \bar{C}$, where $\bar{C}$ denotes the complement of C, in this case, the causal wedge of $\bar{C}$ is the entire time-slice excluding the causal wedge of C, therefore $\phi(x) \in W_C[A \cup B]$ and the bulk field has a CFT representation in $A \cup B$.

The puzzling feature of this argument is that we can take the union of any two regions and the bulk field $\phi(x)$ will always be in the causal wedge of the union, this means that we could obtain three different representations in the boundary, $\phi_{A\cup B}$, $\phi_{B\cup C}$, and $\phi_{C\cup A}$ of the same bulk operator. How are we supposed to use the AdS-Rindler reconstruction to obtain a CFT representation of a bulk operator if we obtain different operators depending on what we arbitrarily call region A, B, and C? Another question one may ask concerning the same result is where is the information that characterizes the operator in the center located in the CFT?

Turns out that, just like the radial commutativity puzzle, the ABC puzzle also has a very neat solution when we rephrase those properties from AdS/CFT in terms of quantum error correction. Once again, for now, we claim that the ABC puzzle is not a problem within our description as it is perfectly solvable in quantum error correction (29, 30), as we will see in Chapter 4.

3 CORRECTING QUANTUM ERRORS AND ALL THAT

"To be an Error and to be Cast out is part of God's Design."
William Blake

In this chapter, we review the fundamentals of quantum error correction, its main properties and important examples. This chapter is intended to provide intuition and solid ground in which we will connect the ideas of quantum error correction with holography later. The theory of quantum error correction is very technical and has a large number of definitions, theorems, and important bounds. The motivation behind this chapter is twofold: in one hand, we lay down useful tools which will be applied later when we discuss connections between quantum information theory and holography. On the other hand, there is beauty to be appreciated on the formalisms themselves, in particular if one is interested in realizability of quantum technologies. It is worth mentioning that research in quantum error correction has been incredibly active as it is among the main research programs of the so-called NISQ[1] era. (33) For an excellent review on the contents of this chapter, we refer to. (34, 35, 75–77)

3.1 An error correction primer

The key word when we think about error correction is *redundancy*, one way or another, every error correction method described in this chapter will amount to redundancy. However, what exactly do we mean by redundancy?

Imagine you want to send a message to your friend through the mail, but it is an important message of your thoughts concerning whether or not Brazil will win its sixth world cup this year (2022), and you do not want the message to be lost. How can you protect the message? No matter how you look at it, the message you send cannot convey more information than the number of bits of information it has, and every single piece of information you want to send is important. Now, imagine you send more information than you intended to, if some bits of information get lost in the transmission process and you are lucky enough, the lost words may be exactly the extra ones you added. Thus, the

[1] Acronym coined by John Preskill to describe "Noisy Intermediate-Scale Quantum".

information you wanted to convey is not lost, since the damaged part was unnecessary in the first place. But how can you guarantee that errors will only affect the extra pieces? This procedure is precisely what error correction intends to do: add redundancy to the message in a way that if something goes wrong, the extra redundant information is damaged in a way that the original message can be recovered by the receiver.

Whenever we are dealing with classical information, this procedure is simpler. Let us say that our information is composed of classical bits, and we wish to send a single bit 0. Instead of simply sending it, we add redundancy in our message by sending 000 instead. An error in the transmission process may happen, say one of the bits is flipped and the received message is 100. Nonetheless, the receiver will still understand that the original message was 0 as long as there is a majority vote previously combined. Had we not included this redundancy, the received message could have been simply 1 and the receiver would be completely lost. This procedure is, of course, not infallible, we could be unlucky in a way that two bits were flipped and the message was corrupted regardless. We could increase the amount of redundancy to make sure that this would not happen, however, there is some cost associated with sending more and more redundancy. This intuitively describes a sort of balance between how protected the message must be and how much redundancy one is willing to insert.

When we are dealing with quantum information, this procedure must be revised. The reason is that there exists a no-go theorem known as the *no cloning theorem* which states that one cannot create independent and identical copies of a given quantum state. This way, our strategy no longer works and we must think of something else. The idea is to still use redundancy but to encode information that we wish to protect into a subspace that carries larger amounts of information, in a way that if some error occurs, it only affects information outside the protected subspace. The encoding procedure is done through clever use of quantum properties, such as entanglement and coherence.

To motivate and give intuition behind the mechanism in which this encoding procedure and how redundancy works for quantum information, we briefly talk about Shor's code. Later on, we will see that there exist general formalisms in which quantum error correction is rigorously defined with a large degree of generality.

3.1.1 A motivating example: Shor's code

Imagine Luíza wishes to send Vitor[2] a message that consists of a single qubit and she wants to protect the message. In Shor's code (36), the idea is to encode the localized information of this single qubit in a non-local way on nine qubits, this way, if some error occurs in the transmission of the message, the receiver has enough information to detect and correct the error. In practice, we define a subspace, called the *code subspace* or *logical subspace*[3], and write its basis elements as a combination of the nine qubits as follows:

$$|0\rangle \to |\tilde{0}\rangle = (|000\rangle + |111\rangle)(|000\rangle + |111\rangle)(|000\rangle + |111\rangle),$$
$$|1\rangle \to |\tilde{1}\rangle = (|000\rangle - |111\rangle)(|000\rangle - |111\rangle)(|000\rangle - |111\rangle).$$

Instead of sending a single qubit, Luíza sends nine qubits and once Vitor gets the message, depending on which combination was sent, he knows whether she sent a $|\tilde{0}\rangle$, and thus the original message was $|0\rangle$, or $|\tilde{1}\rangle$ and therefore the original message was $|1\rangle$. This procedure loosely defines a *code*.

How does this code detect and correct errors? The idea is to exploit the fact that the valid codewords all have the same terms in each block of three qubits as well as the same sign between each block. To detect an error, it suffices to compare the signs between the three blocks and if the qubits that belong to the same block are in the same combination of states. For instance, let us imagine that Luíza sent a message and Vitor got the following information:

$$|\psi\rangle = (|100\rangle + |011\rangle)(|000\rangle + |111\rangle)(|000\rangle + |111\rangle),$$

whenever he makes a comparison between the states on the first block, he will detect that a qubit was "flipped". This procedure is performed through measurements of the *syndrome*. Heuristically, Vitor starts by comparing the first to the second, they are different, and since this is not true for a valid codeword, he already knows an error occurred in either the first or the second qubit. To certify where the error occurred, he compares the first with the third; if they are different, it means that the error is in the first one, if they are equal, the error must be on the second qubit. Another possibility would be that an error

[2] The vast majority of quantum information theorists would call them Alice and Bob. As an act of rebellion, we have decided to change the names in honor of two names which are important for the author.

[3] Elements that belong to a code subspace are called *codewords* or *logical elements*.

introduces some (-1) phase between the blocks of qubits, resulting in

$$|\tilde{0}\rangle \to (|000\rangle - |111\rangle)(|000\rangle + |111\rangle)(|000\rangle + |111\rangle),$$
$$|\tilde{1}\rangle \to (|000\rangle + |111\rangle)(|000\rangle - |111\rangle)(|000\rangle - |111\rangle).$$

The approach to detect such error is also to make comparisons between blocks[4], as the valid codewords all have the same sign. Vitor compares the sign of the first with the second, and then with the third. This way, he detects in which block the phase error occurred. Another possibility is to consider what would happen if both errors occurred simultaneously. As they are independent, the algorithm to detect and correct would be simply comparing the qubits within the blocks, and comparing the signs between blocks, that is, a superposition of the previous two detection methods.

The application of the superposition principle is fundamental and can be further generalized in our context. As we have seen, from simple errors such as "flipping" a qubit or introducing a phase, there could be more complex errors which are a combination of those simpler ones. The error detection and correction procedures follow the same pattern, once we break down complicated errors into simpler ones, correcting those is enough to recover the original message. In particular, the action of "flipping" a qubit is precisely what happens if we acted with a σ_x in our basis element, introducing this phase amounts to the action of σ_z, and so on. If we can define a basis for errors, every possible error that could happen in our code is a mere combination of basis elements, once we figure out how our code detects and corrects[5] each error from the basis, our code becomes robust against any kind of error.

A convenient basis for the errors in Shor's code are Pauli matrices plus the identity, that is, every error is a combination of the elements $\{\sigma_x, \sigma_y, \sigma_z, \mathbf{1}\}$. The most general element of the code subspace can be written as

$$|\tilde{\Psi}\rangle = \alpha|\tilde{0}\rangle + \beta|\tilde{1}\rangle \tag{3.1}$$

[4] As a rule of thumb, whenever we are interested in detecting errors, we always should look for comparative measurements, such as whether or not the signs are the same, or whether or not the qubits are in the same superposition. Note that what we measure directly is the syndrome, as it is a (degenerate) observable that gives us partial information. We do not measure the code itself directly, because the superposition structure would be destroyed.

[5] The "correction" part of this error-correcting code is simple as long as each error is a Pauli matrix. As each Pauli matrix square is the identity, once the error is detected, it suffices to apply the same Pauli matrix at the pertinent qubit.

where $\alpha, \beta \in \mathbb{R}$, this codeword is robust against the most general error possible

$$|\tilde{\Psi}\rangle \to a\sigma_{xi}|\tilde{\Psi}\rangle + b\sigma_{yj}|\tilde{\Psi}\rangle + c\sigma_{zk}|\tilde{\Psi}\rangle + d|\tilde{\Psi}\rangle. \tag{3.2}$$

where $a, b, c, d \in \mathbb{R}$ and the second index in each sigma matrix denotes which qubit the error is acting upon, e.g. σ_{xi} is a σ_x acting on the i-th qubit (i runs from 1 to 9).

3.1.2 A note on conventions and generalities

In this subsection, we establish notation conventions and general properties of the types of systems we will be dealing with.

We will always consider finite dimensional Hilbert spaces denoting them by $\mathcal{H}$. The set of linear bounded operators on $\mathcal{H}$ is denoted by $\mathcal{L}(\mathcal{H})$, and we denote general operators using uppercase latin letters, such as $X, Y, ... \in \mathcal{L}(\mathcal{H})$. The set of density operators on $\mathcal{H}$ is denoted by $\mathcal{L}_1(\mathcal{H})$, and we use lowercase greek letters to denote density operators, such as $\rho, \sigma, \tau, ... \in \mathcal{L}_1(\mathcal{H})$. As a reminder, a density operator is Hermitian ($\rho = \rho^\dagger$), has trace equals unity ($\mathrm{tr}\rho = 1$) and is positive semi-definite ($\rho \geq 0$). The last condition may also be cast as its eigenvalues are always non-negative, i.e. are such that $\mathrm{tr}\rho^2 = \sum_k \lambda_k^2 \leq 1$, the inequality saturates for pure states, as they can be written in the form $\rho = |\psi\rangle\langle\psi|$ and thus have only one eigenvalue which is equal to unity. The quantity $\mathrm{tr}\rho^2$ is called the purity, as it characterizes whether or not the corresponding quantum state is pure or has statistical mixture. In particular, for d-dimensional Hilbert spaces (d is finite, which is our case) the purity also has a lower bound given by $1/d$, which is saturated for the maximally mixed state $\rho = \mathbf{1}_d/d$.

As we sketched, the overall idea of quantum error correction is to protect information contained in the code subspace or the logical subspace, which we will denote as $\mathcal{H}_{code}$ or $\mathcal{H}_L$, depending on the context. Elements which belong to $\mathcal{H}_{code}$ are known as *codewords* or *logical elements* and a basis for $\mathcal{H}_{code}$ is called a *code basis* or *logical basis*.

A code that is used to encode k qubits in n qubits will have a total of 2^k codewords that define a basis which corresponds to the basis of the original states. This result is valid for a general case, had we considered a qudit code, we would have d^k instead. Any logical element may be written as a linear combination of elements of the logical basis. The *distance* between two codewords is defined as the number of places in which they differ. For example, the distance between codewords $(1, 1, 0, 0)$ and $(0, 1, 0, 1)$ is 2. The

distance of a code is defined as the mininum distance between any two codewords. Another way to measure the distance of the code is to consider $d = 2t + 1$, where t denotes the number of errors that the code can correct.

In general, we need to address only the elements that compose an error basis. It is convenient to consider Pauli matrices as an error basis for a large number of codes. The *weight* of an operator which is a tensor product of Pauli matrices is the number of qubits (or qudits) in which it differs from identity, e.g. an error of the form $\sigma_x \otimes \mathbf{1} \otimes \mathbf{1}$ which acts on three qubits has weight one since it differs from the identity in one element. The set of all operators whose structure is a tensor product of Pauli matrices (with a possible overall factor of -1 and $\pm i$) constitutes a group G under multiplication. This group plays a key role in Stabilizer quantum error correction, as we shall see.

In the previous subsection, we briefly stated that error detection methods can be done only through comparative measurements, which is accomplished by the *syndrome*. The idea is to perform a measurement that does not disturb the information in the encoded state, but rather retrieves information about the error. The syndrome measurement is projective, which means that it projects the error in a error basis (combination of Pauli matrices and the identity) which then allows the correction by employing the corresponding Pauli operators on the damaged qubits. This measurement provides information about which error happened but does not provide information about the encoded qubit itself, hence preserving the superposition structure.

In some error-correcting codes, it is required to have a more robust formalism. We will be frequently dealing with three quantum channels, which are completely positive and trace-preserving (CPTP) maps. The first quantum channel is the *encoding* channel, denoted by $\mathcal{E}$, which models the encoding of information in the quantum error-correcting code, sometimes, this channel is loosely called "code". CPTP maps admit a sum representation, in the Schrödinger picture, given by

$$\mathcal{E}(\rho) = \sum_a K_a \rho K_a^\dagger \tag{3.3}$$

where K_a are called Kraus operators. Those Kraus operators are typically called operation elements in the context of error correction. In the Heisenberg picture, the corresponding map is the Hilbert-Schmidt dual $\mathcal{E}^\dagger$, which has sum representation given by

$$\mathcal{E}^\dagger(\rho) = \sum_a K_a^\dagger \rho K_a. \tag{3.4}$$

The second quantum channel often considered is the *noise* channel, denoted by $\mathcal{N}$, which models the action of noise in the information. Given that noise channels are CPTP maps, they also possess a sum representation like equations (3.3, 3.4), with Kraus operators denoted by N_a. The third quantum channel that plays a key role in error correction is called the *recovery* channel, which models the recovery process from the physical to the logical subspace. Just as before, the recovery map is also a CPTP map that admits sum decomposition, with Kraus operators denoted by R_a. For convenience, we will sometimes denote the CPTP maps and their sum decompositions from equations (3.3) and (3.4) as $\mathcal{E}(\rho) \sim \{E_a\}$ and $\mathcal{E}^\dagger(\rho) \sim \{E_a^\dagger\}$, respectively. It is also worth mentioning that sometimes we consider the encoding channel and the noise channel to be a single quantum channel, i.e., we consider a "redefinintion" given by $\mathcal{E} := \mathcal{N} \circ \mathcal{E}$.

Another concept which will be used throughout this chapter is of an *unital* map, which means that

$$\mathcal{E}^\dagger(\mathbf{1}) = \mathbf{1}. \tag{3.5}$$

In Heisenberg's representation, the condition of an unital map is equivalent to the condition of trace-preserving. Unless said otherwise, the quantum channels $\mathcal{E}$, $\mathcal{N}$, and $\mathcal{R}$ are taken to be unital.

We will often consider that the Hilbert space $\mathcal{H}$ has a decomposition structure given by $\mathcal{H} = (A \otimes B) \oplus C$, and we will say that a quantum system $A \subset \mathcal{H}$ is a subsystem of $\mathcal{H}$ that plays a role in its decomposition structure. In a few circumstances, we will also consider the systems A and B to have their own decomposition structure, which means that the Hilbert space has an even more general decomposition as $\mathcal{H} = \bigoplus_k (A_k \otimes B_k) \oplus C$. Such decomposition arises when we treat operator algebras, therefore, it is pertinent to precisely define the concept of an *algebra*.

Definition 3.1 (Algebra)**.** Let $\mathbb{F}$ be a field (such as $\mathbb{R}, \mathbb{C}, ...$) and $\mathcal{A}$ be a vector space equipped with a closed binary operation (denoted by $\cdot$). We say $\mathcal{A}$ is an algebra over $\mathbb{F}$ if, $\forall\ X, Y, Z \in \mathcal{A}$ and $\forall\ \alpha, \beta \in \mathbb{F}$, the following conditions are true:

$$(X + Y) \cdot Z = X \cdot Z + Y \cdot Z$$
$$Z \cdot (X + Y) = Z \cdot X + Z \cdot Y$$
$$(\alpha X) \cdot (\beta Y) = \alpha\beta(X \cdot Y).$$

An algebra is *commutative* or *Abelian* if, $\forall\ X, Y \in \mathcal{A},\ X \cdot Y = Y \cdot X$. If the algebra is not commutative, it is called *non-commutative* or *non-Abelian*.

For our intentions and purposes, we will consider the elements X, Y, Z of an algebra to be operators and we will be talking about an algebra of operators, and we will denote it by $\mathcal{A}$. To be precise, as our Hilbert space $\mathcal{H}$ is finite dimensional and our algebra will be closed under Hermitian conjugation, we will be dealing with C^*-algebras or von Neumann algebras, however, we will refer to them simply as algebras.

3.2 Standard Quantum Error Correction

The standard model of quantum error correction (QEC) is a quantum error-correcting code formalism developed in (38, 39, 78) which consists of a CPTP noise map $\mathcal{E}$, a CPTP recovery map $\mathcal{R}$ and a code subspace $\mathcal{H}_{code}$, with $\mathcal{E}$, $\mathcal{R} \in \mathcal{L}(\mathcal{H})$ and $\mathcal{H}_{code} \subset \mathcal{H}$. We say that a code subspace is *correctable* with respect to $\mathcal{E}$ if

$$(\mathcal{R} \circ \mathcal{E})\rho = \rho, \qquad \forall\ \rho = P_C \rho P_C \in \mathcal{H}_{code}, \tag{3.6}$$

where P_C denotes the code projector, i.e., the projector of $\mathcal{H}$ into $\mathcal{H}_{code}$.

The CPTP maps have a sum decomposition which plays an important role in standard QEC, there is one subtlety involved in the representation, namely, that it is non-unique. For instance, consider the Schrödinger sum representation of the noise:

$$\mathcal{E}(\rho) = \sum_a E_a \rho E_a^\dagger$$

there is another decomposition which expresses the same exact noise operator, e.g., $\mathcal{E}(\rho) = \sum_b F_b \rho F_b^\dagger$. The catch is, if a noise map indeed has different representations, then they are related through scalars u_{ab} which satisfy $F_b = \sum_{ab} u_{ba} E_a$.

Now let us explore how this formalism allows us to identify and correct errors. The first step is to consider the conditions in which we could guarantee that we have a recovery map $\mathcal{R}$ that we can act on our system after an error $\mathcal{E}$ occurred. In other words, we want to know which conditions are sufficient and enough for equation (3.6).

Consider two operation elements E_a and E_b acting on different codewords $|\psi_i\rangle$ and $|\psi_j\rangle$. We must be able to distinguish between those errors acting on two different codewords, otherwise, we cannot correct them. The only way to guarantee distinguishability is if

$E_a|\psi_i\rangle$ and $E_b|\psi_j\rangle$ are orthogonal, this already gives us a hint:

$$\langle\psi_i|E_a^\dagger E_b|\psi_j\rangle = 0, \qquad \forall\ |\psi_i\rangle, |\psi_j\rangle \in \mathcal{H}_{code},\ \forall\ a, b;\ i \neq j. \tag{3.7}$$

Nevertheless, this condition is not sufficient. Whenever we make a measurement to discover the error, it must have a comparative nature and we must not learn anything about the state itself, if we did, we would break the superposition and the entanglement structure of the code. As a consequence, to learn about the error and the operation elements, we should obtain a quantity that must be independent of the codeword choice. The clear candidate is

$$\langle\psi_i|E_a^\dagger E_b|\psi_i\rangle = \langle\psi_j|E_a^\dagger E_b|\psi_j\rangle = \langle\psi_k|E_a^\dagger E_b|\psi_k\rangle = ...\ \ \forall\ |\psi_\ell\rangle \in \mathcal{H}_{code} \tag{3.8}$$

By combining the orthogonality and the codeword invariance conditions we do indeed obtain a condition that is both sufficient and necessary. The only way to simultaneously satisfy equations (3.7) and (3.8) is through:

$$\langle\psi_i|E_a^\dagger E_b|\psi_j\rangle = \lambda_{ab}\delta_{ij}, \qquad \forall\ a, b, \tag{3.9}$$

or in terms of the projection operators onto the code subspace

$$P_C E_a^\dagger E_b P_C = \lambda_{ab} P_C \qquad \forall\ a, b, \tag{3.10}$$

where λ_{ab} is a Hermitian matrix with complex entries. The conditions (3.10) are called the Laflamme-Knill conditions. Note that they are independent of the operator sum representation of $\mathcal{E}$.

Overall, a code has a CPTP recovery map $\mathcal{R}$ that corrects the code subspace from the noise map $\mathcal{E}$ if and only if the Laflamme-Knill conditions (3.10) are satisfied.

3.3 Noiseless subsystems

Apart from the standard model of quantum error correction, there is another important classes of codes, namely, noiseless subsystem codes. (79–84) The way this class of models work is somewhat different from the standard model, as the aim is to explore the underlying algebraic structure.

The model consists of a CPTP operation $\mathcal{E} \sim \{E_a\}$ on $\mathcal{H}$, and an algebra $\mathcal{A}$ generated by those operation elements. As a finite dimensional C^*-algebra, $\mathcal{A}$ admits an

unique decomposition, up to unitary equivalence, as

$$\mathcal{A} \simeq \bigoplus_J \mathcal{M}_{m_J} \otimes \mathbf{1}_{n_J} \tag{3.11}$$

where $\mathcal{M}_{m_J}$ represents the full $(m_J \times m_J)$-matrix algebra and $\mathbf{1}_{n_J}$ is the n_J-dimensional identity. The algebraic structure induces a natural decomposition of the Hilbert space

$$\mathcal{H} = \bigoplus_J A_J \otimes B_J \tag{3.12}$$

where A_J represents the "noisy subsystems" with $\dim(A_J) = m_J$ and B_J represents the "noiseless subsystems" with $\dim(B_J) = n_J$.

The *noise commutant* (denoted by $\mathcal{A}'$) of an algebra $\mathcal{A}$ is defined as the subset of elements such that

$$\mathcal{A}' = \left\{\rho \in \mathcal{L}_1(\mathcal{H}) :\ E\rho = \rho E,\ \forall\ E \in \{E_a, E_a^\dagger\}\right\}, \tag{3.13}$$

whenever $\mathcal{E}$ is an unital map, all states encoded in $\mathcal{A}'$ are immune to errors of $\mathcal{E}$, that is, the noise commutant is equivalent to the fixed points of the map $\mathcal{E}$:

$$\mathcal{A}' = \mathrm{fix}(\mathcal{E}) = \left\{\sigma \in \mathcal{L}_1(\mathcal{H}) :\ \mathcal{E}(\sigma) = \sum_a E_a \sigma E_a^\dagger = \sigma\right\}. \tag{3.14}$$

In this sense, it would be more suitable to classify noiseless subsystem models as "quantum error prevention" rather than quantum error correction. Anyhow, the idea is to encode the information we wish to protect in the noiseless subsystem, this way, we guarantee that it will be preserved regardless of noise.

3.4 Operator Algebra Quantum Error Correction

Operator Algebra Quantum Error Correction (OAQEC) is formalism of quantum error-correcting codes developed in. (85–88) On top of allowing the construction of more general codes, this class also recovers the standard quantum error correction and the noiseless subsystem models. As we shall see in Chapter 4, it is also a natural language for holographic quantum error-correcting codes.

First, we will address a question we have been postponing: Why operator algebras? To answer this question, we will need to recover a few important concepts. In the Heisenberg picture, an operator $X \sim \{X_a\}$ evolves according to a CP unital map $\mathcal{E}^\dagger \sim \{E_a\}$. If $X_a = \mathcal{E}^\dagger(X_a),\ \forall\ a$, the statistical information regarding operator X is conserved

by the noise. On the other hand, if X defines a standard projective measurement, i.e. $X = \sum_a p_a X_a,\ X_a^2 = X_a,\ \forall\ a$, then the projectors X_a linearly span the algebra they generate, which means that the map $\mathcal{E}$ conserves an entire commutative algebra. In this sense, focusing on the correction (or prevention) of sets of operators that belong to an algebra structure is sufficient for the study of all correctable projective observables. Furthermore, it also allows for a complete characterization of those observables.

When we consider operator quantum error correction, rather than asking for the conditions of equation (3.6), we get a generalization where the procedure of having a recovery CPTP map $\mathcal{R}$ which nullifies the action of a noise $\mathcal{E}$ is necessary only on a subset of states, in other words, it suffices

$$(\mathcal{R} \circ \mathcal{E})(\rho \otimes \sigma) = \rho \otimes \tau, \quad \forall\ \rho, \sigma, \tau \in \mathcal{H}_{code} \tag{3.15}$$

this new condition is equivalent to the correction of some special types of algebras, as we shall see. In general, every algebra of observables induces the decomposition structure of the Hilbert space

$$\mathcal{H} = \bigoplus_{k=1}^{d} (A_k \otimes B_k) \oplus C. \tag{3.16}$$

Each operator $X \in \mathcal{A}$ have C in its kernel and acts irreducibly on each share A_k, while trivially acting on B_k; this means that the corresponding algebra decomposes as

$$\mathcal{A} = \bigoplus_{k=1}^{d} [\mathcal{L}(A_k) \otimes \mathbf{1}_{B_k}] \oplus 0_C \tag{3.17}$$

where $\mathcal{L}(A_k)$ is the set of all linear and bounded operators on A_k, $\mathbf{1}_{B_k}$ is the identity operator on B_k. Whenever we consider the standard QEC framework, we deal with codes whose algebra consists of a single share $\mathcal{L}(A) \otimes \mathbf{1}_B$, with $\dim(B) = 1$. Whereas the Operator QEC framework deals with subsystem codes for general subsystems A and B.

The framework of OAQEC works better with the Heisenberg picture because we do not have to deal with the representation theory of the underlying algebra[6]. Evolution is dictated through the unital CP map $\mathcal{E}^\dagger \sim \{E_a\}$, if for each value of a there exists an operator Y_a such that $X_a = \mathcal{E}^\dagger(Y_a)$, then all statistical information regarding the operator has been conserved by the noise, which means that

$$\mathrm{tr}(\rho X_a) = \mathrm{tr}[\rho \mathcal{E}^\dagger(Y_a)] = \mathrm{tr}[\mathcal{E}(\rho) Y_a]. \tag{3.18}$$

[6] It should be noted that this is a mere convenient choice, we could do exactly the same in Schrödinger picture, however, that would require careful treatment of representation theory which is beyond the scope of the present work. For a treatment on representation theory, see e.g. (89)

To correct $\mathcal{E}$, we need a CPTP recovery map $\mathcal{R}$ such that

$$\mathcal{R}^\dagger(X_a) = Y_a \tag{3.19}$$

$$(\mathcal{R} \circ \mathcal{E})^\dagger X_a = (\mathcal{E}^\dagger \circ \mathcal{R}^\dagger) X_a = X_a \tag{3.20}$$

whenever the recovery map exists, we say that the operator X_a is correctable for $\mathcal{E}$ and is *conserved* by $\mathcal{R} \circ \mathcal{E}$. If $X_a^2 = X_a$, then $\mathcal{R} \circ \mathcal{E}$ conserves the entire Abelian algebra.

We have briefly sketched the concept of conservation of operators and algebras, we wish to give it a more rigorous treatment. An observable X is conserved by $\mathcal{E}$ in $\mathcal{H}_{code}$ if

$$P_C \mathcal{E}^\dagger(X_a) P_C = P_C X_a P_C, \quad \forall\ a, \tag{3.21}$$

where P_C is the projector of $\mathcal{H}$ into $\mathcal{H}_{code}$. More generally, an algebra $\mathcal{A}$ is conserved by $\mathcal{E}$ for states in $\mathcal{H}_{code}$ if

$$P_C \mathcal{E}^\dagger(X) P_C = P_C X P_C, \quad \forall\ X \in \mathcal{A}. \tag{3.22}$$

Note that the conservation of an algebra (3.22) is a generalization of noiseless subsystems, to see that, it suffices to choose an operator $X \otimes \mathbf{1}$ and apply the criteria (87,88). This way, any subalgebra $\mathcal{A}$ of $\mathcal{L}(\mathcal{H}_{code})$ for which every operator $X \in \mathcal{A}$ satisfy the conservation criteria (3.22) is a direct sum of noiseless subsystems.

We can also consider the generalization for correctability of algebras in the context of OAQEC. We say that an algebra $\mathcal{A}$ is correctable for the noise $\mathcal{E}$ on states in $\mathcal{H}_{code}$ if there exists an recovery map $\mathcal{R}$ such that

$$P_C (\mathcal{R} \circ \mathcal{E})^\dagger(X) P_C = P_C X P_C, \quad \forall\ X \in \mathcal{A}. \tag{3.23}$$

This condition generalizes the concept of correctability of the standard QEC model, as in that case we were dealing with simple algebras whose structure was $\mathcal{L}(A) \otimes \mathbf{1}_B$. This definition of correctability is valid for any finite-dimensional algebra. In our case, the projector P_C does not necessarily belong to the algebras.

Up to this point, we have shown why it is important to take a step forward and to consider operator algebras, and how OAQEC works in practice. However, as in the standard QEC case, we need a set of conditions to guarantee the existence of the recovery map $\mathcal{R}$ given a noise $\mathcal{E}$. When we go to the operator level, the following conditions certify whether or not a given subalgebra is conserved and correctable with respect to $\mathcal{E}$.

Theorem 3.2. *A subalgebra $\mathcal{A}$ of $\mathcal{L}(\mathcal{H}_{code})$ is conserved in all states of $\mathcal{H}_{code}$ by the noise $\mathcal{E}$ if and only if*

$$[E_a P_C, X] = 0, \quad \forall E_a, \ \forall \ X \in \mathcal{A}. \tag{3.24}$$

In other words, an algebra on a code subspace is conserved when the elements of the algebra commute with the noise generators, restricted to the code subspace.

Theorem 3.3. *A subalgebra $\mathcal{A}$ of $\mathcal{L}(\mathcal{H}_{code})$ is correctable on $\mathcal{H}_{code}$ for the noise $\mathcal{E}$ if and only if*

$$[P_C E_a^\dagger E_b P_C, X] = 0, \quad \forall \ E_a, E_b \ \forall \ X \in \mathcal{A}. \tag{3.25}$$

As before, the correctability condition is built upon orthogonal errors, which enables their distinguishability, and codeword invariance. Note that the algebra elements commute with the errors in both conservation and correction criterias for $\mathcal{H}_{code}$. For a proof of those theorems, we refer to the aforementioned references where this formalism was originally developed. (85–88)

3.5 Stabilizer codes

Stabilizer codes is a remarkable class of quantum error-correcting codes, proposed in. (37) Its inherent structure allows for the realization of efficient codes and construction of complicated codes out of simpler ones. In particular, stabilizer codes have been receiving a lot of attention because they can be used for fault-tolerant quantum computing (90–93), thus having a large interest in applications on the feasibility of quantum computation and quantum technologies in the NISQ era. (33)

This new class of codes have the same principles as before, we are looking to somehow encode redundant information and adopt a protocol (consisting of recovery maps, commutation relations, and so forth) to recover and protect the information. So far, we dealt with very general conditions for error-correction and error prevention. Our exposure will be somewhat technical, and thus, we first revisit Shor's code and lay down the concepts using an example, and then we generalize. After doing so, we go back to an important example, the 5-qubit code, which has applications in holography and AdS/CFT. (29–31, 63)

3.5.1 Shor's code revisited

In Shor's code, the idea is to encode one qubit worth of information into nine qubits and send the message consisting of nine qubits instead. The way to detect and correct errors was to compare the superpositions of the qubits in the same block and to compare the different signs between different blocks, accomplished through syndrome measurements. Since the code corrects any one-qubit error, we have $t = 1$ and distance $d = 3$.

We mentioned that the single-qubit flip error was the action of a σ_x, and the relative phase changing the sign between two blocks was the action of a σ_z. Turns out that the comparison procedure (for the detection of both kinds of errors) can be expressed in terms of combinations of Pauli matrices. For instance, detecting a qubit flip error is equivalent to measuring the eigenvalues of $\sigma_{z1}\sigma_{z2}$ and $\sigma_{z1}\sigma_{z3}$. If the first two qubits are in the same state, the eigenvalue of $\sigma_{z1}\sigma_{z2}$ is $+1$, otherwise, it is -1. Similarly, one interprets the eigenvalues of $\sigma_{z1}\sigma_{z3}$. The sign comparison procedure can also be cast in this language. It is equivalent to measuring the eigenvalues of $\sigma_{x1}\sigma_{x2}\sigma_{x3}\sigma_{x4}\sigma_{x5}\sigma_{x6}$ and $\sigma_{x1}\sigma_{x2}\sigma_{x3}\sigma_{x7}\sigma_{x8}\sigma_{x9}$. If the signs agree, the eigenvalue is $+1$; if they don't, the eigenvalue is -1.

This way, we may construct several operators such that we can completely identify every possible error in order to correct it. For Shor's code, those operators are displayed on the table below, where it indicates how each M_i operator is composed.

M_1	σ_z	σ_z	$\mathbf{1}$	$\mathbf{1}$	$\mathbf{1}$	$\mathbf{1}$	$\mathbf{1}$	$\mathbf{1}$	$\mathbf{1}$
M_2	σ_z	$\mathbf{1}$	σ_z	$\mathbf{1}$	$\mathbf{1}$	$\mathbf{1}$	$\mathbf{1}$	$\mathbf{1}$	$\mathbf{1}$
M_3	$\mathbf{1}$	$\mathbf{1}$	$\mathbf{1}$	σ_z	σ_z	$\mathbf{1}$	$\mathbf{1}$	$\mathbf{1}$	$\mathbf{1}$
M_4	$\mathbf{1}$	$\mathbf{1}$	$\mathbf{1}$	σ_z	$\mathbf{1}$	σ_z	$\mathbf{1}$	$\mathbf{1}$	$\mathbf{1}$
M_5	$\mathbf{1}$	$\mathbf{1}$	$\mathbf{1}$	$\mathbf{1}$	$\mathbf{1}$	$\mathbf{1}$	σ_z	σ_z	$\mathbf{1}$
M_6	$\mathbf{1}$	$\mathbf{1}$	$\mathbf{1}$	$\mathbf{1}$	$\mathbf{1}$	$\mathbf{1}$	σ_z	$\mathbf{1}$	σ_z
M_7	σ_x	σ_x	σ_x	σ_x	σ_x	σ_x	$\mathbf{1}$	$\mathbf{1}$	$\mathbf{1}$
M_8	σ_x	σ_x	σ_x	$\mathbf{1}$	$\mathbf{1}$	$\mathbf{1}$	σ_x	σ_x	σ_x

For instance,

$$M_1 = \sigma_z \otimes \sigma_z \otimes \mathbf{1} \otimes \mathbf{1} \otimes \mathbf{1} \otimes \mathbf{1} \otimes \mathbf{1} \otimes \mathbf{1} \otimes \mathbf{1}.$$

The two basis codewords in Shor's code $|\tilde{0}\rangle$ and $|\tilde{1}\rangle$ are eigenvectors of all eight M_i operators with eigenvalue $+1$. In this sense, any operator which leaves the codewords invariant can

be written as a combination of those eight operators. The set of operators that fix the codewords $|\tilde{0}\rangle$ and $|\tilde{1}\rangle$ have a group structure which is called the *stabilizer group* S of the code, or the stabilizer of the code, for short. The M_i operators are generators of the stabilizer S. In other words, the operators M_i leave the code subspace invariant.

The generators of S have a special property: to detect errors in a stabilizer code, it is enough to measure the eigenvalues of the stabilizer generators, if every single one of them yields $+1$, that means no error occurred. If one yields -1, we are capable of pointing out which error occurred. For instance, let us imagine we measure M_1, as it anti-commutes with σ_{x1} and σ_{x2}, if one of those two errors occurred, by the resulting eigenvalue we would be able to tell; whereas if let us say σ_{x7} occurred, we could not tell, since σ_{x7} commutes with M_1. We would need another stabilizer generator to detect this error. Generally, if we consider an arbitrary error E and a stabilizer generator $M_i \in S$, the stabilizer element can detect the error as long as they anti-commute. Once the error is detected, we apply the pertinent Pauli matrices (each Pauli matrix squared is the identity) and recover the message, thus correcting the error.

3.5.2 Going back to general stabilizer codes

A stabilizer code is characterized by its stabilizer S, which is an Abelian subgroup of G[7], and the code subspace $\mathcal{H}_{code}$ which is fixed by S. The group G has some useful properties which S inherits:

- σ_x, σ_y and σ_z are unitary, thus every element of G and S is unitary;
- σ_x, σ_y, σ_z are Hermitian, which means that if $A \in G$, then $A^\dagger \in G$;
- σ_x, σ_y and σ_z commute while acting in the same qubit and anti-commute while acting in different qubits. This means that every element in G and S either commutes or anti-commutes.

As S is Abelian, $\{-1, \pm i\} \notin S$. The code subspace is invariant under the action of any $M \in S$ and has dimension 2^k. In other words, if $M \in S$, $|\psi_i\rangle \in \mathcal{H}_{code}$ and $\{M, E\} = 0$, then the action of the stabilizer element after an error E occured is $ME|\psi_i\rangle = -EM|\psi_i\rangle =$

[7] Recall that G is the group of operators whose structure is a tensor product of Pauli matrices under multiplication.

$-E|\psi_i\rangle$. This allows us to conclude:

$$\langle\psi_i|E|\psi_j\rangle = \langle\psi_i|ME|\psi_j\rangle = -\langle\psi_i|E|\psi_j\rangle = 0, \tag{3.26}$$

thus the code satisfies the condition (3.7) whenever we take $E = E_a^\dagger E_b$. This means that stabilizer codes satisfy the condition we required that errors must be orthogonal to guarantee they are distinguishable. In order to recover Laflamme-Knill conditions (3.10) for stabilizer codes, it remains to show codeword invariance, which means that the errors can be corrected regardless of the codeword choice. However, as long as the anti-commutation is satisfied, $\{M, E\} = 0$, the condition (3.26) is indeed independent of the codeword choice, since $\langle\psi_i|E|\psi_i\rangle = \langle\psi_j|E|\psi_j\rangle$. Furthermore, as we have seen, to accomodate both conditions, it suffices to consider

$$\langle\psi_i|E_a^\dagger E_b|\psi_j\rangle = \lambda_{ab}\delta_{ij}, \tag{3.27}$$

which are the Laflamme-Knill conditions. (39) As long as $E_a^\dagger E_b$, $\forall\ E_a, E_b$, anti-commutes with some element of S, the Laflamme-Knill conditions are satisfied and the code can correct for the set of errors.

There are some subtleties associated with the elements of S. It is an Abelian subgroup, which means that every element of S commutes with each other. As it is a group, the identity must be in S, and it also commutes with everything. Note, however, that the identity is incorporated in the error basis and thus is an error itself. How can we make sense of that?

There are no problems with having an error that belongs to the stabilizer group, this motivates two new definitions. The *centralizer* of S, denoted $C(S)$, is defined as the set of all elements in G that commutes with all of S. The *normalizer* of S, denoted $N(S)$, is defined as the set of all elements in G that fix S under conjugation, in other words

$$A^\dagger M A = \pm A^\dagger A M = \pm M, \quad \forall\ A \in G, M \in S. \tag{3.28}$$

In our case, the centralizer and the normalizer of S are the same, this is a consequence of the structure and properties of G and S. Since $-1 \notin S$, every element $A \in N(S)$ also commutes with every element in S, and thus $A \in C(S)$.

If $E \in [N(S) - S]$, then the error E rearranges elements in the code subspace $\mathcal{H}_{code}$ in a closed fashion, which means that the error acting on a codeword is still a codeword.

Consider $M \in S$ and $|\psi\rangle \in \mathcal{H}_{code}$, then

$$ME|\psi\rangle = EM|\psi\rangle = E|\psi\rangle \tag{3.29}$$

which means that $E|\psi\rangle \in \mathcal{H}_{code}$. However, note that because $E \notin S$, there is some state in the code subspace which is not fixed by E.

By taking into consideration those subtleties associated with the normalizer and the centralizer of the code, and by addressing the question of elements that are errors and belong to S, we can state a more precise notion. A quantum code with stabilizer S will detect all errors E that are either in S or anti-commute with some element of S. More precisely, the error can be detected as long as $E \in S \cup [G - N(S)]$.

The distance d of a code is a synonym to how many qubits can be protected by the code. In stabilizer codes, however, there is a convenient way to cast this concept as an upper bound: the code has distance d if and only if the set $[N(S) - S]$ contains no elements whose weight is less than d.

3.5.3 The 5-qubit code

In the study of stabilizer quantum error-correcting codes, the 5-qubit code is one of the fundamental cornerstones. It has many useful properties, the most notable one is the fact that this is the smallest code that corrects a single qubit error. (94) This code is also cyclic, which means that the stabilizer and the codewords are invariant under cyclic permutations of the qubits. On top of that, it also has a holographic interpretation with profound applications in AdS/CFT and quantum gravity.

The 5-qubit code encodes one qubit into five qubits. As we have seen, the fundamental concept to characterize stabilizer codes is the elements that generate the stabilizer group. For this code, those are shown in the table below.

M_1	σ_x	σ_z	σ_z	σ_x	$\mathbf{1}$
M_2	$\mathbf{1}$	σ_x	σ_z	σ_z	σ_x
M_3	σ_x	$\mathbf{1}$	σ_x	σ_z	σ_z
M_4	σ_z	σ_x	$\mathbf{1}$	σ_x	σ_z

The code subspace of the encoded qubit has a basis that consists of two codewords, $|\tilde{0}\rangle$ and $|\tilde{1}\rangle$. The logical basis elements can be generated, up to normalization, from the

five physical qubits and the stabilizer generators as follows:

$$|\tilde{0}\rangle = \sum_{M \in S} M|00000\rangle \tag{3.30}$$

where the sum goes through every possible combination of the four stabilizer generators, in this case, a total of 16. That is,

$$\begin{aligned}
|\tilde{0}\rangle &= |00000\rangle + M_1|00000\rangle + M_2|00000\rangle + M_3|00000\rangle + M_4|00000\rangle \\
&+ M_1M_2|00000\rangle + M_1M_3|00000\rangle + M_1M_4|00000\rangle + M_2M_3|00000\rangle \\
&+ M_2M_4|00000\rangle + M_3M_4|00000\rangle + M_1M_2M_3|00000\rangle + M_1M_2M_4|00000\rangle \\
&+ M_1M_3M_4|00000\rangle + M_2M_3M_4|00000\rangle + M_1M_2M_3M_4|00000\rangle,
\end{aligned}$$

by applying the combinations of Pauli operators in the qubits, we calculate explicitly obtaining

$$\begin{aligned}
|\tilde{0}\rangle &= |00000\rangle + |10010\rangle + |01001\rangle + |10100\rangle + |01010\rangle \\
&- |11011\rangle - |00110\rangle - |11000\rangle - |11101\rangle - |00011\rangle - |11110\rangle \\
&- |01111\rangle - |10001\rangle - |01100\rangle - |10111\rangle + |00101\rangle.
\end{aligned}$$

In principle, we could do the same procedure and obtain $|\tilde{1}\rangle$ as a sum over the stabilizer generators and the corresponding physical states. However, there is a much simpler way to do so. Note that for the physical qubits, the action of σ_x is precisely to flip the qubit, i.e., $|1\rangle = \sigma_x|0\rangle$. For the 5-qubit code, this property is carried over to the logical subspace, that is

$$|\tilde{1}\rangle = \sigma_x\sigma_x\sigma_x\sigma_x\sigma_x|\tilde{0}\rangle \tag{3.31}$$

where instead of a single Pauli operator, we must replace it by five, since the logical states are five-qubit states. It is important to note that this is not general, but rather a specific feature of the 5-qubit code. Explicitly,

$$\begin{aligned}
|\tilde{1}\rangle &= |11111\rangle + |01101\rangle + |10110\rangle + |01011\rangle + |10101\rangle \\
&- |00100\rangle - |11001\rangle - |00111\rangle - |00010\rangle - |11100\rangle - |00001\rangle \\
&- |10000\rangle - |01110\rangle - |10011\rangle - |01000\rangle + |11010\rangle.
\end{aligned}$$

The idea is to calculate the commutation relations of the errors E with elements of S, as long as $E \in S \cup [G - N(S)]$, this code is capable of detecting the error. Note that this

code has distance $d = 3$ given its code subspace structure. For instance, one could check that operators such as $\sigma_{y1}\sigma_{z4}\sigma_{y3}$ are in the normalizer of S but are not in S itself, i.e., are in $[N(S) - S]$. Error operators with weight higher than 3 surpasses the distance of the code and thus cannot be detected.

In a more concrete sense, let us consider an example. Say that a single-qubit error σ_x occurred in the first qubit. The first step is to calculate the commutation relations with the stabilizer generators:

$$[\sigma_x\mathbf{1111}, \sigma_x\sigma_z\sigma_z\sigma_x\mathbf{1}] = 0,$$
$$[\sigma_x\mathbf{1111}, \mathbf{1}\sigma_x\sigma_z\sigma_z\sigma_x] = 0,$$
$$[\sigma_x\mathbf{1111}, \sigma_x\mathbf{1}\sigma_x\sigma_z\sigma_z] = 0,$$
$$[\sigma_x\mathbf{1111}, \sigma_z\sigma_x\mathbf{1}\sigma_x\sigma_z] \neq 0.$$

For the error-correction procedure itself, we recognize the syndrome and apply the operation to correct the error. In our example, the error commuted with every generator except M_4, which means that the syndrome is 0001. The error-correction protocol associated with a syndrome 0001 is to apply σ_x on the first qubit. (75, 77) Since $\sigma_x^2 = \mathbf{1}$, whenever we reapply the Pauli matrix, we recover the original message.

3.6 Outlook

In this chapter, we reviewed the basics of different quantum error correction approaches. We began by motivating quantum error correction as a tool to protect quantum information, used Shor's code to illustrate the main ideas behind the error-detection and error-correction mechanisms. Albeit simple, Shor's code has several interesting properties which allow one to concrete see quantum error correction in action without having to worry too much with definitions and concepts.

After motivating, we explored standard quantum error correction, which consists of a code where one is interested in the sufficient and necessary conditions for the existence of a map that could recover the message from any errors. Following, we studied noiseless subsystems; the idea behind those codes is the use of algebraic structures of the operators in view of exploring a subsystem that is immune to errors.

We followed our discussion by exploring two of the most important quantum error-correcting code models: Operator Algebra Quantum Error Correction and Stabilizer Error

Correction. The former consists of a generalization of the previously discussed models. The idea is to go to the operator level and explore algebraic properties underlying the Hilbert space structure in a way that the code protects a subalgebra of the code's full logical algebra. We saw how those generalizations recover the previous models under the correct circumstances. Apart from being a clear generalization, and thus having more general applicability, OAQEC also provides a natural approach to codes that possess a holographic interpretation, as we will see later.

Stabilizer codes, on the other hand, work somewhat differently from OAQEC despite having the same purpose: protecting quantum information through redundancy and wise use of Hilbert space properties. The idea here is to define a group called the stabilizer group, which consists of operators whose commutation relation with the errors tell us whether or not the code is capable of detecting and correcting them. This class of codes found great success in applications, in particular, stabilizer codes have been one of the most explored topics within quantum computing research lately, in particular, they seem to be a very solid candidate to push further noisy intermediate-scale quantum computers. The fact that those codes found large success in fault-tolerant computation as well as holography reveals how versatile they are.

4 HOLOGRAPHY MEETS QUANTUM INFORMATION

"Unforeseen surprises are the rule in science, not the exception.
Remember: Stuff happens."
Leonard Susskind

In this chapter, we establish the connection between holography and quantum error correction. As we previously mentioned, it seems that AdS/CFT has some built-in redundancy in its description and thus cannot realize an isomorphism as one would like to. We will argue that, rather than a problem, this redundancy is a feature of AdS/CFT that appears whenever we understand the correspondence through the lenses of quantum error correction. Instead of paradoxes, we have rich features which can be deeply explored. We begin the chapter by presenting the groundbreaking result of Ryu and Takayanagi which relates entanglement entropy with spacetime geometry, the vast majority of ideas relating quantum information theory with holography are built upon this famous result. Following, we present the 3-qutrit and the HaPPY codes and how they can be used to solve the paradoxes and further explore the correspondence. In the end, we discuss recent work which uses error correction to point out incompatibilities between global symmetries and the AdS/CFT correspondence structure. We propose a slightly different view of the incompatibility and use it to motivate the introduction of quantum resource theories in the next chapter.

4.1 Entanglement Entropy and the legendary Ryu-Takayanagi formula

The first remarkable result which connects quantum information theory and gravity is the Ryu-Takayanagi formula (27, 28). This result states that we can calculate the entanglement entropy of the CFT on a boundary region by calculating the area of a minimal surface related to the bulk AdS theory. The physical consequences are endless, and the overall idea can be roughly thought of as entropy equals geometry.

First, let us begin by stating what we mean by entanglement entropy. Say that we have a system at zero temperature whose ground state can be described by the pure state

$|\Psi\rangle$. The corresponding density matrix $\rho \in \mathcal{L}_1(\mathcal{H})$ is

$$\rho = |\Psi\rangle\langle\Psi|. \tag{4.1}$$

Since it describes a pure state, the von Neumann entropy is zero $S = -\mathrm{tr}(\rho \log \rho) = 0$. Now, say that we divide our system into two subsystems, A and B. The corresponding Hilbert space is split into two subspaces $\mathcal{H} = \mathcal{H}_A \otimes \mathcal{H}_B$. The reduced density matrix of subsystem A is given by

$$\rho_A = \mathrm{tr}_B \rho, \tag{4.2}$$

where the partial trace is taken over the degrees of freedom of subsystem B. As such, the entanglement entropy of the subsystem A is the von Neumann entropy of the reduced density matrix,

$$S_A = -\mathrm{tr}_A(\rho_A \log \rho_A). \tag{4.3}$$

The entanglement entropy (4.3) quantifies how entangled a given wavefunction such as $|\Psi\rangle$ is. It is a legitimate entropy measure, as it satisfies subadditivity as well as strong subadditivity; for other useful properties of the entanglement entropy, see e.g. (34).

The Ryu-Takayanagi proposal goes as follows: define the entanglement entropy S_A in a CFT on a spacetime $\mathbb{R} \times S^d$ (or $\mathbb{R}^{1,d}$) for a subsystem A which has an arbitrary $(d-1)$-dimensional boundary $\partial A \in S^d$ (or $\in \mathbb{R}^d$). Then, the entanglement entropy may be evaluated as

$$S_A = \frac{\mathrm{area}(\gamma_A)}{4G_N^{(d+2)}} \tag{4.4}$$

where γ_A is the d-dimensional static minimal surface whose boundary is ∂A. γ_A belongs to the AdS_{d+2} space; $G_N^{(d+2)}$ is the $(d+2)$-dimensional Newton's constant.

The above statement is the original formulation of the Ryu-Takayanagi result, and despite its gargantuan success, it has some clear drawbacks. First of all, this result is static, as we have implicitly fixed a time t and chosen a timeslice Σ. The evolution of the system imposes that $\rho \to \rho(t)$ and thus the entanglement entropy and its evaluation through equation (4.3) must evolve with time. Furthermore, the way the Ryu-Takayanagi result is stated so far is only valid in the semiclassical limit (2.11), where we have taken N to be large, the string coupling g_S to be very small and the AdS radius ℓ to be much larger than the Planck length. Not everything is lost, however, as there has been several works addressing both drawbacks, in particular, its covariant formulation (sometimes called the HRT formula) (95), and its validity beyond the aforementioned limits. (96–100)

Nonetheless, the Ryu-Takayanagi result also plays a key role in quantum error correction. The direct relation between the result and error correction was first explored by Harlow. (32) Moreover, the Ryu-Takayanagi formula also has direct consequences on AdS-Rindler reconstruction, in particular, the Ryu-Takayanagi surface (or geodesic in the case of AdS_3) can be used to determine the causal wedge of a given boundary region. This allows us to sharpen up the construction of the causal wedge in a more applicable way.

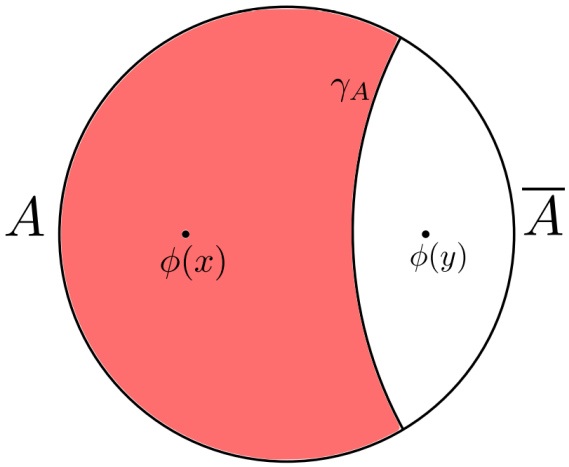

Figure 6 – AdS_3 setup where we have a boundary region A and its corresponding Ryu-Takayanagi geodesic γ_A. The region limited by the boundary region and the geodesic is precisely the causal wedge of A (shaded red). The error correction interpretation is due to the fact that a bulk operator $\phi(x)$ can be reconstructed in A regardless of the information contained in $\bar{A}$, therefore, one could erase the entire boundary region $\bar{A}$ and still be able to reconstruct $\phi(x)$. In other words, $\phi(x)$ is protected against erasures of $\bar{A}$. Conversely, $\phi(y)$ is protected against erasures of A.
Source: Adapted from HARLOW. (32)

Additionally, it also offers a clearer error correction interpretation. For example, consider the system disposed in Figure 6, the causal wedge associated with the boundary region A (shaded red in the Figure) is the region delimited by A and the Ryu-Takayanagi geodesic γ_A. The error correction interpretation arises from the fact that the bulk field $\phi(x)$ is within the causal wedge of A, and thus can be reconstructed in A. However, the bulk field $\phi(y)$ is outside the wedge and may not be reconstructed in A. In other words, the information in the causal wedge of A is protected against erasures over the boundary region $\bar{A}$, because the bulk field $\phi(x)$ can be reconstructed regardless of what information lies in $\bar{A}$. This feature is a manifestation of the subregion duality we have encountered in the AdS-Rindler reconstruction. The Ryu-Takayanagi geodesic is precisely what determines

the boundary of one wedge to the other, also note that $\gamma_A = \gamma_{\bar{A}}$.

Beyond error correction, the Ryu-Takayanagi result is the "Rosetta Stone" for several important applications and insights for quantum gravity and quantum information. Particularly, in the ER=EPR proposal of Maldacena and Susskind (101, 102), and the Black Hole Information Paradox. (103–106) Those proposals are very exciting as it not only is a paradigm shift where one takes gravity to be emergent out of quantum information, but also an incredibly active area of research.

4.2 Holographic codes that correct quantum errors

In this section we begin our discussion of quantum error-correcting codes in AdS/CFT, those ideas will permeate the rest of the Chapter and, to some extent, the rest of this work. Holographic codes are nothing but usual quantum error-correcting codes employed in a seemingly exotic context where we reinterpret some of its features. The way error correction works for holographic codes is the same as typical codes, i.e. following the procedures described in Chapter 3. Those codes can be thought of as toy models for the correspondence as well as tools to elucidate and solve the puzzles we have discussed. The literature on holographic codes has been rapidly increasing, and many new models and codes have been proposed with varying degrees of success. It is beyond the scope of this work to promote a broad discussion of all models, instead, we focus on the two most consolidated ones with the idea of discussing the recent results by Harlow and Ooguri (40, 41) that suggest that quantum gravity (and its incarnation through AdS/CFT) is incompatible with global symmetries.

4.2.1 Solving puzzles and paradoxes with the 3-qutrit code

The first code we will discuss was originally proposed in (29), the idea is to protect the information of a single qutrit by encoding it into the non-local structure of three qutrits. A qutrit is a three-level system and its basis can be identified with the states $\{|0\rangle, |1\rangle, |2\rangle\}$. In error correction terminology, we encode a logical qutrit into three physical qutrits, and the logical basis will exploit the entanglement between the physical qutrits:

$$|\psi\rangle = \sum_{k=0}^{2} c_k |k\rangle \rightarrow |\tilde{\psi}\rangle = \sum_{k=0}^{2} c_k |\tilde{k}\rangle \tag{4.5}$$

where $|k\rangle$ is a basis for the 27-dimensional Hilbert space $\mathcal{H}$ spanned by the three physical qutrits, and $|\tilde{k}\rangle$ is a basis for the 3-dimensional subspace $\mathcal{H}_{code}$ spanned by the logical

qutrit. The logical basis is explicitly given by

$$|\tilde{0}\rangle = \frac{1}{\sqrt{3}}(|000\rangle + |111\rangle + |222\rangle),$$
$$|\tilde{1}\rangle = \frac{1}{\sqrt{3}}(|012\rangle + |120\rangle + |201\rangle),$$
$$|\tilde{2}\rangle = \frac{1}{\sqrt{3}}(|021\rangle + |102\rangle + |210\rangle).$$

The code subspace is symmetric under permutation of its basis elements. Note that any logical state $|\tilde{\psi}\rangle \in \mathcal{H}_{code}$ is highly entangled, and the reduced density matrix of any of the qutrits is given by

$$(\rho)_1 = \mathrm{tr}_{23}(\tilde{\rho}) = (\rho)_2 = (\rho)_3 = \frac{1}{3}\left(|0\rangle\langle 0| + |1\rangle\langle 1| + |2\rangle\langle 2|\right),$$

that is, a maximally mixed state which means that any single qutrit has no information at all about the encoded message. The claim is any two qutrits have complete information about the encoded message, thus a single qutrit may be completely erased without damaging the encoded information.

Let us say that the third qutrit was lost in the process. There exists a unitary operation whose support is only the first and second qutrits that accomplish the following:

$$U_{12}|\tilde{k}\rangle = |k\rangle_1 \otimes |\chi\rangle_{23}, \quad |\chi\rangle_{23} = \frac{1}{\sqrt{3}}(|00\rangle + |11\rangle + |22\rangle), \tag{4.6}$$

it acts upon any basis element of the code subspace and recovers the corresponding physical basis element overwriting what was stored in the first qutrit, while the second and the third will be in a entangled state. As the encoded message is a combination of the basis elements $|\tilde{k}\rangle$, it follows

$$U_{12}|\tilde{\psi}\rangle = |\psi\rangle_1 \otimes |\chi\rangle_{23}, \quad \tilde{\rho} = U_{12}^{\dagger}(\rho_1 \otimes |\chi\rangle\langle\chi|_{23})U_{12}, \tag{4.7}$$

in words, the unitary acts in the first and second qutrits of the code and recovers the original message in the first qutrit. The remaining second and third qutrits are in the entangled state $|\chi\rangle_{23}$. This means that losing the third qutrit was not a problem at all, as the encoded information could be recovered using the unitary whose support is only the first and the second qutrits. In this model, the unitary U_{12} is simply a permutation, and its explicit form is given by

$$|00\rangle \to |00\rangle \quad |11\rangle \to |01\rangle \quad |22\rangle \to |02\rangle$$
$$|01\rangle \to |12\rangle \quad |12\rangle \to |10\rangle \quad |20\rangle \to |11\rangle$$
$$|02\rangle \to |21\rangle \quad |10\rangle \to |22\rangle \quad |21\rangle \to |20\rangle.$$

For details on the explicit calculations of the recovery procedure, see Appendix B. In this particular case, we considered that the third qutrit was lost and thus we could only work with the first and the second ones. However, given the permutation symmetry structure of $\mathcal{H}_{code}$, it is clear that we could also apply a unitary U_{13} with support on the first and third qutrits or U_{23} with support on the second and third qutrits.

On top of recovering the encoded information, it is also desirable to perform operations. Imagine we want to implement a general and linear transformation like $O|k\rangle = (O)_{jk}|j\rangle$ as a logical operator $\tilde{O}$ acting on the code subspace as

$$\tilde{O}|\tilde{k}\rangle = (O)_{jk}|\tilde{j}\rangle;$$

generally speaking, this operator is not unique and has support on all three qutrits[1], however, we can construct it in a way that we force it to operate only on the two qutrits that were not lost. Considering the case where the third qutrit was lost, we can be clever and construct the operator

$$\tilde{O} \to \tilde{O}_{12} = U_{12}^{\dagger} O U_{12}, \tag{4.8}$$

with support only on the first and second qutrits. The idea is to recover the encoded message with the unitary U_{12}, act with the desired operator O, and then encode back the message through $U_{12}^{\dagger}$. This ensures that we obtain the matrix elements $(O)_{jk}$ for the logical operator $\tilde{O}$. Note that we can also construct other operators manipulating the support depending on which qutrit was lost, that is, $\tilde{O}_{13}$ and $\tilde{O}_{23}$, and obtain the same matrix elements $(O)_{jk}$.

The operators $\tilde{O}_{12}, \tilde{O}_{13}$ and $\tilde{O}_{23}$ act distinctly in the Hilbert space of the three qutrits but act the same way in the code subspace. In other words, we have a logical operator that has three different representations as physical operators with different supports. Such situation precisely resembles the "ABC puzzle", where we had a bulk field that had three different boundary representations. Indeed, the 3-qutrit code may be thought of as a toy model for AdS/CFT because of how redundancy is explored in those two contexts. We interpret the boundary degrees of freedom as very coarse-grained in the three physical qutrits, the bulk operator is associated with the encoded logical qutrit, and the three boundary reconstructions $\phi_{A\cup B}, \phi_{B\cup C}, \phi_{C\cup A}$ are akin to the three

[1] Note that the notation $(O)_{jk}$ indicate matrix elements, rather than which qutrits are being dealt with.

implementations $\tilde{O}_{12}, \tilde{O}_{13}, \tilde{O}_{23}$ of the logical operator $\tilde{O}$. For a graphical representation, see Figure 7.

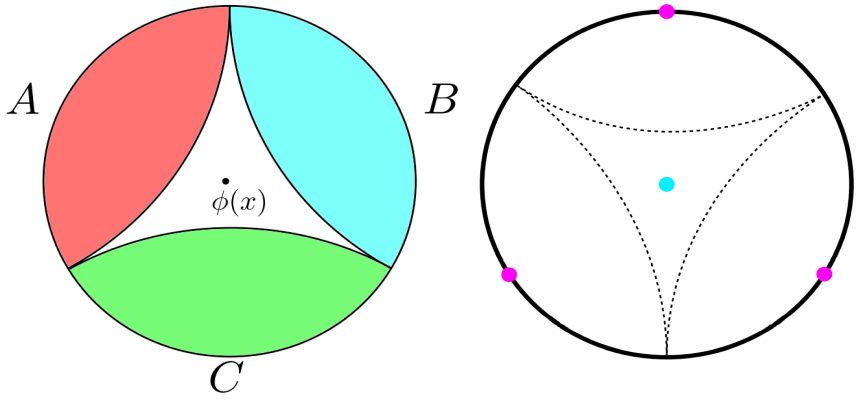

Figure 7 – The 3-qutrit code as a toy model for the AdS/CFT correspondence. The left figure is the ABC puzzle setup, where the boundary is divided into three regions and there is a bulk field in the center. The right figure is the 3-qutrit interpretation, where the magenta dots represent the physical qutrits which are interpreted as very coarse-grained CFT degrees of freedom, and the cyan dot in the middle represents the logical (encoded) qutrit and is interpreted as the bulk field operator $\phi(x)$.
Source: Adapted from HARLOW. (30)

Furthermore, the 3-qutrit code also provides insight in how information is recovered in the ABC puzzle setup. A single physical qutrit does not have enough information to restore the information of the encoded logical qutrit, just like the causal wedge of a single boundary region does not have enough information to reconstruct the bulk field $\phi(x)$. However, if we take any two qutrits, we have enough information to completely restore the information; whereas if we take the union of any two boundary regions, the bulk field will be within the corresponding causal wedge and thus can be reconstructed. In other words, from subregion duality, the 3-qutrit code protects the information against erasure of one qutrit just like the bulk field is protected against erasure of any single boundary region in the ABC puzzle setup.

So far, we have discussed the interpretation of the 3-qutrit code as a toy model for AdS/CFT, but how exactly does it solve the puzzles? In both the ABC and the radial commutativity puzzles, the answer lies on the limits we have taken whenever we discussed the global and AdS-Rindler reconstruction procedures (see equation (2.11) and its discussion). The error correction interpretation comes from the redundancy which arises when we consider a CFT region that corresponds to multiple wedges. On top of that, we

also discussed that the kinds of CFTs we would be dealing with had a semiclassical dual near the vacuum, in other words, we were working in the large N limit with small string coupling g_S and large AdS radius ℓ. When we take those three limits, we are selecting a particular region of the entire Hilbert space of quantum gravity states, choosing those that have a semiclassical dual. What happens is that by doing this selection, we are implicitly defining a subspace that works just like a code subspace.

This way, whenever we use the AdS-Rindler procedure to reconstruct a bulk operator in the boundary, we are implicitly dealing with error correction redundancies. This becomes evident when we consider the ABC puzzle setup, where a single bulk operator can have three different reconstructions. The solution of the ABC puzzle comes from the fact that we are not dealing with the entire quantum gravity Hilbert space, but rather a code subspace of it and thus it does not violate any sort of isomorphism structure. Furthermore, the reconstructions $\phi_{A\cup B}, \phi_{B\cup C}, \phi_{C\cup A}$ are different CFT operators that have the same action on the code subspace, just like the logical operator $\tilde{O}$ and its physical counterparts $\tilde{O}_{12}, \tilde{O}_{13}$, $\tilde{O}_{23}$ in the 3-qutrit code.

For the radial commutativity puzzle, the solution also resides in the fact that we thought we were considering the full quantum gravity Hilbert space, when in fact we were dealing with a code subspace of it. The "paradox" can be rephrased as

$$\langle\tilde{\psi}|[\phi(x), \mathcal{O}(Y)]|\tilde{\psi}\rangle = 0, \quad \forall\ |\tilde{\psi}\rangle \in \mathcal{H}_{code}, \tag{4.9}$$

however, now there is no contradiction with the time-slice axiom because the operator $\phi(x)$ commutes with the CFT operator $\mathcal{O}(Y)$ only within the code subspace. The 3-qutrit code can also be used to illustrate this "paradox". Consider a logical operator $\tilde{O}$ and a physical operator X_3 acting on the third qutrit. In principle, we have $\langle\tilde{\psi}|[\tilde{O}, X_3]|\tilde{\psi}\rangle = 0$, however, this commutation is identically null because we could always choose $\tilde{O} \to \tilde{O}_{12}$ and then the commutation would be between two operators that have no matching support. If we choose an operator X_1, we could employ $\tilde{O} \to \tilde{O}_{23}$ and repeat the process.

The 3-qutrit code is also a stabilizer code (see section 3.5) whose code subspace may be defined as the simultaneous eigenspace of the set of stabilizer operators. For this

particular code, the stabilizers are defined[2] as

$$M_x = X \otimes X \otimes X, \qquad M_z = Z \otimes Z \otimes Z, \tag{4.10}$$

where M_x commutes with M_z[3], which means that they can be simultaneously diagonalized. Any non-trivial Pauli operator with weight-one must fail to commute with at least one of the two stabilizers, as a consequence, no non-trivial operator with weight-one can preserve the code subspace. Nonetheless, one can construct weight-two Pauli operators that do commute with both M_x and M_z, thus preserving the code subspace, e.g.

$$X_L = X \otimes X^{-1} \otimes \mathbf{1}, \qquad Z_L = Z \otimes \mathbf{1} \otimes Z^{-1}. \tag{4.11}$$

Those operators act non-trivially and preserve the code subspace. In other words, X_L and Z_L are non-trivial logical operators of the code, furthermore, they have the same commutation relations as X and Z and thus generate the Pauli group acting upon the encoded qutrit. Those considerations are precisely the stabilizer formulation of the statement that we could create operators with different supports on the physical qutrits but that acted in the same way on the code subspace.

4.2.2 Happiness is subjective, the HaPPY code is not

The second holographic quantum error-correcting code we discuss is known as the HaPPY code (31), which bears one of the best acronyms[4] in theoretical physics, and it unfortunately does not have anything to do with the feeling of happiness[5]. This code is actually a family of stabilizer codes (see section 3.5) that consists of a tensor network structure[6] whose building block is a specific kind of tensor with maximal entanglement along any bipartition, this class of tensors is known as *perfect tensors*. The network of perfect tensors give rise to an isometry from the bulk degrees of freedom to the boundary

[2] X and Z denote a generalized version of the corresponding Pauli matrices, adapted to qutrits. The tensor product structure indicates that we operate at each qutrit.

[3] It is important to clarify that this property is valid for qutrits, but not qubits.

[4] HaPPY stands for Harlow-Preskill-Pastawski-Yoshida which are the surnames of the authors of the paper in which this code was proposed.

[5] This statement is debatable, as the original article is one of the most relevant papers in theoretical physics of the past decade, so it is safe to assume that it brought quite a bit of happiness to the authors.

[6] Tensor networks were originally developed as a tool for quantum many-body systems, however, there are several interesting applications of those structures in connections of high-energy physics and quantum information theory. It is beyond the scope of this work to give tensor networks proper treatment, hence, we refer to the reviews. (107–110)

degrees of freedom, thus establishing an isometry between two different Hilbert spaces. Following the error correction language, bulk degrees of freedom can be identified as logical degrees of freedom, likewise, boundary degrees of freedom can be identified as physical degrees of freedom. Let us begin our discussion by precisely defining the notion of a tensor.

Definition 4.1. (Tensor). Say we have two Hilbert spaces denoted by $\mathcal{H}_A$ and $\mathcal{H}_B$ with a basis $|a\rangle$ and $|b\rangle$ associated with them, respectively. A tensor is a linear map between (different) Hilbert spaces that obeys

$$T : \mathcal{H}_A \to \mathcal{H}_B; \quad |a\rangle = \sum_b |b\rangle T_{ba}. \tag{4.12}$$

A tensor is said to be *isometric* if it preserves the inner product structure. This property can be expressed as

$$\sum_b T^\dagger_{a'b} T_{ba} = \delta_{a'a}. \tag{4.13}$$

Sometimes we will refer isometric tensors simply as *isometries*. Isometric tensors have the "operator-pushing" property, that is, for any operator O and another equal norm operator O',

$$OT = TT^\dagger OT = T(T^\dagger OT) = TO', \tag{4.14}$$

this property follows from equations (4.12) and (4.13). The operator-pushing property (4.14) will be widely used in the AdS-Rindler reconstruction procedure for the HaPPY code. The aforementioned property is represented in Figure 8, borrowing from the diagramatic representation of tensor networks. We are now ready to define perfect tensors.

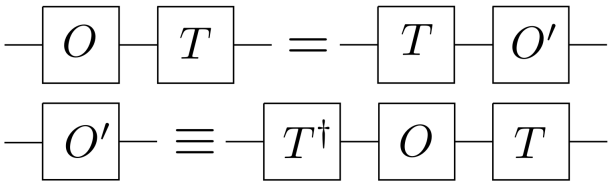

Figure 8 – Operator-pushing property of an isometric tensor T with a given operator O and another equal norm operator O'.
Source: PASTAWSKI. (31)

Definition 4.2. (Perfect tensor). A tensor with $2n$ indices denoted $T_{a_1 a_2 \ldots a_n \ldots a_{2n}}$ is said to be a perfect tensor if, for any bipartition of the indices into A and $\bar{A}$ with $|A| \leq |\bar{A}|$, the tensor T is proportional to an isometric tensor from A to $\bar{A}$.

Where $|A|$ denotes the cardinality of the set A. The bipartitions follow from the division of the $2n$ indices of the tensor in a way that $|A|+|\bar{A}| = 2n$. We can also attribute the meaning that T is a linear map from the span of indices in the subset A to the span of indices in $\bar{A}$. Furthermore, we will assume that each index a_i $(i = 0, ..., n)$ runs from $0, 1, ..., \zeta$; in this case, ζ is called the *bond dimension*. One sufficient condition to assure that T is indeed a perfect tensor is for it to be a unitary transformation when $|A| = |\bar{A}| = n$, which translates as the saturation of the inequality in the definition (4.2).

Now we explore how perfect tensors can be interpreted as error-correcting codes. Then, we address the tensor network structure and its properties under the light of the AdS/CFT correspondence. The code we discuss is an embedded version of the 5-qubit code (see subsection 3.5.3) where we consider a 6-index perfect tensor. In other words, this code consists of a 5-qubit code which encodes one logical qubit and has distance $d = 3$. The encoding tensor is given by a map

$$T : \mathcal{H}_2 \to \mathcal{H}_{32}$$

that is, the tensor is an isometry from the 2-dimensional Hilbert space of the encoded logical qubit to the 32-dimensional Hilbert space of the five physical qubits. We can write it explicitly as

$$|T\rangle = \sum_{abcdef} T_{abcdef}|abcdef\rangle, \tag{4.15}$$

and the stabilizer structure is such that

$$[M_i, M_j] = 0 \Rightarrow \quad M_i|T\rangle = |T\rangle, \tag{4.16}$$

where the stabilizers of this code are given by

M_1	σ_x	σ_z	σ_z	σ_x	$\mathbf{1}$	$\mathbf{1}$
M_2	$\mathbf{1}$	σ_x	σ_z	σ_z	σ_x	$\mathbf{1}$
M_3	σ_x	$\mathbf{1}$	σ_x	σ_z	σ_z	$\mathbf{1}$
M_4	σ_z	σ_x	$\mathbf{1}$	σ_x	σ_z	$\mathbf{1}$
M_5	σ_x	σ_x	σ_x	σ_x	σ_x	σ_x
M_6	σ_z	σ_z	σ_z	σ_z	σ_z	σ_z

the way stabilizer codes work in terms of error detection and correction is through the syndrome of the error, as we have discussed.

Given the fundamental building blocks, which are the 6-index perfect tensors (5-qubit codes), we shall describe the tensor networks consisting of those blocks, and how this network can be interpreted holographically and may be used to perform the AdS-Rindler reconstruction procedure.

The idea consists of a uniform tilling of the hyperbolic disc by attaching together pentagons which represent the 5-qubit code, this way, each pentagon has other four adjacent pentagons at each vertex. The perfect tensor with six legs is placed at each pentagon, where each side of the pentagon represents one tensor that is being contracted and each pentagon carries a free index tensor which is interpreted as the logical encoded qubit (that is, the bulk index). For a schematic representation of this setup, see Figure 9.

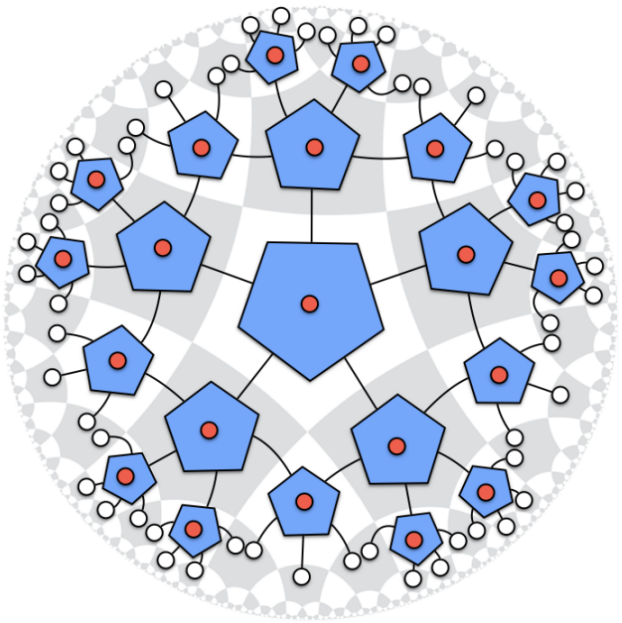

Figure 9 – Schematic representation of the HaPPY code. Each blue pentagon is interpreted as a 5-qubit quantum error-correcting code, each red dot is a free bulk (logical) index. The white dots close to the boundary represent the physical uncontracted qubits.
Source: Adapted from PASTAWSKI. (31)

The pentagon-tilling code is an isometry from the bulk to the boundary, this can be seen by noting that in a given layer (we adopt the first layer to be the central pentagon, the second layer to be the adjacent pentagons to the central one, and so forth), each tensor is contracted with a maximum of two tensors from the previous layer, as a consequence, each free index which represents the encoded qubit can be thought of as the input tensor, which means that each layer describes an isometry. Given that layers define isometries,

and that contraction of isometries is a isometry itself, the contraction of the first layer (that is, the central pentagon) with every layer until the boundary is reached is indeed an isometry.

The entire network structure can be seen as the encoding of a quantum error-correcting code. In particular, we can estimate how effective this code is when it comes to encoding logical qubits into physical qubits. Each pentagon carries one logical qubit (illustrated as the red dots inside each pentagon in Figure 9), and thus the number of logical qubits is the number of pentagons of the network. The number of physical qubits amounts to the uncontracted indices in the boundary (illustrated as the white dots in Figure 9). According to a numerical argument laid down in (31), in the large limit of layers, the ratio between logical and physical qubits converge to $1/\sqrt{5}$.

Apart from the encoding of logical qubits, the HaPPY code has two important features when it comes to holography. The first one is the fact that it satisfies a inequality which may be thought of as a discretized version of the Ryu-Takayanagi result, yielding

$$S_R \leq |\gamma_R| \log \zeta, \tag{4.17}$$

where γ_R denotes a cut throughout the network which splits it into two different (disjoint) sets of perfect tensors, $|\gamma_R|$ denotes the number of tensor legs that were cut through (which is interpreted as the "discrete length"), and R denotes a CFT boundary region, interpreted as a set of physical uncontracted legs. This cut is analogous to the "minimal area" or "minimal length" of the continous Ryu-Takayanagi result. The proof concerning this result is sketched in (31) and relies on sophisticated arguments from graph theory (111, 112) which are beyond the scope of this work. For a illustration of this result in the HaPPY code, see Figure 10.

The other important holographic feature of the HaPPY code concerns the explicit AdS-Rindler reconstruction procedure (see section 2.6). The idea consists of exploiting the perfect tensor structure and the operator-pushing property from equation (4.14), the algorithm is roughly sketched at Figure 11.

We begin by coupling the free bulk (logical) index with an operator (represented as the blue and green squares in Figure 11), and then use the operator-pushing property of equation (4.14). Given the perfect tensor structure, the tensor is a unitary map that maps any three tensor legs into the complementary set of three legs. Because of that, it

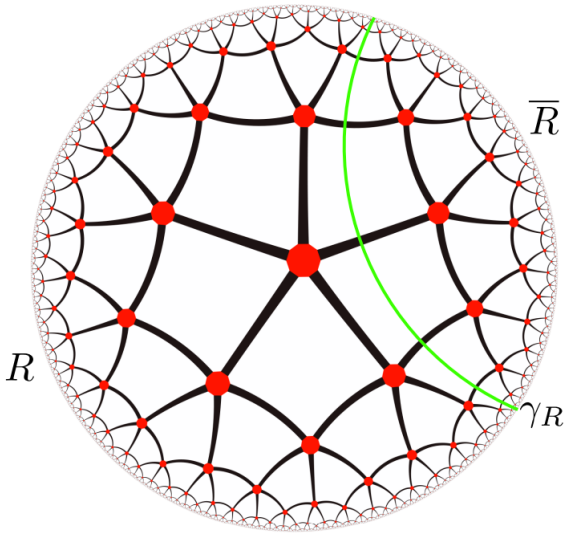

Figure 10 – The Ryu-Takayanagi geodesic γ_R depicted in the HaPPY tensor network in green; $|\gamma_R|$ is equal to the number of tensor legs it crosses. Each red dot represents a bulk logical index, each black line represents a tensor contraction of the physical qubits.
Source: Adapted from HARLOW. (30)

defines an isometry between any set of three input legs and a set of three output legs. This algorithm is carried further down the layers of the network, using the fact that a combination of isometries is also an isometry. This procedure also reproduces the "built-in redundancy" of AdS/CFT; we could implement the same bulk operator but considering a different set of three legs propagating throughout the network, as a result, we would reach a different corresponding boundary region and thus a different boundary representation. Overall, the boundary operator is obtained from the network structure together with the isometric embedding of the free bulk (indices) into the code subspace which is associated with the boundary Hilbert space. In other words, although we obtain different boundary operators depending on which set of legs we choose, every boundary operator reconstructed this way acts on the code subspace in the same way.

In terms of AdS/CFT, one often requires that only a subalgebra of operators must be protected and reconstructed. For instance, following the two operators depicted in Figure 11, say that we are interested only in the blue operator which acts upon the central free bulk index. In this case, the boundary subregion associated with the green operator could be completely erased and have all information lost, regardless, we would be able to reconstruct the blue operator in the boundary without any problems. The converse is also true, had our interest been on the green operator instead, the entire boundary region that

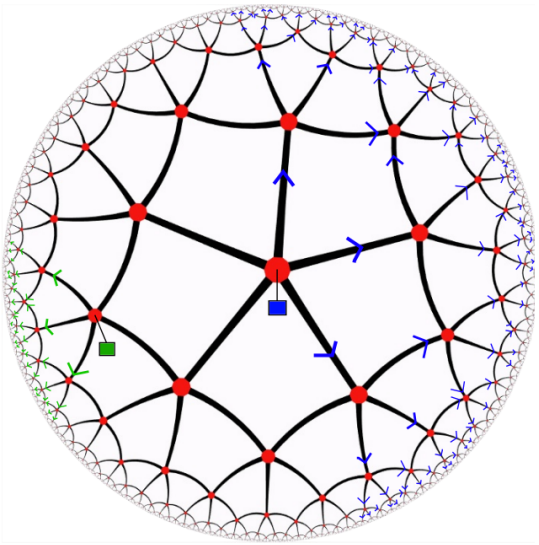

Figure 11 – Explicit reconstruction in the HaPPY code. The blue and green squares represent operators being coupled with the free bulk (logical) index. The isometric perfect tensor structure is exploited in order to carry on with the contractions.
Source: PASTAWSKI. (31)

supports the blue operator could be erased. Furthermore, there is an associated degree of protection associated with how deep one operator is within the bulk. It is clear that if a random piece of the boundary is lost, it is way more likely that the support of the green operator will completely vanish than the support of the blue one. The framework that rigorously describes the preservation of subalgebras of operators is the Operator Algebra Quantum Error Correction (see section 3.4).

4.3 Symmetries in AdS/CFT

The concept of symmetry is one of the most important concepts in physics, particularly in the context of field theories. With that said, it is no surprise that symmetries play a fundamental role in quantum gravity and the AdS/CFT correspondence. There are conjectures about symmetries in quantum gravity that have become almost folklore for theoretical physicists, in the sense that it is agreed that they are true but their proof remains elusive. One striking conjecture with deep implications is that global symmetries are incompatible with a consistent theory of quantum gravity. Recently, by using modern tools from AdS/CFT and quantum error correction, Harlow and Ooguri (40, 41) showed that indeed global symmetries cannot exist in AdS/CFT. In this section, we will reproduce their argument and propose a slightly different interpretation that, despite leading to

the same conclusion, may be rephrased in terms of quantum resource theories and thus explored in this context. First of all, we must precisely define what we mean by "global symmetry".

Definition 4.3 (Global symmetry)**.** A quantum field theory has an (internal, zero-form) global symmetry with symmetry group G if, on the manifold $\mathbb{R}^d$, the following are true:

1. There exists a homeomorphism $U(g)$ from G to the set of unitary operators on $\mathcal{H}_{\mathbb{R}^d}$;
2. $U^\dagger(g)\mathcal{A}(R)U(g) = \mathcal{A}(R),\ \forall\ R \subset \mathbb{R}^d,\ \forall\ g \in G$, where $\mathcal{A}(R)$ denotes a von Neumann algebra on the region R;
3. $\forall\ g \neq e$, there exists an operator $\mathcal{O}(x)$ such that $U^\dagger(g)\mathcal{O}(x)U(g) \neq \mathcal{O}(x)$;
4. $U^\dagger(g)T_{\mu\nu}(x)U(g) = T_{\mu\nu}(x),\ \forall\ g \in G$, where $T_{\mu\nu}(x)$ denotes the energy momentum tensor at a spacetime point $x \in \mathbb{R}^d$.

The first condition requires the existence of the homeomorphism, one could ask for a representation instead; however, representations must be continuous and therefore impose a stronger requirement. The second requires that the algebra is conserved, that is, by applying symmetry transformations we cannot increase or decrease the number of operators that belong to the algebra. The third represents the uniqueness of the group element, the homeomorphism is said to be *faithful* whenever this condition is satisfied. The last condition implies conservation of the energy content, in a slightly more general fashion than the typical criteria of commuting with the Hamiltonian. It is important to mention that gauge symmetries do not satisfy this definition of "global symmetry", there are several subtleties associated with gauge symmetries in this context which are beyond the scope of this work, one must take into consideration Wilson and 't Hooft lines, as well as so-called "operator dressings".

The next important definition to carry on the argument concerns the so-called splittability property of global symmetries. (113–115)

Definition 4.4 (Splittability)**.** A given global symmetry is said to be splittable on an arbitrary differential spatial manifold Σ if, $\forall\ R \subset \Sigma$, $\forall\ g \in G$, there exists a homeomorphism $U(g, R)$ such that

$$U^\dagger(g,R)\mathcal{O}U(g,R) = \begin{cases} U^\dagger(g,\Sigma)\mathcal{O}U(g,\Sigma),\ \mathcal{O} \in \mathcal{A}(R) \\ \mathcal{O},\ \mathcal{O} \in \mathcal{A}(\mathrm{int}(\Sigma \backslash R)) \end{cases} \tag{4.18}$$

where $\mathcal{A}$ denotes a von Neumann algebra and int($\Sigma \backslash R$) denotes the interior of the spatial manifold Σ excluding the region R. As a consequence, if we have the union of disjoint regions R_i, the symmetry operators can be written as

$$U(g, \cup_i R_i) = \prod_i U(g, R_i), \tag{4.19}$$

this manifestation of splittability is essential for the argument.

Let us say we have an algebra of operators $\mathcal{A}$ on a bulk region a_0 with a global symmetry. The bulk homeomorphism is denoted by $U_L(g)$ and the AdS/CFT structure implies that there exists a corresponding global symmetry homeomorphism $U_{CFT}(g)$ that applies the symmetry transformation over an algebra of operators in the boundary. Furthermore, the boundary CFT is indeed a quantum field theory and the definition of splittability is satisfied, hence the CFT symmetry can be written as

$$U_{CFT}(g) = \bigotimes_i W_i(g), \tag{4.20}$$

where each $W_i(g)$ operator has support over a small boundary region A_i, we denote the causal wedge of each A_i region as a_i. The setup is shown in Figure 12.

The bulk operators are symmetric under a global transformation, and according to Noether's theorem, they must be charged as the symmetry has a Noether current associated with it, given by

$$U(g, \Sigma) \sim \exp\left(i\epsilon^a \int_\Sigma \star J_a\right),$$

this implies that every bulk operator that belong to the algebra $\mathcal{A}(a_0)$ is charged, and the total charge of the global symmetry is Q. In the same way, it is expected that the global symmetry on the CFT has the same charge Q, however, given the splittability condition, this charge must be distributed over the CFT boundary regions A_i. Therefore, we should expect $Q = \sum_i Q_i$, where each Q_i is associated with a corresponding boundary region A_i.

From the AdS-Rindler reconstruction procedure, we have seen that a necessary condition for reconstruction of an operator is that it must lie within the causal wedge of the associated boundary region, e.g., bulk operators in a_1 can be reconstructed in the boundary region A_1. In our case, we may split the boundary k times in a way that not a single charged operator from the algebra $\mathcal{A}(a_0)$ is contained inside any causal wedge

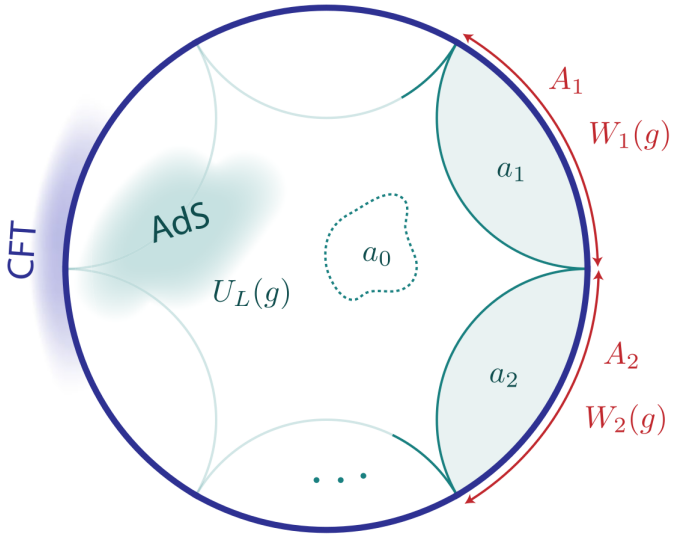

Figure 12 – Illustration of the setup regarding the incompatibility between global symmetries and AdS/CFT. The assumption is that there is an algebra $\mathcal{A}$ of charged operators on a_0, the corresponding global symmetry unitary on the CFT is splittable and can be written as a tensor product $\otimes_i W_i(g)$, where each individual $W_i(g)$ has support only on the corresponding A_i region of the boundary. Each boundary region A_i is associated with a causal wedge a_i. Given the AdS-Rindler reconstruction procedure, there are no charged operators in any causal wedge a_i $(i \neq 0)$, and thus the total charge according to the CFT side must be zero. This contradicts the fact that there exists an algebra of charged operators in the bulk. As a consequence, global symmetries cannot be compatible with the structure of the AdS/CFT correspondence. Source: FAIST. (45)

from any of the $\{A_i\}$ regions[7]. In other words, each boundary region A_i "sees" no charged operators as there are indeed no charged operators on a_i $(i \neq 0)$, and thus the individual charge Q_i of each boundary region A_i must be zero. As the global charge of the CFT symmetry is the sum of the individual charges, and each charge is zero, we conclude that the global charge is zero. This clearly contradicts the fact that there is a charged algebra of operators in the bulk, and thus, one concludes that non-trivial global symmetries cannot be consistent with the AdS/CFT structure.

This is the argument provided by Harlow and Ooguri, it relies on two important assumptions that seem quite reasonable, namely, that AdS-Rindler reconstruction works exactly and that the CFT operator is splittable. The error correction argument is present in the AdS-Rindler reconstruction. We argued that there were no charged operators on any

[7] This argument is robust in the sense that we can enlarge the bulk algebra as much as we want, as long as it remains finite, because we can always split the boundary even more, certifying that no bulk operators lie inside any causal wedge.

causal wedges, which implied that the CFT operator was not charged, in contradiction with the algebra of charged operators in the bulk. We like to think about this result in a slightly different way, motivated by the so-called Eastin-Knill Theorem (42), which we discuss next.

4.3.1 The Eastin-Knill result

This result is one of the central results of quantum error correction theory. In many aspects, it is quite unfortunate because it is a no-go result (42) which severely constrains what can be done in error correction.

Theorem 4.5. *No quantum error-correcting code can exactly correct errors, possess a continuous symmetry and implement a universal set of gates that act transversely on physical qubits.*

In other words, this result implies that we cannot build a quantum code that has the three following properties simultaneously: exact error correction, continuous symmetries and transversal gates. As such, in order to create quantum codes, we must give up on one of those requirements. There are pros and cons to each requirement, however, some are more impactful than others. In a nutshell, one does not want to give up on transversal gates, because this condition is essential for assuring that errors will not propagate throughout the computation, and this is precisely the idea behind fault tolerance. This way, it is clear that one must give up on either exact error correction or continuous symmetries. There have been several recent works (44–46, 48, 49) exploring both possibilities. In particular, we use those ideas to motivate the introduction of quantum resource theories in the next chapter, where we intend to study how the "lack of symmetry" and the "lack of exact correction" can be rephrased in this context.

Going back to the holographic argument, we interpret that "global symmetries are incompatible with AdS/CFT" is a particular realization of the Eastin-Knill theorem. In the original argument, we had splittable CFT operators and exact AdS-Rindler reconstruction which led to global symmetries being incompatible. However, we can reinterpret those quantities in contrast to what the Eastin-Knill theorem proposes. The exact correction part is analogous to the exact AdS-Rindler reconstruction, and the splittability condition for the boundary symmetry is analogous to the transversal gate implementation. As a

consequence, global symmetries are “incompatible”, just like continuous symmetries are incompatible for a quantum code if we demand exact error correction and transversal gate implementation.

The Harlow-Ooguri argument can, therefore, be seen as a version of the Eastin-Knill theorem where they were not willing to give up on both exact AdS-Rindler reconstruction (exact error correction) and splittability (transversal gates), and consequently, they were left with the option that global symmetries (continuous symmetries) were no longer possible.

It would be very interesting to study what could happen if, for instance, we had an approximate version of AdS-Rindler reconstruction, would that allow global symmetries (in some form, e.g. asymptotically)? What about a splittable CFT operator up to some factor? With those questions in mind, we motivate the introduction of quantum resource theories in Chapter 5 to study approximate error correction and asymmetry. Despite recent progress (116, 117), the regime of validity of the AdS-Rindler procedure is still unknown, let alone if approximate AdS-Rindler works.

5 USING RESOURCES TO OUR ADVANTAGE: A TESTIMONY FROM A QUANTUM INFORMATION THEORIST

"Dream Team da rima, essa união me dá alta estima
Mestre das armas do microfone à esgrima
Vê se me entende, o estudante aprende
O professor ensina."
Sabotage

In this chapter, motivated by the results about global symmetries in AdS/CFT and the Eastin-Knill theorem, we introduce the concept of quantum resource theories (QRTs) and discuss how this framework may be employed to systematically characterize approximations and asymmetry in quantum error correction. We also propose a new distance measure based on sub- and super-fidelities which can be used to bound approximations in quantum error correction. Beyond measuring distances, those bounds generate a legitimate metric, which means that they can be employed to explore the underlying geometry. We calculate our bounds for three quantum channels that commonly arise in the theory of error correction: the dephasing, depolarizing, and the amplitude damping channels.

5.1 Quantum resource theories in a nutshell

Quantum resource theories are a robust and versatile framework to study generic phenomena in quantum information theory. (43) The idea is to quantify a given desirable quantum effect, develop protocols to manipulate such effects, and identify optimized processes for certain applications. The methodology consists of classifying all possible quantum states of the system into *free states* or *resource states*. Tied with free states, there is a set of *free operations* that arise from natural physical constraints of the system. The resource theory essentially tells us which state manipulation processes are possible using certain restricted or free operations. There are several robust resource theories that describe a large variety of phenomena, such as entanglement (118, 119), coherence (120), asymmetry and quantum reference frames (50, 51), non-locality (121), quantum thermodynamics (122, 123), and quantum channels. (47, 124)

There are several advantages to reinterpreting the study of certain quantum

phenomena in terms of resource theories. First of all, there are results, theorems and corollaries which are valid for every resource theory, therefore, once it is shown that the quantum phenomena can be cast as a resource theory, there is a large set of tools at the disposal. Furthermore, it is possible to explore many emergent similarities between different physical phenomena which, in principle, had no relation whatsoever, but once they are rephrased as resource theories, similarities become evident. There is also very rich literature exploring the relations between different resource theories, see for instance. (125–129) From a practical standpoint, resource theories tell us how to quantify the amount of resources and how to convert those into useful operations. Let us state precisely what we mean by a quantum resource theory.

Definition 5.1. (Quantum Resource Theory). Let A and B denote two physical subsystems, and $\mathcal{H}_A$, $\mathcal{H}_B$ be their corresponding Hilbert spaces. Let Φ be a map that assigns a set of completely positive and trace preserving (CPTP) maps, $\Phi(\mathcal{H}_A \to \mathcal{H}_B) \subset \mathcal{L}(\mathcal{H}_A \to \mathcal{H}_B)$. Let $\mathcal{F}$ be a map induced as $\mathcal{F}(\mathcal{H}) := \Phi(\mathbb{C} \to \mathcal{H})$ for an arbitrary Hilbert space $\mathcal{H}$. If the two following properties are satisfied,

1. For every physical subsystem A, $\mathbf{1}_A \in \Phi(\mathcal{H}_A \to \mathcal{H}_A)$;
2. For any three physical subsystems A, B, and C; $\sigma \in \Phi(\mathcal{H}_A \to \mathcal{H}_B)$, $\Lambda \in \Phi(\mathcal{H}_B \to \mathcal{H}_C) \Rightarrow (\sigma \circ \Lambda) \in \Phi(\mathcal{H}_A \to \mathcal{H}_C)$,

then the set $(\mathcal{F}, \Phi)$ is called a quantum resource theory.

The set $\mathcal{F}(\mathcal{H}) \subset \mathcal{L}_1(\mathcal{H})$ defines the set of *free states* in $\mathcal{H}$, and CPTP maps in $\Phi(\mathcal{H}_A \to \mathcal{H}_B)$ are called *free operations*. States that belong to $\mathcal{L}_1(\mathcal{H})\backslash\mathcal{F}(\mathcal{H})$ are called *resource states* in $\mathcal{H}$. CPTP maps that do not belong in the set of free operations are called *dynamical resources* or *resource operations*.

Although the definition of a QRT looks quite abstract at first glance, the two requirements simply state that the identity is always a free state and that the composition structure of CPTP maps is preserved, that is, the composition of free operations is also a free operation. Operations are "free" in the sense that they may be realized any number of times in any order and do not consume resources, at the same time, they cannot convert any non-free state into a free state. For example, say we have two subsystems A and B, if

$\xi \in \Phi(\mathcal{H}_A \to \mathcal{H}_B)$ and $\rho \in \mathcal{F}(\mathcal{H}_A)$, then $\xi(\rho) \in \mathcal{F}(\mathcal{H}_B)$. This property is sometimes called the *golden rule* of QRTs.

The structure presented so far is already robust enough to describe many different phenomena. (130) Nonetheless, in the resource theories we are interested (asymmetry, and to some extent, coherence), it is necessary to add an extra requirement related to a tensor product structure.

Definition 5.2. (QRT with tensor product structure). A quantum resource theory $(\mathcal{F}, \Phi)$ admits a tensor product structure if

1. For any three physical subsystems A, B, and C, and for $\xi \in \Phi(\mathcal{H}_A \to \mathcal{H}_B)$, then $(\mathbf{1}_C \otimes \xi) \in \Phi(\mathcal{H}_{CA} \to \mathcal{H}_{CB})$, where $\mathbf{1}_C$ denotes the identity on subsystem C;
2. $\forall\ \sigma \in \mathcal{F}(\mathcal{H}_B)$, the CPTP map $\xi_\rho = (\rho \otimes \sigma)$ is a free operation, that is, $\xi_\rho \in \Phi(\mathcal{H}_A \to \mathcal{H}_{AB})$;
3. $\forall\ \mathcal{H}$, the set $\Phi(\mathcal{H} \to \mathbb{R})$ is not empty.

Once again, those conditions are quite natural in the sense that those properties are expected for a large number of physical phenomena. The first condition simply implies that free operations remain free once they act only on a part of a joint system. One may think of the first condition as if $\xi \in \Phi(\mathcal{H}_A \to \mathcal{H}_B)$ and $\xi' \in \Phi(\mathcal{H}'_A \to \mathcal{H}'_B)$ are both free, then $(\xi \otimes \xi') = (\mathbf{1}_B \otimes \xi') \circ (\xi \otimes \mathbf{1}_A)$ must be free. This follows from the definition of a QRT, where the composition of free maps is also free and coupling a free map with the identity is a free operation. The second condition requires that attaching an auxiliary subsystem is a free operation and the third requires that discarding a subsystem is a free operation. A practical way to rephrase the third condition is to recognize that the partial trace is a free operation, following from the first and third properties of Definition 5.2. Now, we shall explore a particular resource theory with rich applications in quantum error correction, namely, the asymmetry resource theory.

5.2 The asymmetry resource theory

"Symmetric states are all alike; every asymmetric state is asymmetric in its own way."

Anna Karenina (not quite)

Given the general definitions of the previous section, we are now ready to explore the resource theory of asymmetry, which is the resource-theoretic formulation of the study of reference frames, symmetries and covariant operations. In particular, we want to explore how asymmetry (or lack of symmetry) may be used in the context of error correction. The discussion on quantum reference frames and symmetries begins with the dispute between *speakable* and *unspeakable* information. (51)

Whenever we are dealing with speakable information, the means of encoding is irrelevant to the information processing task at hand. For instance, in Shannon's coding theorem (131), it does not matter what the two values of 0 and 1 of a classical bit represent, as the whole information can be transmitted simply by sharing strings of bits. A large number of information processing tasks belong to this class.

Nonetheless, there are several information processing tasks of high interest which cannot simply be stated in such a way. For example, synchronization of clocks or the alignment of Cartesian frames. Say that we have two parties, which we will call Luíza and Vitor. Say that Luíza wants to send Vitor information about her position (and they do not share a pre-aligned reference frame), there is no way that Luíza can precisely describe her position by just sending strings of classical bits of information. She must also include some sort of system which points toward some direction and say her position in relation to this direction; this system must have a degree of freedom that allows the encoding of this information, for example, she cannot use a spherically symmetry system to "point" at some direction. Those information processing tasks are called unspeakable.

There are two natural resource-theoretic approaches to describing speakable information and unspeakable information. In the former case, one employs the resource theory of coherence (120); in the latter, one employs the resource theory of asymmetry. (50) In fact, as argued in (51, 132), one can transform unspeakable information into speakable information through the insertion of a reference frame. The "unspeakable coherence" resource theory[1] is what we study next.

Consider two parties, Luíza and Vitor, that do not share a common reference frame. Given a compact symmetry group G and unitary representations $U(g),\ \forall\ g \in G$, such

[1] Also known as asymmetry resource theory.

that if $\rho \in \mathcal{L}_1(\mathcal{H})$ is the density matrix that characterizes Luíza's state, then

$$\mathcal{U}_g(\rho) := U(g)\rho U^\dagger(g) \tag{5.1}$$

is the state described by Vitor. Suppose that Luíza has no information whatsoever about g; her description of Vitor's density matrix is obtained through the integration over all possible g, in other words, over the Haar measure

$$\mathcal{G}(\rho) = \int_G \mathcal{U}_g(\rho)\ dg \tag{5.2}$$

where dg denotes the Haar measure (for details, see Appendix C). For discrete groups, the result is same but with a sum over g (for $g = 1, ..., \dim G$) in place of the integration. The map $\mathcal{G}(\cdot)$ is called the G-twirling map and plays a key role in asymmetry resource theory.

The basic idea of asymmetry resource theory is that lack of a shared reference frame naturally imposes a restriction on the types of states that Luíza can prepare in relation to Vitor's reference frame. In particular, she can only prepare states using the G-twirling map, and states prepared this way constitute the free states of the resource theory:

$$\mathcal{F}(\mathcal{H}) := \{\mathcal{G}(\rho) \mid \rho \in \mathcal{L}_1(\mathcal{H})\}. \tag{5.3}$$

States that satisfy the property $\rho = \mathcal{G}(\rho)$ are called *G-invariant* states. On top of that, representation theory (89) may be used to further characterize free states of the resource theory. Following (51), we may decompose the Hilbert space into its irreducible representations as

$$\mathcal{H} = \sum_k \mathcal{H}_k := \sum_k \mathcal{M}_k \otimes \mathcal{N}_k, \tag{5.4}$$

where $\mathcal{M}_k$ denotes the representation space and $\mathcal{N}_k$ denotes the multiplicity space. As an example, we may take $G = U(1)$. The unitary representation is simply $U_\theta = e^{i\hat{n}\theta}$ where $\theta \in U(1)$ and $\hat{n}$ denotes the number operator. All irreducible unitary representations of $U(1)$ can be labelled by the eigenvalue of the number operator, e.g. $n \in \mathbb{N}$. In this case, a pure state is given by $|\psi\rangle = \sum_n \sqrt{p_n}|n\rangle$ and the action of the G-twirling map produces the state

$$\mathcal{G}(|\psi\rangle\langle\psi|) = \sum_n p_n |n\rangle\langle n|. \tag{5.5}$$

The form of this state points toward a so-called *superselection rule* which means that the lack of a shared reference frame imposes a constrain on which sort of states Luíza can prepare. For instance, Luíza cannot prepare states that are in a $U(1)$-coherent superposition

in eigenstates of the number operator, because those cannot be generated through a G-twirling map and thus are not free states.

Now we discuss how free operations are realized in the asymmetry resource theory. Once again, we have our favorite players Luíza and Vitor. Say that Vitor possesses a state $\sigma \in \mathcal{L}_1(\mathcal{H})$ and Luíza wants to perform a CPTP operation $\xi : \mathcal{L}(\mathcal{H}) \to \mathcal{L}(\mathcal{H})$ on her reference frame. How does Luíza describe the initial and final states on her reference frame? What about Vitor? In this setup, there are three quantities one would be interested:

- Luíza's description of the initial state: $\mathcal{U}_g^\dagger(\sigma)$;
- Luíza's description of the final state: $\xi \circ \mathcal{U}_g^\dagger(\sigma)$;
- Final state relative to Vitor's reference: $\mathcal{U}_g \circ \xi \circ \mathcal{U}_g^\dagger(\sigma)$;

in particular, Vitor and Luíza will agree upon the description of the CPTP map only if her operation is of the form

$$\int_G \mathcal{U}_g \circ \xi \circ \mathcal{U}_g^\dagger \, dg \tag{5.6}$$

which is precisely the description of Luíza's operation from Vitor's point of view if he does not know which $g \in G$ relates the two reference frames. Hence he must calculate the Haar integral averaging over all possible group elements. Channels that satisfy the structure of equation (5.6) are precisely the free operations of the asymmetry resource theory. In other words, we can define the set of free operations as

$$\Phi(\mathcal{H}) := \{\xi \text{ is CPTP} \mid [\xi, \mathcal{U}_g] = 0\}. \tag{5.7}$$

Quantum channels that satisfy the property $\xi = \int_G \mathcal{U}_g \circ \xi \circ \mathcal{U}_g^\dagger \, dg$ are said to be *G-covariant*.

Up to this point we have considered channels whose input and output Hilbert spaces have the same dimension, this is not a necessary condition, we can extend this notion for Hilbert spaces of different dimensionalities (as long as they are finite). For instance, a quantum channel $\xi : \mathcal{H}_A \to \mathcal{H}_B$ is said to be G-covariant with respect to the unitary representations $\{U_A(g)\}_{g\in G}$ and $\{U_B(g)\}_{g\in G}$ of the Hilbert spaces $\mathcal{H}_A$ and $\mathcal{H}_B$, respectively, if

$$\xi \circ \mathcal{U}_g^A = \mathcal{U}_g^B \circ \xi, \ \forall \ g \in G. \tag{5.8}$$

This extension is particularly important in the context of quantum error correction, where one deals with a physical Hilbert space and a logical Hilbert space with different dimensions.

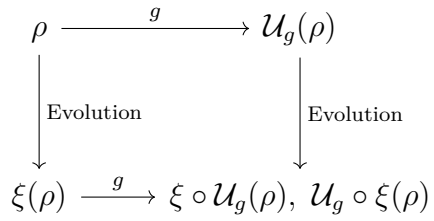

Figure 13 – Diagram which summarizes the asymmetry resource theory. Given a state ρ, it can evolve under a CPTP map ξ or one could employ a symmetry transformation according to a group G and its corresponding unitary $\mathcal{U}_g$. If the diagram commutes, then the ρ state is a free state and is G-invariant whereas the quantum channel ξ is a free operation and is G-covariant.
Source: By the author.

In summary, in the asymmetry resource theory, the set of free states consists of the states that are symmetric under the unitary transformations $U(g)$ related to a symmetry group G; the set of free operations consists of CPTP maps that are symmetric under unitary compositions described by $\mathcal{U}_g$ which are related to a symmetry group. A schematic representation of the asymmetry resource theory can be seen at Figure 13.

The introduction of an asymmetry resource theory is motivated by the description of physical systems that lack a shared reference frame, however, applications of this resource theory go well beyond the original context. In particular, we employ this resource theory to study covariant and approximate quantum error-correcting codes in the next section.

5.3 Covariant codes and approximate error correction

With the foundations of quantum resource theories and, in particular, the asymmetry resource theory at hand, we are ready to enhance our discussion of quantum error correction. Covariant codes are quantum codes that possess a symmetry transformation on the logical subspace (or the logical subsystem) that is realized by a corresponding symmetry on the physical space (or the physical subsystem). This is accomplished in a fault-tolerant way through the transversal implementation of a universal set of logical gates, because if one particular realization of the logical gate in the physical system is faulty, the error does not propagate. Unfortunately, the Eastin-Knill theorem forbids such realization if one demands exact error correction, therefore, the study of covariant codes is inevitably tied down to the study of approximate error-correcting codes. We now precisely

define what we mean by "covariant codes" and "approximate error correction".

We employ a formalism that closely follows the Operator Algebra formalism (see section 3.4), with a slightly different notation. A quantum error-correcting code consists of a physical subsystem A (and its corresponding finite-dimensional Hilbert space $\mathcal{H}_A$) which is the image of an CPTP map called the encoding channel that acts upon the logical subsystem L (and its corresponding finite-dimensional Hilbert space $\mathcal{H}_L$). We assume that the physical subsystem consists of n smaller subsystems such that $A = \otimes_{i=1}^{n} A_i$. We denote this encoding channel as $\mathcal{E}_{A\leftarrow L}$ and say that the code is *covariant* if

$$\mathcal{E}_{A\leftarrow L} \circ \mathcal{U}_L^\theta = \mathcal{U}_A^\theta \circ \mathcal{E}_{A\leftarrow L} \tag{5.9}$$

where the symmetry unitaries act as $\mathcal{U}_L^\theta(\cdot) = U_L^\theta(\cdot)U_L^{\theta\dagger}$ and $\mathcal{U}_A^\theta(\cdot) = U_A^\theta(\cdot)U_A^{\theta\dagger}$. Using the exponential map, the unitaries can be written as $U_L^\theta = e^{-iT_L\theta}$ and $U_A^\theta = e^{-iT_A\theta}$, where T_L is the generator of the symmetry over the logical subspace, T_A is the generator of the symmetry over the physical subsystem, and $\theta \in G$ is the group parameter. The covariance condition from equation (5.9) may also be cast as

$$\mathcal{E}_{A\leftarrow L}[U_L(g)(\cdot)U_L^\dagger(g)] = U_A(g)\mathcal{E}_{A\leftarrow L}(\cdot)U_A^\dagger(g). \tag{5.10}$$

In terms of the asymmetry resource theory (see section 5.2), free states are symmetric states which means that they commute with the symmetry generators

$$[\rho, T_L] = 0, \qquad [\rho, T_A] = 0, \tag{5.11}$$

and the free operations are symmetric operations, in the sense of equations (5.9, 5.10).

A covariant code is *error-correcting* if, given a CPTP map $\mathcal{N}_A$ which acts upon the physical subsystem A and models the noise, there exists another CPTP map $\mathcal{R}_{L\leftarrow A}$ such that

$$\mathcal{R}_{L\leftarrow A} \circ \mathcal{N}_A \circ \mathcal{E}_{A\leftarrow L} = \mathbf{1}_L. \tag{5.12}$$

In practice, the Eastin-Knill theorem does not allow such codes to exist, and this is exactly where approximate error correction enters. Instead of recovering precisely the logical identity on equation (5.12), we have

$$\mathcal{R}_{L\leftarrow A} \circ \mathcal{N}_A \circ \mathcal{E}_{A\leftarrow L} = \mathcal{I}_L \neq \mathbf{1}_L. \tag{5.13}$$

The condition (5.13) is the statement of approximate error correction. The natural question to ask is "how approximate" is the code? In other words, how far[2] is the quantum channel $\mathcal{I}_L$ from the logical identity? In principle, there are several ways to quantify this approximation, and the overwhelmingly popular approach in the literature (44, 45, 47, 48) is through the use of *fidelity*. We will call the typical procedure adopted in the literature as the "standard approach".

Fidelity is a measure of distinguishability between quantum states, formulated as we know in (133, 134), with its historic beginnings tracing back to. (135–137) Given two quantum states $\rho, \sigma \in \mathcal{L}_1(\mathcal{H})$, their fidelity is defined as

$$F(\rho, \sigma) := \left[\mathrm{tr}\left(\sqrt{\sqrt{\rho}\sigma\sqrt{\rho}}\right)\right]^2. \tag{5.14}$$

The fidelity has the following several desirable properties (in what follows, we always take $\forall\ \rho, \sigma, \tau, \mu \in \mathcal{L}_1(\mathcal{H}),\ \forall a \in [0,1] \subset \mathbb{R}$):

1. *Bounds*: $0 \leq F(\rho, \sigma) \leq 1$, with $F(\rho, \sigma) = 1 \Leftrightarrow \rho = \sigma$ and $F(\rho, \sigma) = 0 \Leftrightarrow$ the support of ρ and σ are orthogonal;
2. *Symmetry*: $F(\rho, \sigma) = F(\sigma, \rho)$;
3. *Unitary invariance:* $F(\rho, \sigma) = F(U\rho U^\dagger, U\sigma U^\dagger)$, $\forall\ U$ unitary;
4. *Concavity:* $F(\rho, a\sigma + (1-a)\tau) \geq aF(\rho, \sigma) + (1-a)F(\rho, \tau)$;
5. *Multiplicativity*: $F(\rho \otimes \sigma, \tau \otimes \mu) = F(\rho, \tau)F(\sigma, \mu)$;
6. *Monotonicity*: $F(\rho, \sigma) \leq F(\mathcal{E}(\rho), \mathcal{E}(\sigma))$, $\forall\ \mathcal{E} \in \mathcal{L}(\mathcal{H})$ CPTP map.

In the standard approach, one defines the approximation error as

$$\epsilon(\mathcal{I}_L, \mathbf{1}_L) := \sqrt{1 - F(\mathcal{I}_L, \mathbf{1}_L)}, \tag{5.15}$$

that is, one calculates the square root of one minus the fidelity between the code $\mathcal{I}_L$ and the logical identity $\mathbf{1}_L$ acting implicitly in a quantum state. If the code recovers precisely the logical identity, it means that the error correction is exact and thus the approximation error (5.15) is zero. On the other hand, if somehow the code has an orthogonal support with respect to the logical identity, the fidelity is zero and the approximation error is maximum.

[2] Note that in the definitions of covariant and approximate quantum error-correcting codes there is an implicit quantum state under consideration. That is, we must have a logical state ρ_L in which the channels $\mathcal{E}_{A\leftarrow L}$, $\mathcal{N}_A$ and $\mathcal{R}_{L\leftarrow A}$ will act upon.

Although the fidelity properties are quite useful which makes fidelity (and the error approximation) good measures of quantum state distinguishability, there is a serious drawback that severely hinders its applicability scope. The definition of fidelity (5.14) requires the computation of square roots of Hermitian matrices in successive manner, this way, it is necessary to at least diagonalize an Hermitian matrix twice. As a result, the fidelity can rarely be evaluated, which means that the the standard approach to define the error approximation is of little use. With that in mind, we propose a different approach to quantify the error approximation which will be explored in the next section.

5.4 Geometric bounds for approximate quantum error correction

Given the difficulties associated with evaluating the fidelity generically, we propose two new distance quantifiers for quantum channels. In our proposal, we make use of two quantities originally proposed in (52, 53) called the *sub-fidelity* and the *super-fidelity*. We begin by considering the former, which is defined as

$$E(\rho,\sigma) := \mathrm{tr}(\rho\sigma) + \sqrt{2(\mathrm{tr}\rho\sigma)^2 - 2\mathrm{tr}(\rho\sigma\rho\sigma)}, \tag{5.16}$$

and the latter is defined as

$$G(\rho,\sigma) := \mathrm{tr}(\rho\sigma) + \sqrt{(1-\mathrm{tr}\rho^2)(1-\mathrm{tr}\sigma^2)}. \tag{5.17}$$

The sub- and super-fidelities are lower- and upper-bounds to the fidelity, respectively:

$$E(\rho,\sigma) \leq F(\rho,\sigma) \leq G(\rho,\sigma), \tag{5.18}$$

and they inherit the following desirable properties (in what follows, we always take $\forall\ \rho,\sigma,\tau,\mu \in \mathcal{L}_1(\mathcal{H}), \forall\ a \in [0,1] \subset \mathbb{R}$):

1. *Bounds*: $0 \leq E(\rho,\sigma) \leq 1$ and $0 \leq G(\rho,\sigma) \leq 1$;
2. *Symmetry*: $E(\rho,\sigma) = E(\sigma,\rho)$ and $G(\rho,\sigma) = G(\sigma,\rho)$;
3. *Unitary invariance*: $E(\rho,\sigma) = E(U\rho U^\dagger, U\sigma U^\dagger)$ and $G(\rho,\sigma) = G(U\rho U^\dagger, U\sigma U^\dagger)$, $\forall\ U$ unitary;
4. *Concavity*: $E(\rho, a\sigma + (1-a)\tau) \geq E(\rho,\sigma) + (1-a)E(\rho,\tau)$, and $G(\rho, a\sigma + (1-a)\tau) \geq G(\rho,\sigma) + (1-a)G(\rho,\tau)$;
5. *Multiplicativity*:
   - Sub-fidelity is *sub-multiplicative*: $E(\rho\otimes\sigma, \tau\otimes\mu) \leq E(\rho,\tau)E(\sigma,\mu)$;

- Super-fidelity is *super-multiplicative*: $G(\rho\otimes\sigma,\tau\otimes\mu)\geq G(\rho,\tau)G(\sigma,\mu)$.

Given the definitions and properties of sub- and super-fidelity, we are now ready to discuss our proposal of distance measures:

$$\mathcal{D}_{\text{sub}}(\mathcal{I}_L,\mathbf{1}_L):=\sqrt{1-E(\mathcal{R}_{L\leftarrow A}\circ\mathcal{N}_A\circ\mathcal{E}_{A\leftarrow L},\mathbf{1}_L)} \tag{5.19}$$

$$\mathcal{D}_{\text{super}}(\mathcal{I}_L,\mathbf{1}_L):=\sqrt{1-G(\mathcal{R}_{L\leftarrow A}\circ\mathcal{N}_A\circ\mathcal{E}_{A\leftarrow L},\mathbf{1}_L)} \tag{5.20}$$

where we are taking the quantum channels to act upon some implicit quantum state and $\mathcal{I}_L=\mathcal{R}_{L\leftarrow A}\circ\mathcal{N}_A\circ\mathcal{E}_{A\leftarrow L}$.

The relation between the newly proposed distances and the standard approach error approximation is obtained from the fidelity inequalities (5.18) and the definition of the error approximation (5.15), which yields

$$\mathcal{D}_{\text{super}}(\mathcal{I}_L,\mathbf{1}_L)\leq\epsilon(\mathcal{I}_L,\mathbf{1}_L)\leq\mathcal{D}_{\text{sub}}(\mathcal{I}_L,\mathbf{1}_L). \tag{5.21}$$

Therefore, the distance measures based on the sub- and on the super-fidelity are upper- and lower-bounds, respectively. The inequalities are saturated when the sub- and the super-fidelity recover the fidelity. Overall, this happens if at least one of the states is pure[3] or if both states are single-qubit states[4]. For error-correction applications, both conditions are in general not satisfied, which means that the distance measures provide powerful bounds to the error approximation. The great advantage of our proposal over the fidelity-based error is the fact that calculating $\mathcal{D}_{\text{super}}$ and $\mathcal{D}_{\text{sub}}$ require only the evaluation

[3] Note that the fidelity can be written in terms of the eigenvalues of the matrix $\sqrt{\sqrt{\rho}\sigma\sqrt{\rho}}$, in particular, it follows

$$\sqrt{F(\rho,\sigma)}=\text{tr}\sqrt{\sqrt{\rho}\sigma\sqrt{\rho}}=\sum_{i=1}^{N}a_i,$$

by considering that $\text{tr}\rho\sigma=\text{tr}\sqrt{\sqrt{\rho}\sigma\sqrt{\rho}}=\sum_{i=1}^{N}\lambda_i^2$ and squaring the above result, we obtain

$$F(\rho,\sigma)=\text{tr}\rho\sigma+2\sum_{i<j}a_ia_j$$

where a_i with $i=1,...,N$ denotes the eigenvalues. In the case where one of the states is pure, the sum over i and j such that $i<j$ has only a single term $2a_ia_j=\sqrt{2\text{det}(\rho\sigma)}=\sqrt{2\text{det}(\rho)}\sqrt{2\text{det}(\sigma)}$.

[4] For single-qubit states, the density matrices will be two-dimensional, and e.g. in the case of the super-fidelity which rely on the purity of the density matrices, we recover

$$G(\rho,\sigma)=\text{tr}(\rho\sigma)+\sqrt{1-\text{tr}\rho^2}\sqrt{1-\text{tr}\sigma^2}=\text{tr}(\rho\sigma)+2\sqrt{\text{det}(\rho)}\sqrt{\text{det}(\sigma)}=F(\rho,\sigma).$$

A similar line of reasoning recovers the fidelity out of the sub-fidelity.

of three traces, which is astonishingly easier to compute than the squares roots of successive diagonalization of Hermitian matrices.

Furthermore, the bound related to the super-fidelity is geometric in the sense that it can be used to measure distances and legitimately define a metric. For three arbitrary quantum states ρ, σ, $\tau \in \mathcal{L}_1(\mathcal{H})$, it satisfies $\mathcal{D}_{\text{super}}(\rho, \sigma) \geq 0$ and $\mathcal{D}_{\text{super}}(\rho, \sigma) = 0$ if and only if $\rho = \sigma$, it is symmetric $\mathcal{D}_{\text{super}}(\rho, \sigma) = \mathcal{D}_{\text{super}}(\sigma, \rho)$, and last but not least it also satisfies the triangle inequality, $\mathcal{D}_{\text{super}}(\rho, \tau) \leq \mathcal{D}_{\text{super}}(\rho, \sigma) + \mathcal{D}_{\text{super}}(\sigma, \tau)$. (52, 53) The second property follow by construction for the distance measure based on the sub-fidelity, however, the distance based on the sub-fidelity is not positive semi-definite and thus does not define a metric.

From the fact that the distance measure based on the super-fidelity define a metric, it would be quite interesting to further enhance this result and see if it can be extended to differential or Riemannian geometry. If that were the case, it would be possible to reinterpret the robust machinery of charts, covariant derivatives, connections, geodesics, curvature, and fiber bundles using concepts from quantum error correction and information geometry.

In a more concrete sense, an immediate and desirable result would be to test the new bounds "in action" and see the results they yield. With that motivation, we calculated both distance measures for three quantum channels that frequently arise in the theory of error correction: dephasing, depolarizing, and amplitude damping channels. Those results are discussed in the following section.

5.5 Computing bounds

In this section, we put our proposal to the test by evaluating it with regards to three typical quantum channels which model the "failure" of exact error correction. In general, our results are valid for any finite-dimensional system, beyond the usual use of fidelity for qubit states (restricted to $2-$dimensional density operators).

For numerical computations, we adopted the calculations for five qubits (as we have seen, five is a magic number of qubits, motivated by the five-qubit code) whose Hilbert space is $32-$dimensional. We also must adopt a "test" state, which is the initial state that the quantum channels will act upon. There are several choices, we take a state which

interpolates, with a parameter λ, between an arbitrary pure state $|\psi\rangle$ and a maximally mixed state $\mathbf{1}_N/N$ ($\mathbf{1}_N$ denotes the $N \times N$ identity matrix) as follows

$$\rho = \lambda|\psi\rangle\langle\psi| + (1-\lambda)\frac{\mathbf{1}_N}{N}, \tag{5.22}$$

with $\lambda \in [0,1]$. Clearly, for $\lambda = 1$ our test state becomes a pure state and for $\lambda = 0$ our state becomes the maximally mixed state. As the pure state $|\psi\rangle$ is arbitrary, we have taken it to be a N-dimensional[5] GHZ state (138, 139)

$$|\psi\rangle = \frac{1}{\sqrt{2}}(|0\rangle^{\otimes n} + |1\rangle^{\otimes n}),$$

for five qubits ($n = 5$), the GHZ state becomes $|\psi\rangle = (|00000\rangle + |11111\rangle)/\sqrt{2}$ and the corresponding density matrix is 32×32, every matrix element is zero except $\rho_{(1,1)}, \rho_{(32,32)}, \rho_{(1,32)}$ and $\rho_{(32,1)}$, which are $1/2$. As a consequence, we take $N = 32$ and consider a 32×32 identity matrix composing the test state (5.22).

As we are dealing with a composite system, the sum operator representation (see equation 3.3) adopted must be modified accordingly. The quantum channels have local action, which means that they act only on a single qubit at any given time. For illustration purposes, consider a bipartite system whose state is ρ_{AB}. The sum representation of a local quantum channel $\mathcal{E}$ becomes

$$\mathcal{E}(\rho_{AB}) = \sum_{i,j}(K_i^A \otimes \mathbf{1}_B)(\mathbf{1}_A \otimes K_j^B)\rho_{AB}(\mathbf{1}_A \otimes K_j^B)^\dagger(K_i^A \otimes \mathbf{1}_B)^\dagger, \tag{5.23}$$

where $K_{i,j}^{A,B}$ denotes the pertinent Kraus operators. The structure for a system composed of n qubits with the local action of the quantum channel is a generalization of the result (5.23), that is,

$$\begin{aligned}\mathcal{E}(\rho_{A_1\ldots A_n}) = \sum_{i_1,\ldots,i_n}(K_{i_1}^{A_1} \otimes \mathbf{1}_{A_2} \otimes \ldots \otimes \mathbf{1}_{A_n})(\mathbf{1}_{A_1} \otimes K_{i_2}^{A_2} \otimes \ldots \otimes \mathbf{1}_{A_n})\ldots(\mathbf{1}_{A_1} \otimes \mathbf{1}_{A_2} \otimes \ldots \otimes K_{i_n}^{A_n}) \\ \times \rho_{A_1\ldots A_n}(\mathbf{1}_{A_1} \otimes \mathbf{1}_{A_2} \otimes \ldots \otimes K_{i_n}^{A_n})^\dagger\ldots(\mathbf{1}_{A_1} \otimes K_{i_2}^{A_2} \otimes \ldots \otimes \mathbf{1}_{A_n})^\dagger(K_{i_1}^{A_1} \otimes \mathbf{1}_{A_2} \otimes \ldots \otimes \mathbf{1}_{A_n})^\dagger.\end{aligned} \tag{5.24}$$

Hereinafter, our work consists of taking $n = 5$ (remember the five-qubit code) in equation (5.24) and computing the distance measures based on the sub- and super-fidelities

[5] Dear reader, be careful: n denotes the number of qubits we will be dealing with. N denotes the dimension of the matrices and states we will be dealing with. They are connected through $2^n = N$. In our case, five-qubits ($n = 5$) and matrices which are 32×32 ($N = 32$). We would like to stress that this choice is merely for numerical purposes, as our results are valid for arbitrary n.

($\mathcal{D}_{\text{sub}}$ and $\mathcal{D}_{\text{super}}$, respectively) for a given set of Kraus operators. The calculation of the distance measures will provide us the geometric bounds for the error approximation. What changes from one quantum channel to the other is precisely the set of Kraus operators.

5.5.1 Geometric bounds for the dephasing channel

We begin with the dephasing channel, as it is the one with the least Kraus operators in the sum representation we choose. Our choice consists of taking

$$K_0 = \begin{pmatrix} 1 & 0 \\ 0 & \sqrt{1-p} \end{pmatrix}, \quad K_1 = \begin{pmatrix} 0 & 0 \\ 0 & \sqrt{p} \end{pmatrix},$$

where $p \in [0,1]$ denotes the probability of the channel affecting the system.

The result for the distance measure based on the sub-fidelity, considering five qubits with local action of the dephasing channel and initial state interpolating between a pure GHZ state and a maximally mixed state (5.22), is given by

$$\mathcal{D}_{\text{sub}}(\mathcal{E}_{\text{deph}}(\rho),\rho) = \frac{1}{8}\left[\left(62 - 2\left(15+16\sqrt{1-p}\right)\lambda^2 - \frac{1}{2}\{(-1+\lambda)[-31 \right.\right.$$
$$\left.\left. -31\lambda - (869+960\sqrt{1-p}+16p)\lambda^2 + (931+960\sqrt{1-p}-496p)\lambda^3]\right\}^{1/2}\right]^{1/2}, \quad (5.25)$$

and for the super-fidelity based measure we obtain

$$\mathcal{D}_{\text{super}}(\mathcal{E}_{\text{deph}}(\rho),\rho) = \frac{1}{4\sqrt{2}}\sqrt{31-(15+16\sqrt{1-p})\lambda^2 - \sqrt{31(1-\lambda^2)}\sqrt{31+(-31+16p)\lambda^2}}. \quad (5.26)$$

Those results provide us bounds for the error approximation whenever we model the resulting composition of quantum channels $\mathcal{R}_{L\leftarrow A}\circ\mathcal{N}_A\circ\mathcal{E}_{A\leftarrow L}$ to be a dephasing channel.

For concreteness, we look for the numeric behavior of the geometric bounds, equations (5.25, 5.26), with respect to the two free parameters: the mixture of the initial state (parameter λ in equation 5.22) and the probability p (see Kraus operators of the dephasing channel). The distance measure based on the sub-fidelity will provide us the error upper-bound and the one based on super-fidelity the error lower-bound.

We start by considering variations of the geometric bounds with respect to the mixture λ, to accomplish that, we fix $p = 0.2$ and run the numerical simulation, whose result is shown in Figure 14.

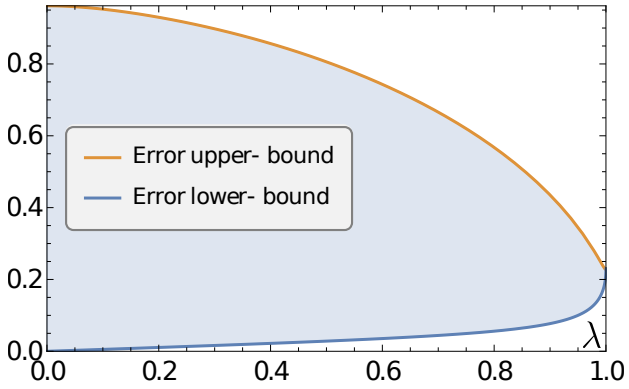

Figure 14 – Bounds for the error approximation considering the dephasing channel. In this realization, the mixture λ of the initial state is a free parameter whereas the probability is fixed $p = 0.2$. The possible values for the error approximation are shaded light blue.
Source: by the author.

For λ close to zero, the initial state is "almost" maximally mixed and the geometric bounds are not very restrictive. On a second note, as λ goes to 1, the initial state becomes more and more pure, to the point where it becomes a completely pure GHZ state for $\lambda = 1$. As a consequence, the sub- and the super-fidelity become the fidelity, and the two bounds converge to a single value.

The second analysis we employ concerns the behavior of the geometric bounds in relation to the probability p that characterizes the quantum channel. In this instance, we fix $\lambda = 0.7$ and run the numerical simulation, with result displayed in Figure 15.

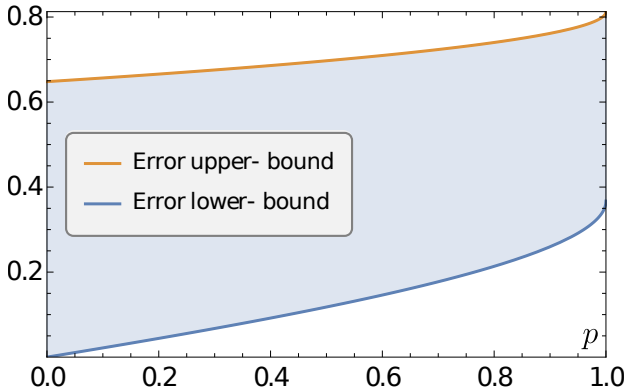

Figure 15 – Bounds for the error approximation considering the dephasing channel. In this realization, the probability p of the quantum channel is a free parameter whereas the initial state mixture is fixed $\lambda = 0.7$. The possible values for the error approximation are shaded light blue.
Source: by the author.

We observe that the probability "modulates" the possible numerical values for the geometric bounds, but it is not possible to conclude whether or not the bounds are more limiting in certain regions of values for p. Clearly, the numerical values for the bounds increases as p increases, in other words, the error approximation gets higher as we take larger values of p. This is precisely what one would expect from a practical point of view, as the more likely errors are to occur, the more likely the final and initial states will be distinct, which implies larger approximations because the error approximation is nothing but a measure of how distinct two quantum states are.

Moreover, our result also satisfies another important eye-test: the value $p = 0$ is equivalent to the channel not happening at all, which means that the sub-fidelity and the super-fidelity are evaluated for two equal states. The super-fidelity for two equal states is always one[6], which implies that its associated geometric bound must be zero; this is exactly the result we obtained. Unfortunately, the sub-fidelity is, in general, not equal to one if the two states are equal and thus nothing can be said about its distance based measure.

Given that the dephasing channel and our initial state rely solely on two parameters, we can explore the resulting numerical bounds whilst we vary both simultaneously. By letting both p and λ run from 0 to 1, we obtain the plot of Figure 16.

For a fixed p, the value of the mixture significantly changes the sharpness of the geometric bounds; moreover, the two bounds converge to the same unique value whenever $\lambda = 1$, this property is irrespective of p, but the value itself in which the bounds converge depends on the value of p. In more geometrical terms, the two hyperplanes have a common end-line (they intersect each other) whose value varies with p. On the other hand, the range of possible values for the error approximation is influenced by the value of the probability, in particular, smaller p allows for a range of smaller values; whereas as p goes to 1, the allowed values increases, as it is more likely that errors will occur, resulting in overall higher approximations.

[6] It follows from the definition: $G(\rho, \rho) = \mathrm{tr}\rho^2 + \sqrt{1 - \mathrm{tr}\rho^2}\sqrt{1 - \mathrm{tr}\rho^2} \equiv 1$.

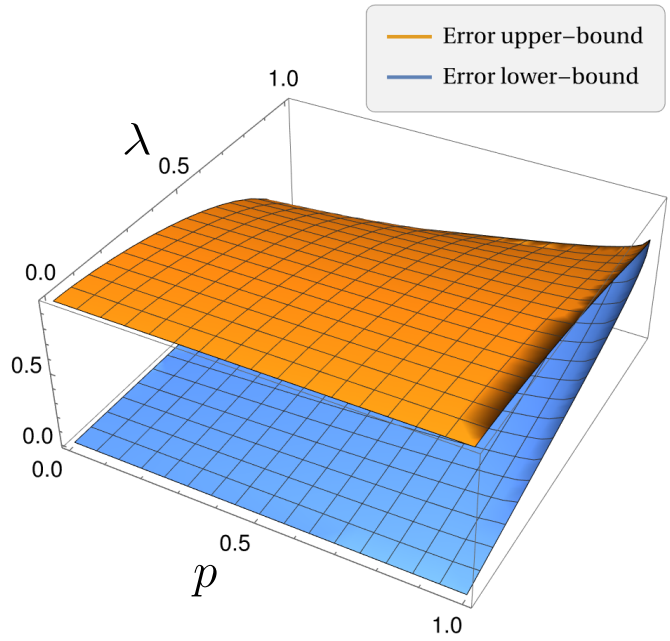

Figure 16 – Bounds for the error approximation considering the dephasing channel. In this realization, both the probability p and the initial state mixture λ are free parameters. The possible values for the error approximation are within the volume delimited by the upper-bound hyperplane (orange) and the lower-bound hyperplane (blue).
Source: by the author.

5.5.2 Geometric bounds for the depolarizing channel

The second quantum channel we consider is the depolarizing channel, whose Kraus operators can be written as

$$K_0 = \sqrt{1 - \frac{3p}{4}} \begin{pmatrix} 1 & 0 \\ 0 & 1 \end{pmatrix}, \quad K_1 = \sqrt{\frac{p}{4}} \begin{pmatrix} 0 & 1 \\ 1 & 0 \end{pmatrix},$$

$$K_2 = \sqrt{\frac{p}{4}} \begin{pmatrix} 0 & -i \\ i & 0 \end{pmatrix}, \quad K_3 = \sqrt{\frac{p}{4}} \begin{pmatrix} 1 & 0 \\ 0 & -1 \end{pmatrix},$$

where $p \in [0, 1]$ denotes the probability. It is worth mentioning that one could write the Kraus operators compactly through the use of Pauli matrices.

We begin with the results for the geometric bounds as functions of the parameters λ and p. Once again, we consider five qubits with initial state (5.22) and local action of

the quantum channel. The distance measure based on the sub-fidelity is given by

$$\mathcal{D}_{\text{sub}}(\mathcal{E}_{\text{depo}}(\rho),\rho) = \frac{1}{16}\Big[248 - 248\lambda^2 + 4p(1+47\lambda^2) - \Big[(-1+\lambda)\Big(4p(31+31\lambda+2293\lambda^2 - 2867\lambda^3) + 124(-1-\lambda-59\lambda^2+61\lambda^3) + p^2(-31-31\lambda-2725\lambda^2+4323\lambda^3)\Big)\Big]^{1/2}\Big]^{1/2}, \tag{5.27}$$

and the calculation for the super-fidelity yields

$$\mathcal{D}_{\text{super}}(\mathcal{E}_{\text{depo}}(\rho),\rho) = \frac{1}{8}\Big[62 + p - 62\lambda^2 + 47p\lambda^2 - \sqrt{31(1-\lambda^2)} \times\sqrt{-124\,(-1+\lambda^2) + 4p\,(1+47\lambda^2) - p^2(1+95\lambda^2)}\Big]^{1/2}. \tag{5.28}$$

For the depolarizing quantum channel, the first numerical analysis we employ consists of solving equations (5.27, 5.28) while varying λ from 0 to 1 with fixed value $p = 0.2$ for the probability. The numerical experiment is illustrated in Figure 17.

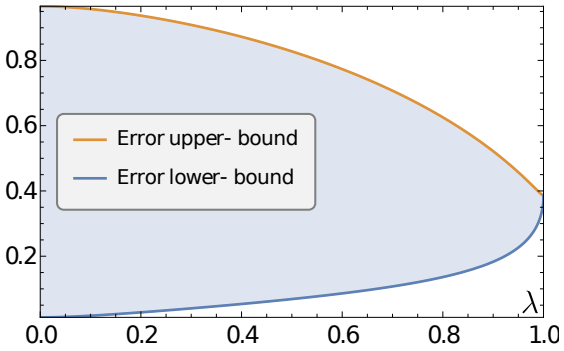

Figure 17 – Bounds for the error approximation considering the depolarizing channel. In this realization, the mixture λ of the initial state is a free parameter whereas the probability is fixed $p = 0.2$. The possible values for the error approximation are shaded light blue.
Source: by the author.

The behavior of the geometric bounds for the depolarizing channel is quite similar to the one for the dephasing channel. For small λ, which means an initial state close to maximally mixed, the bounds are not restrictive at all; nonetheless, as the initial state mixture goes towards 1, the bounds gets more and more restrictive, which implies that the range of allowed values for the error approximation diminishes. In particular, the sub- and super-fidelity based measures converge to the same value whenever the initial state is completely pure. This is in accordance with the definition of sub- and super-fidelities, as we have seen, whenever one of the two states is completely pure, they reduce to the fidelity, which means that both bounds from equation (5.18) are saturated.

Just like for the dephasing channel, it is also important to see the effect that the probability p has over the geometric bounds. For that matter, we fix $\lambda = 0.7$ and vary p from 0 to 1. The results are revealed in Figure 18.

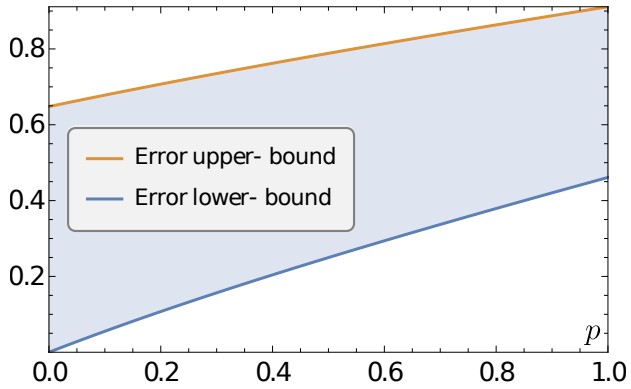

Figure 18 – Bounds for the error approximation considering the depolarizing channel. In this realization, the probability p of the quantum channel is a free parameter whereas the initial state mixture is fixed $\lambda = 0.7$. The possible values for the error approximation are shaded light blue.
Source: by the author.

The effect that the probability has over the bounds is once again "modulating" the possible numerical values. The overall effect is to increase the numerical values as we go from a smaller probability to a higher probability of the quantum channel action. Such result is expected, as the larger the value of p, the more likely the error to occur, and thus more likely that the final state is different from the initial state. If we take $p = 0$, this amounts to the channel not happening at all, as such, the final state will be exactly the initial state, the super-fidelity is one and its associated distance measure is zero. This is exactly what is observed. The sub-fidelity does not capture this behavior and we cannot conclude anything else from the geometric upper-bound.

The icing on the cake of our analysis is understanding how the geometric bounds vary when both parameters are free. We vary λ and p to obtain the numerical simulation exhibited in Figure 19.

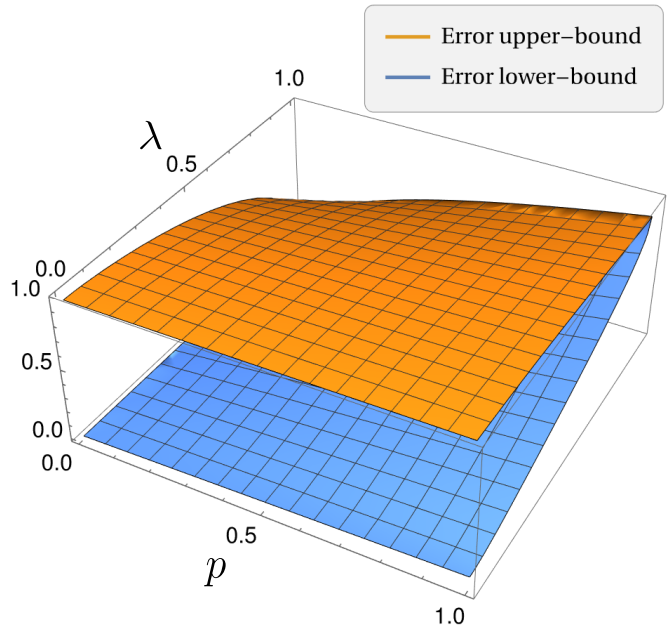

Figure 19 – Bounds for the error approximation considering the depolarizing channel. In this realization, both the probability p and the initial state mixture λ are free parameters. The possible values for the error approximation are within the volume delimited by the upper-bound hyperplane (orange) and the lower-bound hyperplane (blue).
Source: by the author.

The behavior observed in the joint analysis is straightforward, for any fixed λ, we obtain the influence of p on the bounds; for any fixed p, we obtain the influence of λ. The remarkable features may all be recovered. For small λ, the bounds are not restrictive at all and they become sharper as λ increases. For $\lambda = 1$, the two hyperplanes converge to a line whose value depends solely on p. The features of p are also recovered: for $p = 0$, the lower hyperplane indicates that the super-fidelity based measure is zero; for increasing p, the overall range of values of the error approximation increases accordingly.

5.5.3 Geometric bounds for the amplitude damping channel

The third and last example we discuss is the amplitude damping channel. In the sum representation, its Kraus operators are given by

$$K_0 = \sqrt{p}\begin{pmatrix} 1 & 0 \\ 0 & \sqrt{1-\gamma} \end{pmatrix}, \quad K_1 = \sqrt{p}\begin{pmatrix} 0 & \sqrt{\gamma} \\ 0 & 0 \end{pmatrix},$$

$$K_2 = \sqrt{1-p}\begin{pmatrix} \sqrt{1-\gamma} & 0 \\ 0 & 1 \end{pmatrix}, \quad K_3 = \sqrt{1-p}\begin{pmatrix} 0 & 0 \\ \sqrt{\gamma} & 0 \end{pmatrix},$$

where $p \in [0,1]$ denotes the probability and $\gamma \in [0,1]$ denotes the "strength" of the damping. The two main differences of this channel[7] in comparison to the previous ones we have discussed is the fact that it is not unital, which means that it does not map the identity to itself, and that it has one extra free parameter.

The closed form for the sub-fidelity based measure, considering five qubits with local action of the amplitude damping channel and initial state (5.22) is

$$\begin{aligned}\mathcal{D}_{\text{sub}}(\mathcal{E}_{\text{AD}}(\rho),\rho) = \frac{1}{8}\Big\{62 - 2(15 + 16\sqrt{1-\gamma} - 8\gamma)\lambda^2 - \frac{1}{2}\Big[(-1+\lambda)\Big(-64\gamma\lambda^2\,[-7 \\ +(15+8\sqrt{1-\gamma})\lambda\Big] + \gamma^2\Big(1 + 4(-1+p)p + \lambda + 4(-1+p)p\lambda + (43 + 140(-1+p)p)\lambda^2 \\ +(211 + 364(-1+p)p)\lambda^3\Big) + (-1+\lambda)\Big[31 + \lambda(62 + (931 + 960\sqrt{1-\gamma})\lambda)\Big]\Big)\Big]^{1/2}\Big\}^{1/2},\end{aligned} \tag{5.29}$$

and the closed expression for the super-fidelity based distance measure is

$$\begin{aligned}\mathcal{D}_{\text{super}}(\mathcal{E}_{\text{AD}}(\rho),\rho) = \frac{1}{4\sqrt{2}}\Big\{31 + (-15 - \frac{32}{2}\sqrt{1-\gamma} + 8\gamma)\lambda^2 - \sqrt{31}\sqrt{1-\lambda^2} \\ \times\Big[32\gamma\lambda^2 - 31(-1+\lambda^2) + \gamma^2\Big(-1 - 15\lambda^2 - 4(-1+p)p(1+7\lambda^2)\Big)\Big]^{1/2}\Big\}^{1/2}.\end{aligned} \tag{5.30}$$

In other words, equations (5.29, 5.30) provide bounds for the error approximation whenever we model the resulting composition $\mathcal{R}_{L\leftarrow A}\circ\mathcal{N}_A\circ\mathcal{E}_{A\leftarrow L}$ to be an amplitude damping channel acting locally on the five-qubit code.

To obtain further insights from the analysis of the distance measures, we look for the behavior of the upper- and lower-bounds of the error (see equation 5.21) varying the initial state mixture λ and the strength of the channel (parameter γ of the Kraus operators).

[7] Sometimes the channel we are calling "amplitude damping" is referred to as "generalized amplitude damping" in the literature. The "generalized" version, as the name suggests, is more general hence why we have decided to use it. We could have called it "generalized" but we have used this word way too many times thus far, so we have decided against its use in the end.

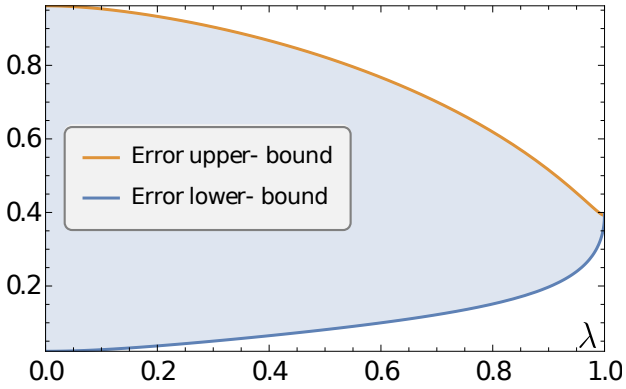

Figure 20 – Bounds for the error approximation considering the amplitude damping channel. In this realization, the mixture λ of the initial state is a free parameter whereas the probability and the strength are fixed $p = 0.2$, $\gamma = 0.3$. The possible values for the error approximation are shaded light blue.
Source: by the author.

We begin by taking fixed $p = 0.2$ and $\gamma = 0.3$ and solving equations (5.29, 5.30) with λ varying from 0 to 1. The numerical result is displayed in Figure 20. The behavior observed once more follows similarly to the case of the other two quantum channels previously analyzed. For a very mixed initial state, the error approximation is bounded very broadly, as the initial state becomes closer to a pure state, the bounds become tighter. This is a consequence of the fact that as the states become purer, the sub- and super-fidelities become closer to the fidelity (in the limit case that the state is completely pure, the sub- and super-fidelities recover precisely the fidelity), which is manifested as sharper bounds for the error approximation.

Yet another interesting analysis is to observe how sensitive are the distance measures with regards to the strength of the amplitude damping. In this realization, we let γ vary from 0 to 1 and fix the probability $p = 0.2$ and the mixture $\lambda = 0.5$. The numerical results are shown in Figure 21.

Although the bounds are clearly sensitive to the strength of the channel, their tightness seems to not rely on this parameter, in stark contrast with the mixture chosen for the initial state. The effect that the strength has over the bounds is to increase their numerical value as the strength of the channel increases. This result is expected from an intuitive perspective, as the stronger the action of the channel, the more likely that the final state and the initial state differ significantly, yielding smaller values for the sub- and super-fidelities, which in turn provides higher values for the bounds.

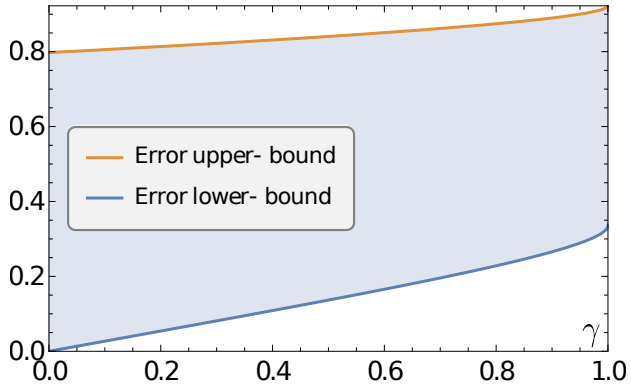

Figure 21 – Bounds for the error approximation considering the amplitude damping channel. In this realization, the strength γ of the channel is a free parameter whereas the probability and the initial state mixture are fixed $p = 0.2$, $\lambda = 0.5$. The possible values for the error approximation are shaded light blue.
Source: by the author.

To finish our numerical analysis with glory, we ought to observe the effect of the two parameters simultaneously. In the following simulation, we vary both λ and γ whereas the probability is fixed $p = 0.2$. The results are displayed in Figure 22.

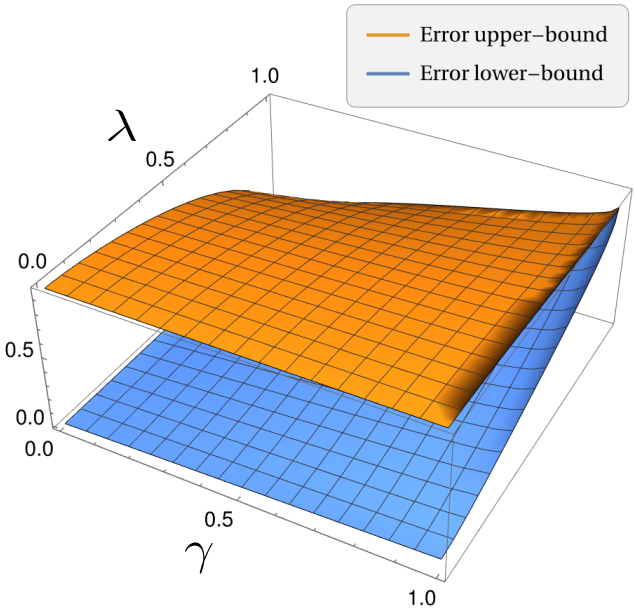

Figure 22 – Bounds for the error approximation considering the amplitude damping channel. In this realization, the only fixed parameter is the probability, taken to be $p = 0.2$. The possible values for the error approximation are within the volume delimited by the upper-bound hyperplane (orange) and the lower-bound hyperplane (blue).
Source: by the author.

As expected given the previous two numerical results: for a fixed λ, the strength

of the channel has little influence in regards to the sharpness of the bounds. However, for a fixed strength γ, the initial state mixture characterized by λ significantly alters the geometric bounds. In particular, for an "almost" pure initial state, the bounds are much tighter than for an "almost" maximally mixed state. Furthermore, for a completely pure initial state, the bounds converge to a set of values that describe a line. The value in which the bounds converge depends on the channel strength, but the fact that both bounds converge to a unique value (for a fixed γ) is regardless of the channel strength.

6 CONCLUSIONS AND FURTHER WORK

The Universe is indeed full of surprises. Who would have thought that the way information is reliably encoded in quantum computers is also the way information is encoded in quantum gravity? This somewhat exotic connection was the main motivation behind this work.

We began by providing a review of the main concepts in AdS/CFT. Given the fact that the original paper is the most cited in theoretical physics (as far as the authors are concerned), the amount of information related to different applications and subtleties of AdS/CFT is way beyond the scope of this work. This way, our brief review of the subject has the ambition of pointing out why we need quantum error correction. We accomplish that by exploring one facet of the correspondence: operator reconstruction. As the AdS/CFT statement is of equivalence between different theories, it is natural to ask what is the relation between objects of one theory to the other. In particular, this relation is, supposedly, one-to-one. Turns out that the reconstruction procedures developed in the literature (known as global and AdS-Rindler reconstructions) had an annoying inconvenience: the one-to-one isomorphism was nowhere to be seen; there was redundancy everywhere. To address this inconsistency properly, we argued that quantum error correction is necessary.

We also provided a review of quantum error correction, presenting concepts and formalizing results that were going to be used later. In particular, we illustrated the main idea of redundancy through the simple Shor's code. Following, we discussed the two most common formalisms for quantum error correction, namely Operator Algebra Quantum Error Correction and Stabilizer codes. Just like in the case of AdS/CFT, the study of quantum error correction is an incredibly active area of research, and our brief review does not nearly address everything that those formalisms have to offer. We limited ourselves to the main concepts which would be useful in connections with holography.

Following, we connected the dots by exploring what quantum information theory has to say in holography. The first result we discuss is the Ryu-Takayanagi formula which was the first and arguably the most important result in this direction. Once the Achilles' heel of AdS/CFT, redundancy became a desired good when it was realized that AdS/CFT

works just like an error-correcting code. There are several examples of how quantum error correction can be used in AdS/CFT for various purposes. We presented two codes, the 3-qutrit and the HaPPY, which consists of stabilizer codes that are sufficient to solve the puzzles that arose when we discussed the operator reconstruction procedures in holography.

As a further motivating example of how the relation between holography and quantum error correction has been a formidable one, we explored the recent results of Harlow and Ooguri that point out an intrinsic inconsistency between AdS/CFT and global symmetries. As quantum information theorists, we understood those results under the light of the Eastin-Knill theorem, which is a restricting no-go theorem that provides what can and what cannot be done in quantum error-correcting codes. From the Eastin-Knill result, there are two possibilities: either consider approximate quantum error-correcting codes or asymmetric quantum error-correcting codes. In order to understand those ideas more concretely, we employed the formalism of quantum resource theories.

Motivated by the use of resource theories in the context of error correction, we delve deeper into approximate error correcting codes. Rather than asking for exact error correction, one asks for recovery of the message up to some factor; despite being a clear drawback, in some cases, it is enough for practical purposes and, on the other hand, one can free itself from the no-go theorem of Eastin and Knill. There are several recent works in the literature which propose different approaches to approximate error correction, however, they all have one feature in common: the use of fidelities as a measure of quantum state distinguishability.

The final goal of an error correcting code is to find a recovery channel such that the recovered quantum state (after the action of some noise and encoding channels) is as close as possible to the original state, the fidelity is employed in this context exactly as a way to evaluate "how close is the recovered state to the original one". Given that the fidelity is equal to one if and only if both states are equal and zero if and only if the two states have completely orthogonal support, it is necessary to take a complementary measure (one minus the fidelity) to quantify the actual approximation; that is precisely what we called the standard approach to the error approximation. As not everything that glitters is gold, calculating fidelities for generic states is a tough task, as one must (at least) diagonalize a Hermitian matrix twice in order to calculate the trace of its square root.

Part of this work and our proposal emerge as a way to circumvent this issue. Instead of using the fidelity to evaluate the distinguishability between the original state and the recovered state, we take a step back and look into the sub- and super-fidelities which are bounds for the fidelity. Although those quantities are "just" bounds, they have an overwhelming advantage from the computational point of view: they require evaluating only three traces. From the definition of our proposed distance measures, it is clear that the sub-fidelity based provides the upper-bound to the standard error approximation whereas the super-fidelity based provides the lower-bound. This way, rather than trying to evaluate a complicated error approximation, we calculate its bounds in a much simpler fashion.

As a way to advocate for concreteness, we put our proposed bounds to the test by calculating them for three quantum channels that frequently appear in the theory of quantum error correction. The idea is to model the composition of the recovery, noise and encoding channels as a single noisy channel (this is where the "approximate error correction" resides, had we taken the identity instead, we would have exact error correction), which we take to be the dephasing, depolarizing, and the amplitude damping channels. Although our proposed bounds are valid for any finite-dimensional system and for any quantum state (in particular, if one of the states in which we evaluate the sub- and super-fidelity is pure, we recover the fidelity and our bounds simply become the standard error approximation), to actually perform calculations we have to compromise. Motivated by the 5-qubit code, we fix the number of qubits to be five and perform the quantum channels acting locally. It is also necessary to consider an initial "test" state, which we take to be an interpolation between a GHZ state and a maximally mixed state.

The numerical results we obtained displayed clear features that would be expected for bounds on error approximation in the context of error correction. First of all, given that our initial state interpolates between a pure state and a completely mixed state, we need to address the behavior of our bounds in those two cases. For pure states, the bounds converge to a unique value, this is what one would expect given that both the sub- and the super-fidelity are reduced to the fidelity if one of the states in which they are evaluated is pure. For completely mixed states, the result is quite the opposite. As a mixed state is the "least pure" state possible, the bounds evaluated over the maximally mixed states are as far as possible from each other, which results in a broader range of values for the error approximation. Therefore, it is expected that the mixture which dictates the purity of the

initial state severely modifies the bounds, with the bounds being much tighter for purer states. This is exactly what we observed for the three channels we considered.

The second feature we recovered is the effect that the probability of the channel has over the values for the bounds. Every quantum channel in the sum representation amounts to evaluating a combination of Kraus operators. Any Kraus operator for noisy quantum channels is characterized by a probability which indicates the likelihood of that quantum channel performing a noisy operation. The intuitive behavior is that as we increase the probability, the more likely the outcome is noisy, and the more likely that the final state is distinct from the initial state. This amounts to smaller sub- and super-fidelities which in turn amount to larger bounds. In other words, we expect that for lower probabilities, the bounds for the error approximation are numerically smaller and for larger probabilities, the bounds should be numerically greater. This is indeed what we obtained. Furthermore, for null probability, one would expect the final and initial states to be exactly the same (as there are no noisy operations), which means that the super-fidelity is one and its distance measure is zero. Once again, this behavior was observed in our numerical results for the three channels. The amplitude damping channel has one extra parameter which models the strength of the damping, for smaller strength values, the numerical bounds for the error are also smaller, and for increasing strength values, the numerical bounds increase accordingly.

There is a "brave new world" waiting to be explored when it comes to those bounds. As we mentioned, the bound related to the super-fidelity defines a genuine metric because it satisfy the three following properties: positive semi-definiteness, symmetry and the triangle inequality. Nonetheless, those requisites are concerning "metric" in the theory of metric spaces. It would be of utmost interest to see whether or not this notion of metric can be extended into the richer differential and Riemannian geometric notion of metric tensors. If that were the case, there is vast uncharted territory; it would be possible to use tools from differential geometry (covariant derivatives, geodesics, connections, fiber bundles, and all that jazz) to explore this result. We hope to address this question soon, and whether or not differential geometric tools can be used or will be useful at all only time will tell.

A second path to glory consists of going back to our original motivation: what about AdS/CFT? The logical concatenation of ideas is clear: beginning with the Harlow-

Ooguri result, we like to think of it in terms of the Eastin-Knill theorem, as a way to deal with this no-go theorem, we employ resource theories and consider approximate error correction; turns out that the typical approaches are difficult to calculate because of the fidelity, therefore, we propose a different approach by considering sub- and super-fidelity, we propose and calculate distance measures for typical quantum channels and confirm that they behave as expected (they even define a metric). Now what? How to close the circle and interpret those bounds under the light of AdS/CFT? We also hope to address those questions in future work.

There are a few other interesting questions whose answers would certainly enrich the discussion. First of all, it would be interesting to further enhance the scope of applicability of our bounds. So far, we performed calculations modelling the lack of exact error correction by considering single quantum channels; what about the composition of more complicated channels? What results would our bounds yield? To finalize, we save the best for last: how tight are those bounds? Whenever one is dealing with bounds and inequalities, this is the main question that has to be answered. In particular, it would be quite interesting to know whether or not methods borrowed from information geometry and AdS/CFT may play a role in this answer or give us a hint.

REFERENCES

1 ZYLA, P. A. *et al.* Review of particle physics. **Progress of Theoretical and Experimental Physics**, v. 2020, n. 8, p. 083C01, 2020.

2 CARROLL, S. **Spacetime and geometry**: an introduction to general relativity. Cambridge: Cambridge University Press, 2019.

3 WALD, R. **General relativity**. Chicago: University of Chicago Press, 2010.

4 GREEN, M. *et al.* **Superstring theory**: an introduction. Cambridge: Cambridge University Press, 1988. v. 1.

5 GREEN, M. *et al.* **Superstring theory**: loop amplitudes, anomalies and phenomenology. Cambridge: Cambridge University Press, 1988. v. 2.

6 POLCHINSKI, J. **String theory**. Cambridge: Cambridge University Press, 2001. v. 1.

7 POLCHINSKI, J. **String theory**. Cambridge: Cambridge University Press, 2001. v. 2.

8 VIRASORO, M. A. Alternative constructions of crossing-symmetric amplitudes with Regge behavior. **Physical Review**, v. 177, n. 5, p. 2309–2311, 1969.

9 VENEZIANO, G. Construction of a crossing-symmetric, Regge behaved amplitude for linearly rising trajectories. **Nuovo Cimento**, v. 57, n. 1, p. 190–197, 1968.

10 SUSSKIND, L. Harmonic-oscillator analogy for the veneziano model. **Physical Review Letters**, v. 23, n. 10, p. 545–547, 1969.

11 SUSSKIND, L. Structure of hadrons implied by duality. **Physical Review D**, v. 1, n. 4, p. 1182–1186, 1970.

12 J.SCHERK; H.SCHWARZ, J. Dual models for non-hadrons. **Nuclear Physics B**, v. 81, n. 1, p. 118–144, 1974.

13 YONEYA, T. Connection of dual models to electrodynamics and gravidynamics. **Progress of Theoretical Physics**, v. 51, n. 6, p. 1907–1920, 1974.

14 GLIOZZI, F.; SCHERK, J.; OLIVE, D. Supersymmetry, supergravity theories and the dual spinor model. **Nuclear Physics B**, v. 122, n. 2, p. 253–290, 1977.

15 GREEN, M. B.; SCHWARZ, J. H. Supersymmetrical string theories. **Physics Letters B**, v. 109, n. 6, p. 444–448, 1982.

16 GREEN, M. B.; SCHWARZ, J. H. Anomaly cancellations in supersymmetric d = 10 gauge theory and superstring theory. **Physics Letters B**, v. 149, n. 1, p. 117–122, 1984.

17 GROSS, D. J. *et al.* Heterotic string. **Physical Review Letters**, v. 54, n. 6, p. 502–505, 1985.

18 HAWKING, S. W. Particle creation by black holes. **Communications in Mathematical Physics**, v. 43, n. 1, p. 199–220, 1975.

19 BEKENSTEIN, J. D. Black holes and entropy. **Physical Review D**, v. 7, n. 8, p. 2333–2346, 1973.

20 SUSSKIND, L. The world as a hologram. **Journal of Mathematical Physics**, v. 36, n. 11, p. 6377–6396, 1995.

21 HOOFT, G. 't. **Dimensional reduction in quantum gravity**. 1993. Available from: https://arXiv.org/pdf/gr-qc/9310026.pdf. Acessible at: 23 Jan. 2022.

22 MALDACENA, J. M. The large N limit of superconformal field theories and supergravity. **International Journal of Theoretical Physics**, v. 38, n. 4, p. 1113–1133, 1997.

23 AMMON, M.; ERDMENGER, J. **Gauge/gravity duality**: foundations and applications. Cambridge: Cambridge University Press, 2015.

24 AHARONY, O. *et al.* Large N field theories, string theory and gravity. **Physics Reports**, v. 323, n. 3, p. 183–386, 2000.

25 NASTASE, H. **Introduction to the AdS/CFT correspondence**. Cambridge: Cambridge University Press, 2015.

26 D'HOKER, E.; FREEDMAN, D. Z. **Supersymmetric gauge theories and the AdS/CFT correspondence**. 2002. Available from: https://arXiv.org/pdf/hep-th/0201253.pdf. Acessible at: 23 Jan. 2022.

27 RYU, S.; TAKAYANAGI, T. Holographic derivation of entanglement entropy from the anti–de Sitter space/conformal field theory correspondence. **Physical Review Letters**, v. 96, n. 18, p. 181602, 2006.

28 RYU, S.; TAKAYANAGI, T. Aspects of holographic entanglement entropy. **Journal of High Energy Physics**, v. 2006, n. 08, p. 045–045, 2006.

29 ALMHEIRI, A.; DONG, X.; HARLOW, D. Bulk locality and quantum error correction in AdS/CFT. **Journal of High Energy Physics**, v. 2015, n. 4, p. 1–34, 2015.

30 HARLOW, D. **TASI lectures on the emergence of the bulk in AdS/CFT**. 2018. Avaliable from: https://arXiv.org/pdf/1802.01040.pdf. Acessible at: 18 Nov. 2021.

31 PASTAWSKI, F. *et al.* Holographic quantum error-correcting codes: toy models for the bulk/boundary correspondence. **Journal of High Energy Physics**, v. 2015, n. 6, 2015. DOI:10.1007/JHEP06(2015)149.

32 HARLOW, D. The Ryu–Takayanagi formula from quantum error correction. **Communications in Mathematical Physics**, v. 354, n. 3, p. 865–912, 2017.

33 PRESKILL, J. Quantum computing in the NISQ era and beyond. **Quantum**, v. 2, p. 79, 2018. DOI:10.22331/q–2018–08–06–79.

34 NIELSEN, M.; CHUANG, I. **Quantum computation and quantum information**. Cambridge: Cambridge University Press, 2000.

35 TERHAL, B. M. Quantum error correction for quantum memories. **Reviews of Modern Physics**, v. 87, n. 2, p. 307–346, 2015.

36 SHOR, P. W. Scheme for reducing decoherence in quantum computer memory. **Physical Review A**, v. 52, n. 4, p. 2493–2496, 1995.

37 GOTTESMAN, D. **Stabilizer codes and quantum error correction**. 1997. Available from: https://arXiv.org/pdf/quant-ph/9705052.pdf. Acessible at: 17 Apr. 2022.

38 STEANE, A. M. Error correcting codes in quantum theory. **Physical Review Letters**, v. 77, n. 5, p. 793–797, 1996.

39 KNILL, E.; LAFLAMME, R. Theory of quantum error-correcting codes. **Physical Review A**, v. 55, n. 2, p. 900–911, 1997.

40 HARLOW, D.; OOGURI, H. Constraints on symmetries from holography. **Physical Review Letters**, v. 122, n. 19, p. 191601, 2019.

41 HARLOW, D.; OOGURI, H. Symmetries in quantum field theory and quantum gravity. **Communications in Mathematical Physics**, v. 383, n. 1, p. 1669–1804, 2021.

42 EASTIN, B.; KNILL, E. Restrictions on transversal encoded quantum gate sets. **Physical Review Letters**, v. 102, n. 11, p. 110502, 2009.

43 CHITAMBAR, E.; GOUR, G. Quantum resource theories. **Reviews of Modern Physics**, v. 91, n. 2, p. 025001, 2019.

44 ZHOU, S.; LIU, Z.-W.; JIANG, L. New perspectives on covariant quantum error correction. **Quantum**, v. 5, p. 521, 2021. DOI:10.22331/q–2021–08–09–521.

45 FAIST, P. *et al.* Continuous symmetries and approximate quantum error correction. **Physical Review X**, v. 10, n. 4, p. 041018, 2020.

46 WOODS, M. P.; ALHAMBRA, Á. M. Continuous groups of transversal gates for quantum error correcting codes from finite clock reference frames. **Quantum**, v. 4, p. 245, 2020. DOI:10.22331/q–2020–03–23–245.

47 LI, L.; BU, K.; LIU, Z.-W. Quantifying the resource content of quantum channels: an operational approach. **Physical Review A**, v. 101, n. 2, p. 022335, 2020.

48 KUBICA, A.; DEMKOWICZ-DOBRZANSKI, R. Using quantum metrological bounds in quantum error correction: a simple proof of the approximate eastin-knill theorem. **Physical Review Letters**, v. 126, n. 15, p. 150503, 2021.

49 HAYDEN, P. *et al.* Error correction of quantum reference frame information. **PRX Quantum**, v. 2, n. 1, p. 010326, 2021.

50 GOUR, G.; SPEKKENS, R. W. The resource theory of quantum reference frames: manipulations and monotones. **New Journal of Physics**, v. 10, n. 3, p. 033023, 2008.

51 BARTLETT, S. D.; RUDOLPH, T.; SPEKKENS, R. W. Reference frames, superselection rules, and quantum information. **Reviews of Modern Physics**, v. 79, n. 2, p. 555–609, 2007.

52 MISZCZAK, J. A. *et al.* **Sub- and super-fidelity as bounds for quantum fidelity**. 2008. Available from: https://arxiv.org/pdf/0805.2037.pdf. Acessible at: 13 June 2022.

53 MENDONCA, P. E. M. F. *et al.* Alternative fidelity measure between quantum states. **Physical Review A**, v. 78, n. 5, p. 052330, 2008.

54 CASALDERREY-SOLANA, J. *et al.* **Gauge/string duality, hot QCD and heavy ion collisions**. Cambridge: Cambridge University Press, 2014.

55 KARCH, A. Recent progress in applying gauge/gravity duality to quark-gluon plasma physics. **AIP Conference Proceedings**, v. 1441, n. 1, p. 95–102, 2012.

56 HOROWITZ, G. **Introduction to holographic superconductors**. 2010. Avaliable from: https://arxiv.org/pdf/1002.1722.pdf. Acessible at: 18 June 2022.

57 RANGAMANI, M. Gravity and hydrodynamics: lectures on the fluid-gravity correspondence. **Classical and Quantum Gravity**, v. 26, n. 22, p. 224003, 2009.

58 FRANCESCO, P. *et al.* **Conformal field theory**. New York: Springer, 1997.

59 BLUMENHAGEN, R.; PLAUSCHINN, E. **Introduction to conformal field theory**: with applications to string theory. Berlin: Springer, 2009.

60 WEINBERG, S. **The quantum theory of fields**. Cambridge: Cambridge University Press, 1995. v. 1.

61 SUSSKIND, L.; WITTEN, E. **The holographic bound in anti-de Sitter space**. 1998. Available from: https://arXiv.org/pdf/hep-th/9805114.pdf. Acessible at: 30 Apr. 2022.

62 WEINBERG, S. **The quantum theory of fields**. Cambridge: Cambridge University Press, 1995. v. 2.

63 JAHN, A.; EISERT, J. Holographic tensor network models and quantum error correction: a topical review. **Quantum Science and Technology**, v. 6, n. 3, p. 033002, 2021.

64 HARLOW, D.; STANFORD, D. **Operator dictionaries and wave functions in AdS/CFT and dS/CFT**. 2011. Available from: https://arXiv.org/pdf/1104.2621.pdf. Acessible at: 30 Oct. 2021.

65 BANKS, T. *et al.* **AdS dynamics from conformal field theory**. 1998. Available from: https://arXiv.org/pdf/hep-th/9808016.pdf. Acessible at: 30 Oct. 2021.

66 WITTEN, E. **Anti de-Sitter space and holography**. 1998. Available from: https://arXiv.org/pdf/hep-th/9802150.pdf. Acessible at: 23 Jan. 2022.

67 HAMILTON, A. *et al.* Holographic representation of local bulk operators. **Physical Review D**, v. 74, n. 6, p. 066009, 2006.

68 KABAT, D.; LIFSCHYTZ, G.; LOWE, D. A. Constructing local bulk observables in interacting AdS/CFT. **Physical Review D**, v. 83, n. 10, p. 106009, 2011.

69 KABAT, D.; LIFSCHYTZ, G. Decoding the hologram: scalar fields interacting with gravity. **Physical Review D**, v. 89, n. 6, p. 066010, 2014.

70 HEADRICK, M. *et al.* Causality and holographic entanglement entropy. **Journal of High Energy Physics**, v. 2014, n. 12, 2014. DOI: 10.1007/JHEP12(2014)162.

71 DONG, X.; HARLOW, D.; WALL, A. C. Reconstruction of bulk operators within the entanglement wedge in Gauge-Gravity duality. **Physical Review Letters**, v. 117, n. 2, p. 021601, 2016.

72 BOUSSO, R.; RANDALL, L. Holographic domains of anti-de Sitter space. **Journal of High Energy Physics**, v. 2002, n. 04, p. 057–057, 2002.

73 HUBENY, V. E.; RANGAMANI, M. Causal holographic information. **Journal of High Energy Physics**, v. 2012, n. 6, 2012. DOI:10.1007/JHEP06(2012)114.

74 HAAG, R. **Local quantum physics**: fields, particles, algebras. Berlin: Springer, 1996.

75 GOTTESMAN, D. **An introduction to quantum error correction and fault-tolerant quantum computation**. 2009. Available from: https://arXiv.org/pdf/0904.2557.pdf. Acessible at: 17 Apr. 2022.

76 DEVITT, S. J.; MUNRO, W. J.; NEMOTO, K. Quantum error correction for beginners. **Reports on Progress in Physics**, v. 76, n. 7, p. 076001, 2013.

77 ROFFE, J. Quantum error correction: an introductory guide. **Contemporary Physics**, v. 60, n. 3, p. 226–245, 2019.

78 BENNETT, C. H. *et al.* Mixed-state entanglement and quantum error correction. **Physical Review A**, v. 54, n. 5, p. 3824–3851, 1996.

79 KNILL, E.; LAFLAMME, R.; VIOLA, L. Theory of quantum error correction for general noise. **Physical Review Letters**, v. 84, n. 11, p. 2525–2528, 2000.

80 ZANARDI, P. Stabilizing quantum information. **Physical Review A**, v. 63, n. 1, p. 012301, 2000.

81 KEMPE, J. *et al.* Theory of decoherence-free fault-tolerant universal quantum computation. **Physical Review A**, v. 63, n. 4, p. 042307, 2001.

82 DUAN, L.-M.; GUO, G.-C. Preserving coherence in quantum computation by pairing quantum bits. **Physical Review Letters**, v. 79, n. 10, p. 1953–1956, 1997.

83 ZANARDI, P.; RASETTI, M. Noiseless quantum codes. **Physical Review Letters**, v. 79, n. 17, p. 3306–3309, 1997.

84 LIDAR, D. A.; CHUANG, I. L.; WHALEY, K. B. Decoherence-free subspaces for quantum computation. **Physical Review Letters**, v. 81, n. 12, p. 2594–2597, 1998.

85 KRIBS, D.; LAFLAMME, R.; POULIN, D. Unified and generalized approach to quantum error correction. **Physical Review Letters**, v. 94, n. 18, p. 180501, 2005.

86 KRIBS, D. W. *et al.* **Operator quantum error correction**. 2006. Available from: https://arXiv.org/pdf/quant-ph/0504189.pdf. Acessible at: 17 Apr. 2022.

87 BÉNY, C.; KEMPF, A.; KRIBS, D. W. Quantum error correction of observables. **Physical Review A**, v. 76, n. 4, p. 042303, 2007.

88 BÉNY, C.; KEMPF, A.; KRIBS, D. W. Generalization of quantum error correction via the heisenberg picture. **Physical Review Letters**, v. 98, n. 10, p. 100502, 2007.

89 FULTON, W.; HARRIS, J. **Representation theory**: a first course. New York: Springer, 1991.

90 PRESKILL, J. **Fault-tolerant quantum computation**. 1997. Available from: https://arXiv.org/pdf/quant-ph/9712048.pdf. Acessible at: 18 June 2022.

91 AHARONOV, D.; KITAEV, A.; PRESKILL, J. Fault-tolerant quantum computation with long-range correlated noise. **Physical Review Letters**, v. 96, n. 5, p. 050504, 2006.

92 ALIFERIS, P.; PRESKILL, J. Fault-tolerant quantum computation against biased noise. **Physical Review A**, v. 78, n. 5, p. 052331, 2008.

93 KITAEV, A. Y. Fault-tolerant quantum computation by anyons. **Annals of Physics**, v. 303, n. 1, p. 2–30, 2003.

94 KNILL, E. *et al.* Benchmarking quantum computers: the five-qubit error correcting code. **Physical Review Letters**, v. 86, n. 25, p. 5811–5814, 2001.

95 HUBENY, V. E.; RANGAMANI, M.; TAKAYANAGI, T. A covariant holographic entanglement entropy proposal. **Journal of High Energy Physics**, v. 2007, n. 07, p. 062–062, 2007.

96 BARRELLA, T. *et al.* Holographic entanglement beyond classical gravity. **Journal of High Energy Physics**, v. 2013, n. 9, 2013. DOI:10.1007/JHEP09(2013)109.

97 FAULKNER, T.; LEWKOWYCZ, A.; MALDACENA, J. Quantum corrections to holographic entanglement entropy. **Journal of High Energy Physics**, v. 2013, n. 11, 2013. DOI:10.1007/JHEP11(2013)074.

98 LEWKOWYCZ, A.; MALDACENA, J. Generalized gravitational entropy. **Journal of High Energy Physics**, v. 2013, n. 8, 2013. DOI:10.1007/JHEP08(2013)090.

99 ENGELHARDT, N.; WALL, A. C. Quantum extremal surfaces: holographic entanglement entropy beyond the classical regime. **Journal of High Energy Physics**, v. 2015, n. 1, 2015. DOI:10.1007/JHEP01(2015)073.

100 JAFFERIS, D. L. *et al.* Relative entropy equals bulk relative entropy. **Journal of High Energy Physics**, v. 2016, n. 6, 2016. DOI:10.1007/JHEP06(2016)004.

101 MALDACENA, J.; SUSSKIND, L. Cool horizons for entangled black holes. **Fortschritte der Physik**, v. 61, n. 9, p. 781–811, 2013.

102 SUSSKIND, L. **Dear qubitzers, GR=QM**. 2017. Available from: https://arxiv.org/pdf/1708.03040.pdf. Acessible at: 24 Fev. 2022.

103 ALMHEIRI, A. *et al.* The entropy of bulk quantum fields and the entanglement wedge of an evaporating black hole. **Journal of High Energy Physics**, v. 2019, n. 12, 2019. DOI:10.1007/JHEP12(2019)063.

104 HARLOW, D. Jerusalem lectures on black holes and quantum information. **Reviews of Modern Physics**, v. 88, n. 1, p. 015002, 2016.

105 ALMHEIRI, A. *et al.* The entropy of hawking radiation. **Reviews of Modern Physics**, v. 93, n. 3, p. 035002, 2021.

106 PENINGTON, G. **Entanglement wedge reconstruction and the information paradox**. 2019. Available from: https://arxiv.org/pdf/1905.08255.pdf. Acessible at: 18 June 2022.

107 EISERT, J. **Entanglement and tensor network states**. 2013. Available from: https://arXiv.org/pdf/1308.3318.pdf. Acessible at: 18 June 2022.

108 ORUS, R. A practical introduction to tensor networks: matrix product states and projected entangled pair states. **Annals of Physics**, v. 349, n. 1, p. 117–158, 2014.

109 BRIDGEMAN, J. C.; CHUBB, C. T. Hand-waving and interpretive dance: an introductory course on tensor networks. **Journal of Physics A**, v. 50, n. 22, p. 223001, 2017.

110 CIRAC, J. I. *et al.* Matrix product states and projected entangled pair states: concepts, symmetries, theorems. **Reviews of Modern Physics**, v. 93, n. 4, p. 045003, 2021.

111 PAPADIMITRIOU, C.; STEIGLITZ, K. **Combinatorial optimization**: algorithms and complexity. New York: Dover, 1998.

112 TRUDEAU, R. **Introduction to graph theory**. New York: Dover, 1993.

113 DOPLICHER, S. Local aspects of superselection rules. **Communications in Mathematical Physics**, v. 85, n. 1, p. 73–86, 1982.

114 DOPLICHER, S.; LONGO, R. Local aspects of superselection rules II. **Communications in Mathematical Physics**, v. 88, n. 1, p. 399–409, 1983.

115 BUCHHOLZ, D.; DOPLICHER, S.; LONGO, R. On noether's theorem in quantum field theory. **Annals of Physics**, v. 170, n. 1, p. 1–17, 1986.

116 COTLER, J. *et al.* Entanglement wedge reconstruction via universal recovery channels. **Physical Review X**, v. 9, n. 3, p. 031011, 2019.

117 CHEN, C.-F.; PENINGTON, G.; SALTON, G. Entanglement wedge reconstruction using the petz map. **Journal of High Energy Physics**, v. 2020, n. 1, 2020. DOI:10.1007/JHEP01(2020)168.

118 PLENIO, M. B.; VIRMANI, S. An introduction to entanglement measures. **Quantum Information & Computation**, v. 7, n. 1, p. 1–51, 2007.

119 HORODECKI, R. *et al.* Quantum entanglement. **Reviews of Modern Physics**, v. 81, n. 2, p. 865–942, 2009.

120 STRELTSOV, A.; ADESSO, G.; PLENIO, M. B. Colloquium: quantum coherence as a resource. **Reviews of Modern Physics**, v. 89, n. 4, p. 041003, 2017.

121 BRUNNER, N. *et al.* Bell nonlocality. **Reviews of Modern Physics**, v. 86, n. 2, p. 419–478, 2014.

122 GOUR, G. *et al.* The resource theory of informational nonequilibrium in thermodynamics. **Physics Reports**, v. 583, p. 1–58, 2015. DOI:10.1016/j.physrep.2015.04.003.

123 GOOLD, J. *et al.* The role of quantum information in thermodynamics—a topical review. **Journal of Physics A**, v. 49, n. 14, p. 143001, 2016.

124 LIU, Y.; YUAN, X. Operational resource theory of quantum channels. **Physical Review Research**, v. 2, n. 1, p. 012035, 2020.

125 HORODECKI, M.; OPPENHEIM, J. (quantumness in the context of) resource theories. **International Journal of Modern Physics B**, v. 27, n. 01n03, p. 1345019, 2012.

126 BRANDAO, F. G. S. L.; GOUR, G. Reversible framework for quantum resource theories. **Physical Review Letters**, v. 115, n. 7, p. 070503, 2015.

127 GOUR, G. Quantum resource theories in the single-shot regime. **Physical Review A**, v. 95, n. 6, p. 062314, 2017.

128 LIU, Z.-W.; HU, X.; LLOYD, S. Resource destroying maps. **Physical Review Letters**, v. 118, n. 6, p. 060502, 2017.

129 SPARACIARI, C. *et al.* The first law of general quantum resource theories. **Quantum**, v. 4, p. 259, 2020. DOI:10.22331/q–2020–04–30–259.

130 PALAZUELOS, C. Superactivation of quantum nonlocality. **Physical Review Letters**, v. 109, n. 19, p. 190401, 2012.

131 SHANNON, C. E. A mathematical theory of communication. **The Bell System Technical Journal**, v. 27, p. 379–423, 1948.

132 MARVIAN, I.; SPEKKENS, R. W. How to quantify coherence: distinguishing speakable and unspeakable notions. **Physical Review A**, v. 94, n. 5, p. 052324, 2016.

133 JOZSA, R. Fidelity for mixed quantum states. **Journal of Modern Optics**, v. 41, n. 12, p. 2315–2323, 1994.

134 SCHUMACHER, B. Quantum coding. **Physical Review A**, v. 51, n. 4, p. 2738–2747, 1995.

135 UHLMANN, A. The transition probability in the state space of a *-algebra. **Reports on Mathematical Physics**, v. 9, n. 2, p. 273–279, 1976.

136 ALBERTI, P. M. A note on the transition probability over c*-algebras. **Letters in Mathematical Physics**, v. 7, n. 1, p. 25–32, 1983.

137 ALBERTI, P. M.; UHLMANN, A. Stochastic linear maps and transition probability. **Letters in Mathematical Physics**, v. 7, n. 2, p. 107–112, 1983.

138 GREENBERGER, D.; HORNE, M.; ZEILINGER, A. **Going beyond Bell's theorem**. 1993. Available from: https://arxiv.org/pdf/0712.0921.pdf. Acessible at: 13 July 2022.

139 BOUWMEESTER, D. *et al.* Observation of three-photon Greenberger-Horne-Zeilinger entanglement. **Physical Review Letters**, v. 82, n. 7, p. 1345–1349, 1999.

APPENDIX

APPENDIX A – EXPLICIT RECONSTRUCTION OF A BULK OPERATOR IN ADS/CFT

In this appendix, we perform the explicit reconstruction of a bulk field using the global reconstruction procedure (see section 2.5). For details, we refer to (30, 67–69, 117). The problem amounts to computing the equations of motion in the AdS space and consider the boundary conditions dictated by AdS/CFT.

We begin by considering the AdS space with global coordinates (equation 2.7 with $\ell = 1$)

$$ds^2 = -\left(1 + r^2\right) dt^2 + \frac{dr^2}{1 + r^2} + r^2 d\Omega_{d-1}^2, \tag{A.1}$$

with $r \in [0, +\infty)$, $t \in (-\infty, +\infty)$ and Ω_{d-1} denotes the round metric over the manifold S^{d-1}. We shall consider a free scalar field for simplicity sake. The action is given by

$$I[\phi] = -\frac{1}{2} \int \sqrt{-g} (\partial_\mu \phi \partial_\nu \phi g^{\mu\nu} + m^2 \phi^2)\ d^{d+1}x, \tag{A.2}$$

and the scalar field ϕ obeys the equations of motion, which is the Klein-Gordon equation

$$\nabla^2 \phi = \frac{1}{\sqrt{-g}} \partial_\mu (\sqrt{-g} g^{\mu\nu} \partial_\nu \phi) = m^2 \phi. \tag{A.3}$$

We may choose the spherical harmonics as a basis for the solutions of the equations of motion (A.3). In this case, we can write

$$c_{\omega \ell \vec{m}}(t, r, \Omega) = R_{\omega \ell}(r) e^{-i\omega t} Y_{\ell \vec{m}}(\Omega), \tag{A.4}$$

where ω is associated with the frequency of the solution, ℓ and $\vec{m}$ are the quantum numbers that characterize the solution, and $Y_{\ell \vec{m}}(\Omega)$ denote the spherical harmonics.

The radial component of the solution obeys the differential equation

$$(1 + r^2) R'' + \left(\frac{d-1}{r} (1 + r^2) + 2r \right) R' + \left(\frac{\omega^2}{1 + r^2} - \frac{\ell(\ell + d - 2)}{r^2} - m^2 \right) R = 0, \tag{A.5}$$

where the prime denotes derivative with respect to the variable r. This equation is generally intractable, therefore we deal with the equation for small and large r. For small r, we obtain

$$R'' + \frac{d-1}{r} R' - \frac{\ell(\ell + d - 2)}{r^2} R = 0,$$

and the solutions have the behavior

$$R(r) \sim r^{-\left(\frac{d-2}{2}\right)\pm\frac{1}{2}\sqrt{(d-2)^2+4\ell(\ell+d-2)}}. \tag{A.6}$$

Meanwhile, for large r, we get

$$r^2R'' + (d+1)rR' - m^2R = 0$$

with solutions

$$R(r) \sim r^{-\left(\frac{d}{2}\pm\frac{1}{2}\sqrt{d^2+4m^2}\right)}. \tag{A.7}$$

In general, we have the choice between the positive or negative solutions in equations (A.6, A.7). Given the freedom of choice, we choose the positive solution for both. There are some subtleties associated with the choice, however, for $m^2 \geq 0$ and $d \geq 2$, the positive choice is consistent. In other words, we take

$$R_{\omega\ell}(r) \sim r^{-\Delta}, \tag{A.8}$$

$$\Delta := \frac{d}{2} + \frac{1}{2}\sqrt{d^2+4m^2}. \tag{A.9}$$

This way, the full solution in the Heisenberg representation of the free scalar can be expanded into

$$\phi(r;t,\Omega) = \sum_{n\ell\vec{m}} \left(c_{n\ell\vec{m}}a_{n\ell\vec{m}} + c^*_{n\ell\vec{m}}a^\dagger_{n\ell\vec{m}}\right), \tag{A.10}$$

where $a_{n\ell\vec{m}}$ ($a^\dagger_{n\ell\vec{m}}$) denotes the annihilation (creation) operators that obey the commutation relations described by $[a_{n\ell\vec{m}}\ ,\ a^\dagger_{n\ell\vec{m}}] = \delta_{nn'}\delta_{\ell\ell'}\delta_{mm'}$. The asymptotic behavior provides the quantization of Δ (see equation A.9) which implies a quantization relation for the frequencies of the solutions, on top of that, it also provides the following relation

$$R_{\omega\ell}(r) = A_{n\ell}r^{-\Delta}(1 + O(1/r^2) + ...).$$

The connection with the boundary operators comes from equation (2.12), by substituting the results we have obtained, it follows

$$\mathcal{O}(t,\Omega) = \sum_{n\ell\vec{m}} \left(A_{n\ell}e^{-i\omega_{n\ell}t}Y_{\ell\vec{m}}(\Omega)a_{n\ell\vec{m}} + A^*_{n\ell}e^{i\omega_{n\ell}t}Y^*_{\ell\vec{m}}(\Omega)a^\dagger_{n\ell\vec{m}}\right), \tag{A.11}$$

it is convenient to split the above result into the "positive" and "negative" parts

$$\mathcal{O}_+(t,\Omega) = \sum_{n\ell\vec{m}} A_{n\ell}e^{-i\omega_{n\ell}t}Y_{\ell\vec{m}}(\Omega)a_{n\ell\vec{m}}$$

$$\mathcal{O}_-(t,\Omega) = \sum_{n\ell\vec{m}} A^*_{n\ell}e^{i\omega_{n\ell}t}Y^*_{\ell\vec{m}}(\Omega)a^\dagger_{n\ell\vec{m}},$$

calculating their respective Fourier transformations, it follows

$$a_{n\ell\vec{m}} = \frac{1}{A_{n\ell}} \int_{-\pi}^{\pi} \int e^{i\omega_{n\ell}t} Y^*_{\ell\vec{m}}(\Omega) \mathcal{O}_+(t,\Omega)\ d\Omega dt, \tag{A.12}$$

$$a^\dagger_{n\ell\vec{m}} = \frac{1}{A^*_{n\ell}} \int_{-\pi}^{\pi} \int e^{-i\omega_{n\ell}t} Y_{\ell\vec{m}}(\Omega) \mathcal{O}_-(t,\Omega)\ d\Omega dt. \tag{A.13}$$

With the results of the $c_{\omega\ell\vec{m}}$ functions (see equation A.4) and the annihilation/creation operators $a_{n\ell\vec{m}}$ (see equation A.12), we can substitute both into the Heisenberg representation of the scalar field (equation A.10), which yields

$$\phi(r;t,\Omega) = \int_{\pi}^{\pi} \int K_+(r,t,\Omega;t',\Omega')\mathcal{O}_+(t',\Omega')d\Omega dt + \int_{\pi}^{\pi} \int K_-(r,t,\Omega;t',\Omega')\mathcal{O}_-(t',\Omega')d\Omega' dt' \tag{A.14}$$

where K_+ and K_- are the smearing functions and have explicit form given by

$$K_+(r,t,\Omega;t',\Omega') := \sum_{n\ell\vec{m}} \frac{1}{A^*_{n\ell}} c_{n\ell\vec{m}}(r,t,\Omega) e^{i\omega_{n\ell}t'} Y^*_{\ell\vec{m}}(\Omega'), \tag{A.15}$$

$$K_-(r,t,\Omega;t',\Omega') := \sum_{n\ell\vec{m}} \frac{1}{A_{n\ell}} c^*_{n\ell\vec{m}}(r,t,\Omega) e^{-i\omega_{n\ell}t'} Y_{\ell\vec{m}}(\Omega'). \tag{A.16}$$

This is the explicit reconstruction procedure for a given free scalar bulk field. Note that the final result (equation A.14) is, up to differences in notation and conventions, the equation of the global reconstruction (2.16) in the main text.

APPENDIX B – 3-QUTRIT CODE STATES

In this appendix, we show the explicit recovery of the 3-qutrit code[1]. The logical basis is given by

$$|\tilde{0}\rangle = \frac{1}{\sqrt{3}}(|000\rangle + |111\rangle + |222\rangle),$$
$$|\tilde{1}\rangle = \frac{1}{\sqrt{3}}(|012\rangle + |120\rangle + |201\rangle),$$
$$|\tilde{2}\rangle = \frac{1}{\sqrt{3}}(|021\rangle + |102\rangle + |210\rangle).$$

A given logical state $|\tilde{\psi}\rangle \in \mathcal{H}_{code}$ is simply a combination of the basis elements

$$|\tilde{\psi}\rangle = |000\rangle + |111\rangle + |222\rangle + |012\rangle + |120\rangle + |201\rangle + |021\rangle + |102\rangle + |210\rangle$$
$$\tilde{\rho} = |\tilde{\psi}\rangle\langle\tilde{\psi}| = |\tilde{0}\rangle\langle\tilde{0}| + |\tilde{1}\rangle\langle\tilde{1}| + |\tilde{2}\rangle\langle\tilde{2}|,$$

by expanding the logical basis for the logical density matrix, we obtain

$$\begin{aligned}\tilde{\rho} = &(|000\rangle\langle 000| + |000\rangle\langle 111| + |000\rangle\langle 222| + |111\rangle\langle 000| + |111\rangle\langle 111| + |111\rangle\langle 222| \\ &+ |222\rangle\langle 000| + |222\rangle\langle 111| + |222\rangle\langle 222|) + (|012\rangle\langle 012| + |012\rangle\langle 120| + |012\rangle\langle 201| \\ &+ |120\rangle\langle 021| + |120\rangle\langle 120| + |120\rangle\langle 201| + |201\rangle\langle 012| + |201\rangle\langle 120| + |201\rangle\langle 201|) \\ &+ (|021\rangle\langle 021| + |021\rangle\langle 102| + |021\rangle\langle 210| + |102\rangle\langle 021| + |102\rangle\langle 102| + |102\rangle\langle 210| \\ &+ |210\rangle\langle 021| + |210\rangle\langle 102| + |210\rangle\langle 210|). \end{aligned} \quad \text{(B.1)}$$

Let us say that the third qutrit was erased. We will show explicitly how to recover the physical basis by acting with the unitary U_{12} on each logical basis element. As any message is linear combination of the physical basis elements, this procedure shows how to reconstruct any message encoded. For the first basis element $|\tilde{0}\rangle$, it follows

$$(U_{12} \otimes I_3)|\tilde{0}\rangle = |0\rangle \otimes \frac{1}{\sqrt{3}}(|00\rangle + |11\rangle + |22\rangle)$$
$$(U_{12} \otimes I_3)\frac{1}{\sqrt{3}}(|000\rangle + |111\rangle + |222\rangle) = \frac{1}{\sqrt{3}}(|000\rangle + |011\rangle + |022\rangle)$$
$$\frac{1}{\sqrt{3}}(|000\rangle + |011\rangle + |022\rangle) = \frac{1}{\sqrt{3}}(|000\rangle + |011\rangle + |022\rangle),$$

[1] Throughout this appendix, we will ignore numerical factors, as they are irrelevant for our interests.

for the second element $|\tilde{1}\rangle$, we have

$$(U_{12}\otimes I_3)|\tilde{1}\rangle = |1\rangle\otimes\frac{1}{\sqrt{3}}(|00\rangle+|11\rangle+|22\rangle)$$
$$(U_{12}\otimes I_3)\frac{1}{\sqrt{3}}(|012\rangle+|120\rangle+|201\rangle) = \frac{1}{\sqrt{3}}(|100\rangle+|111\rangle+|122\rangle)$$
$$\frac{1}{\sqrt{3}}(|122\rangle+|100\rangle+|111\rangle) = \frac{1}{\sqrt{3}}(|100\rangle+|111\rangle+|122\rangle),$$

and for the last element,

$$(U_{12}\otimes I_3)|\tilde{2}\rangle = |2\rangle\otimes\frac{1}{\sqrt{3}}(|00\rangle+|11\rangle+|22\rangle)$$
$$(U_{12}\otimes I_3)\frac{1}{\sqrt{3}}(|021\rangle+|102\rangle+|210\rangle) = \frac{1}{\sqrt{3}}(|200\rangle+|211\rangle+|222\rangle)$$
$$\frac{1}{\sqrt{3}}(|211\rangle+|222\rangle+|200\rangle) = \frac{1}{\sqrt{3}}(|200\rangle+|211\rangle+|222\rangle).$$

It is also useful to consider the reconstruction procedure in terms of density matrices. The reconstruction procedure for the logical density matrix (considering that the lost qutrit is the third) goes as follow

$$\begin{aligned}\tilde{\rho} = |\tilde{\psi}\rangle\langle\tilde{\psi}| &= U_{12}^{\dagger}(|\psi\rangle_1\otimes|\chi\rangle_{23})(\langle\psi|_1\otimes\langle\chi|_{23})U_{12}\\ &= U_{12}^{\dagger}(\rho_1\otimes|\chi\rangle\langle\chi|_{23})U_{12}.\end{aligned}\tag{B.2}$$

We want to show that equation (B.2) indeed recovers the full logical density matrix (B.1). The first step is to calculate the tensor product $\rho_1\otimes|\chi\rangle\langle\chi|_{23}$ and then act the permutation unitaries. The reduced density matrix of any qutrit state is maximally mixed, and the $|\chi\rangle$ state must be entangled. In other words,

$$\begin{aligned}\rho_1 &= |0\rangle\langle 0|+|1\rangle\langle 1|+|2\rangle\langle 2|\\ |\chi\rangle\langle\chi|_{23} &= (|00\rangle+|11\rangle+|22\rangle)(\langle 00|+\langle 11|+\langle 22|)\\ &= |00\rangle\langle 00|+|00\rangle\langle 11|+|00\rangle\langle 22|+|11\rangle\langle 00|+|11\rangle\langle 11|\\ &\quad+|11\rangle\langle 22|+|22\rangle\langle 00|+|22\rangle\langle 11|+|22\rangle\langle 22|,\end{aligned}$$

and the full tensor product is given by

$$\begin{aligned}\rho_1\otimes|\chi\rangle\langle\chi|_{23} = {}&|000\rangle\langle 000|+|000\rangle\langle 011|+|000\rangle\langle 022|+|011\rangle\langle 000|+|011\rangle\langle 011|+|011\rangle\langle 022|\\ &+|022\rangle\langle 000|+|022\rangle\langle 011|+|022\rangle\langle 022|+|100\rangle\langle 100|+|100\rangle\langle 111|+|100\rangle\langle 122|\\ &+|111\rangle\langle 100|+|111\rangle\langle 111|+|111\rangle\langle 122|+|122\rangle\langle 100|+|122\rangle\langle 111|+|122\rangle\langle 122|\\ &+|200\rangle\langle 200|+|200\rangle\langle 211|+|200\rangle\langle 222|+|211\rangle\langle 200|+|211\rangle\langle 211|+|211\rangle\langle 222|\\ &+|222\rangle\langle 200|+|222\rangle\langle 211|+|222\rangle\langle 222|.\end{aligned}$$

Now it remains to act with the unitaries. There is an important subtlety in this process. We have shown explicitly the unitary U_{12} acting on ket states, however, now we have $U_{12}^\dagger$ acting on kets and U_{12} acting on bra states and it must be taken into consideration. As the unitaries are simply permutations, their conjugate consists of inverting the map in a one-to-one fashion. This way, we obtain for $U_{12}^\dagger$

$$\begin{aligned}
&|00\rangle \to |00\rangle \quad |01\rangle \to |11\rangle \quad |02\rangle \to |22\rangle \\
&|12\rangle \to |01\rangle \quad |10\rangle \to |12\rangle \quad |11\rangle \to |20\rangle \\
&|21\rangle \to |02\rangle \quad |22\rangle \to |10\rangle \quad |20\rangle \to |21\rangle,
\end{aligned}$$

and for U_{12},

$$\begin{aligned}
&\langle 00| \to \langle 00| \quad \langle 01| \to \langle 11| \quad \langle 02| \to \langle 22| \\
&\langle 12| \to \langle 01| \quad \langle 10| \to \langle 12| \quad \langle 11| \to \langle 20| \\
&\langle 21| \to \langle 02| \quad \langle 22| \to \langle 10| \quad \langle 20| \to \langle 21|.
\end{aligned}$$

Given the explicit permutations stated above, now we act with them, obtaining

$$\begin{aligned}
U_{12}^\dagger(\rho_1 \otimes |\chi\rangle\langle\chi|_{23})U_{12} = {} & |000\rangle\langle 000| + |000\rangle\langle 111| + |000\rangle\langle 222| + |111\rangle\langle 000| + |111\rangle\langle 111| \\
& + |111\rangle\langle 222| + |222\rangle\langle 000| + |222\rangle\langle 111| + |222\rangle\langle 222| + |120\rangle\langle 120| + |120\rangle\langle 201| \\
& + |120\rangle\langle 012| + |201\rangle\langle 120| + |201\rangle\langle 201| + |201\rangle\langle 012| + |012\rangle\langle 120| + |012\rangle\langle 201| \\
& + |012\rangle\langle 012| + |210\rangle\langle 210| + |210\rangle\langle 210| + |210\rangle\langle 102| + |021\rangle\langle 210| + |021\rangle\langle 021| \\
& + |021\rangle\langle 102| + |102\rangle\langle 210| + |102\rangle\langle 021| + |102\rangle\langle 102|.
\end{aligned}$$

and it indeed precisely recovers the logical density matrix $\tilde{\rho}$ from equation (B.1).

APPENDIX C – HAAR MEASURE AND INTEGRATION

In this appendix, we discuss the Haar measure and how to compute integrals using such measure. This sort of integration arises very frequently in the context of resource theories, in particular, in the case of asymmetry resource theories.

The idea is to establish a way to measure distances when considering group elements $g \in G$. Consider a parametrization given by ξ_i from $i = 1, 2, ..., n$, where n denotes the dimension of the group G. This way, the abstract integration over the group manifold may be equipped with a parametrization, which in turn allow us to rewrite

$$\int_G dg \to \int \sqrt{\eta}\; d^n\xi_i, \tag{C.1}$$

where $\eta = \det(M)$ and M denotes the components of the matrix defined as

$$M_{ij} = \mathrm{tr}\left((-i)\frac{\partial g}{\partial \xi^i}g^{-1}(-i)\frac{\partial g}{\partial \xi^j}g^{-1}\right). \tag{C.2}$$

Note that this definition has several useful properties, in particular, the terms $\frac{\partial g}{\partial \xi^i}g^{-1}$ are in Maurer-Cartan form and belong to the Lie algebra associated with G. On top of that, if we choose an unitary representation, the matrix (C.2) will be Hermitian, to see that,

$$\partial(gg^{-1}) = \partial(\mathbf{1}) = 0,$$

on the other hand, $\partial(gg^{-1}) = \partial g g^{-1} + g\partial g^{-1} \Rightarrow \partial g^{-1} = -g^{-1}\partial g g^{-1}$. As we are dealing with unitary representations, $g^\dagger = g^{-1}$, therefore it follows

$$\left(-i\frac{\partial g}{\partial \xi^i}g^{-1}\right)^\dagger = ig\left(\frac{\partial g^{-1}}{\partial \xi^i}\right) = -igg^{-1}\frac{\partial g}{\partial \xi^i}g^{-1} = -i\frac{\partial g}{\partial \xi^i}g^{-1}, \tag{C.3}$$

which leads to $(M_{ij})^\dagger = M_{ij}$. Yet another property of the definition (C.2) is the fact that it is invariant under left and right translations. Consider a fixed $\bar{g} \in G$ and take $g \to g\bar{g}$. It follows

$$\frac{\partial g}{\partial \xi^i}g^{-1} \to \frac{\partial (g\bar{g})}{\partial \xi^i}(g\bar{g})^{-1} = \frac{\partial g}{\partial \xi^i}\bar{g}(\bar{g})^{-1}g^{-1} = \frac{\partial g}{\partial \xi^i}g^{-1} \tag{C.4}$$

and the argument for left-translation follows closely. Given those properties, the natural definition of a line element is

$$ds^2 = M_{ij}\xi^i\xi^j. \tag{C.5}$$

This is the general theory of Haar measure and Haar integration in a nutshell. For concreteness' sake, we will explore two examples which appear in our context (see sections 5.2 and 5.3).

Let us begin with $G = U(1)$, arguably the simplest Lie group. The definition of this group is such that we may parametrize it through $g = \exp(i\theta)$. Once again, from the group definition, the inverse of a given element is its complex conjugate, which implies that $g^\dagger = g^{-1}$. Now it remains to calculate the matrix elements of M_{ij}, as the group is one-dimensional, the family of parameters ξ^i are reduced to a single one denoted by θ. It is necessary to compute only a single component

$$\frac{\partial g}{\partial \theta} = ie^{i\theta} \to -i\frac{\partial g}{\partial \theta}g^{-1} = (-i)ie^{i\theta}e^{-i\theta} = 1,$$

therefore,

$$M_{ij} = M_{\theta\theta} = \mathrm{tr}(1) \Rightarrow \sqrt{\eta} = 1,$$

consequently,

$$\int \sqrt{\eta}\; d^n\xi_i \to \int_0^{2\pi} d\theta.$$

The normalization condition for a given function $f = f(\theta)$, assuming that the function has "good properties" i.e. is of (at least) class $\mathcal{C}^1$, yields

$$\frac{\int_0^{2\pi} f(\theta)\; d\theta}{\int_0^{2\pi}\; d\theta} = \frac{1}{2\pi}\int_0^{2\pi} f(\theta)\; d\theta. \tag{C.6}$$

The second important example we ought to discuss is $G = SU(2)$. First note that there is an diffeomorphism (i.e. a smooth isomorphism between two differentiable manifolds) between this group and the manifold[1] S^3. We can choose an unitary representation as

$$U = \begin{pmatrix} z_1 & z_2 \\ z_3 & z_4 \end{pmatrix}, \qquad U^\dagger = \begin{pmatrix} z_1^* & z_3^* \\ z_2^* & z_4^* \end{pmatrix},$$

[1] This allow us to employ the following strategy to evaluate the Haar integration: complexify the unitary representation by taking

$$U = \begin{pmatrix} z_1 & iz_2 \\ iz_2^* & z_1^* \end{pmatrix},$$

which in turn provides the constrain $|z_1|^2 + |z_2|^2 = 1$, where one could take $z_1 = x_1 + ix_2$ and $z_2 = x_3 + ix_4$, then the constrain becomes $x_1^2 + x_2^2 + x_3^2 + x_4^2 = 1$ which is precisely the equation of the manifold S^3.

meanwhile, the inverse of U is given by

$$U^{-1} = \frac{1}{z_1 z_4 - z_2 z_3} \begin{pmatrix} z_4 & -z_2 \\ -z_3 & z_1 \end{pmatrix}.$$

From the fact that the representation is unitary, we obtain several constrains on the components because $U^{-1} = U^\dagger$. In particular, one could perform a reparametrization where we rely only on three parameters rather than four. One such reparametrization is obtained by considering the so-called Darboux coordinates:

$$\begin{aligned} z_1 &= \sqrt{1-\lambda} e^{i\theta_1} \\ z_2 &= \sqrt{1-\lambda} e^{i\theta_2} \\ \lambda &= \sin^2(\theta_3), \end{aligned}$$

for $\theta_1, \theta_2 \in [0, 2\pi]$ and $\theta_3 \in [0, \pi/2]$. In this reparametrization, a group element $g \in SU(2)$ has the form

$$g = \begin{pmatrix} \sqrt{1-\lambda} e^{i\theta_1} & i\sqrt{\lambda} e^{i\theta_2} \\ i\sqrt{\lambda} e^{-i\theta_2} & \sqrt{1-\lambda} e^{-i\theta_1} \end{pmatrix}, \quad g^{-1} = \begin{pmatrix} \sqrt{1-\lambda} e^{-i\theta_1} & -i\sqrt{\lambda} e^{-i\theta_2} \\ -i\sqrt{\lambda} e^{i\theta_2} & \sqrt{1-\lambda} e^{i\theta_1} \end{pmatrix}$$

and indeed $g^{-1} = g^\dagger$, as well as $\det(g) = 1$. To calculate the metric we must compute the derivatives as follows

$$\frac{\partial g}{\partial \theta_1} = \begin{pmatrix} i\sqrt{1-\lambda} e^{i\theta_1} & 0 \\ 0 & -i\sqrt{1-\lambda} e^{-i\theta_1} \end{pmatrix},$$

including the inverse to the right, we obtain

$$\frac{\partial g}{\partial \theta_1} g^{-1} = \begin{pmatrix} i(1-\lambda) & \sqrt{\lambda(1-\lambda)} e^{i(\theta_1+\theta_2)} \\ -\sqrt{\lambda(1-\lambda)} e^{-i(\theta_1+\theta_2)} & -i(1-\lambda) \end{pmatrix}.$$

The derivatives with respect to the parameter θ_2 follows closely. We now have enough to calculate the matrix (C.2) and the line element (C.5). Performing the calculations yields

$$M_{ij} = \begin{pmatrix} \dfrac{1}{2\lambda(1-\lambda)} & 0 & 0 \\ 0 & 2(1-\lambda) & 0 \\ 0 & 0 & 2\lambda \end{pmatrix}$$

and

$$ds^2 = \frac{d\lambda^2}{2\lambda(1-\lambda)} + 2(1-\lambda) d\theta_1^2 + 2\lambda d\theta_2^2. \tag{C.7}$$

Note that $\det(M)= 2$, therefore, the normalization condition for a given (at least) class $\mathcal{C}^1$ function $f = f(\lambda, \theta_1, \theta_2)$ gives

$$\frac{\int_0^1 \int_0^{2\pi} \int_0^{2\pi} \sqrt{2} f(\lambda, \theta_1, \theta_2)\ d\lambda d\theta_1 d\theta_2}{\int_0^1 \int_0^{2\pi} \int_0^{2\pi} \sqrt{2}\ d\lambda d\theta_1 d\theta_2} = \frac{1}{4\pi^2} \int f(\lambda, \theta_1, \theta_2)\ d\lambda d\theta_1 d\theta_2, \tag{C.8}$$

which is the parametrized Haar integration for the group $SU(2)$.